

9 The strong coupling α_s

Authors¹ : R. Horsley, P. Petreczky, S. Sint

9.1 Introduction

The strong coupling $\bar{g}_s(\mu)$ defined at scale μ , plays a key role in the understanding of QCD and in its application to collider physics. For example, the parametric uncertainty from α_s is one of the dominant sources of uncertainty in the Standard-Model prediction for the $H \rightarrow b\bar{b}$ partial width, and the largest source of uncertainty for $H \rightarrow gg$. Thus higher precision determinations of α_s are needed to maximize the potential of experimental measurements at the LHC, and for high-precision Higgs studies at future colliders and the study of the stability of the vacuum [2–9]. The value of α_s also yields one of the essential boundary conditions for completions of the Standard Model at high energies.

In order to determine the running coupling at scale μ

$$\alpha_s(\mu) = \frac{\bar{g}_s^2(\mu)}{4\pi}, \quad (317)$$

we should first “measure” a short-distance quantity \mathcal{Q} at scale μ either experimentally or by lattice calculations, and then match it to a perturbative expansion in terms of a running coupling, conventionally taken as $\alpha_{\overline{\text{MS}}}(\mu)$,

$$\mathcal{Q}(\mu) = c_1 \alpha_{\overline{\text{MS}}}(\mu) + c_2 \alpha_{\overline{\text{MS}}}(\mu)^2 + \dots \quad (318)$$

The essential difference between continuum determinations of α_s and lattice determinations is the origin of the values of \mathcal{Q} in Eq. (318).

The basis of continuum determinations are experimentally measurable cross sections or decay widths from which \mathcal{Q} is defined. These cross sections have to be sufficiently inclusive and at sufficiently high scales such that perturbation theory can be applied. Often hadronization corrections have to be used to connect the observed hadronic cross sections to the perturbative ones. Experimental data at high μ , where perturbation theory is progressively more precise, usually have increasing experimental errors, and it is not easy to find processes that allow one to follow the μ -dependence of a single $\mathcal{Q}(\mu)$ over a range where $\alpha_s(\mu)$ changes significantly and precision is maintained.

In contrast, in lattice gauge theory, one can design $\mathcal{Q}(\mu)$ as Euclidean short-distance quantities that are not directly related to experimental observables. This allows us to follow the μ -dependence until the perturbative regime is reached and nonperturbative “corrections” are negligible. The only experimental input for lattice computations of α_s is the hadron spectrum which fixes the overall energy scale of the theory and the quark masses. Therefore experimental errors are completely negligible and issues such as hadronization do not occur. We can construct many short-distance quantities that are easy to calculate nonperturbatively in lattice simulations with small statistical uncertainties. We can also simulate at parameter values that do not exist in nature (for example, with unphysical quark masses between bottom

¹There is a strong overlap with the FLAG 19 report’s section on α_s , authored by R. Horsley, T. Onogi and R. Sommer [1]. In particular the introduction, and the description of methods without new data have been taken over almost unchanged.

and charm) to help control systematic uncertainties. These features mean that precise results for α_s can be achieved with lattice-gauge-theory computations. Further, as in the continuum, the different methods available to determine α_s in lattice calculations with different associated systematic uncertainties enable valuable cross-checks. Practical limitations are discussed in the next section, but a simple one is worth mentioning here. Experimental results (and therefore the continuum determinations) of course have all quarks present, while in lattice gauge theories in practice only the lighter ones are included and one is then forced to use the matching at thresholds, as discussed in the following subsection.

It is important to keep in mind that the dominant source of uncertainty in most present day lattice-QCD calculations of α_s are from the truncation of continuum/lattice perturbation theory and from discretization errors. Perturbative truncation errors are of particular concern because they often cannot easily be estimated from studying the data itself. Further, the size of higher-order coefficients in the perturbative series can sometimes turn out to be larger than naive expectations based on power counting from the behaviour of lower-order terms. We note that perturbative truncation errors are also the dominant source of uncertainty in several of the phenomenological determinations of α_s .

The various phenomenological approaches to determining the running coupling constant, $\alpha_{\overline{\text{MS}}}^{(5)}(M_Z)$ are summarized by the Particle Data Group [10]. The PDG review lists five categories of phenomenological results used to obtain the running coupling: using hadronic τ decays, hadronic final states of e^+e^- annihilation, deep inelastic lepton–nucleon scattering, electroweak precision data, and high energy hadron collider data. Excluding lattice results, the PDG quotes the weighted average as

$$\alpha_{\overline{\text{MS}}}^{(5)}(M_Z) = 0.1176(11), \quad \text{PDG 20 [10]} \quad (319)$$

compared to $\alpha_{\overline{\text{MS}}}^{(5)}(M_Z) = 0.1174(16)$ of the older PDG 2018 [11]. For a general overview of the various phenomenological and lattice approaches see, e.g., Ref. [12]. The extraction of α_s from τ data, which is one of the most precise and thus has a large impact on the nonlattice average in Eq. (319), is especially sensitive to the treatment of higher-order perturbative terms as well as the treatment of nonperturbative effects. This is important to keep in mind when comparing our chosen range for $\alpha_{\overline{\text{MS}}}^{(5)}(M_Z)$ from lattice determinations in Eq. (396) with the nonlattice average from the PDG.

9.1.1 Scheme and scale dependence of α_s and Λ_{QCD}

Despite the fact that the notion of the QCD coupling is initially a perturbative concept, the associated Λ parameter is nonperturbatively defined

$$\begin{aligned} \Lambda &\equiv \mu \varphi_s(\bar{g}_s(\mu)), \\ \varphi_s(\bar{g}_s) &= (b_0 \bar{g}_s^2)^{-b_1/(2b_0^2)} e^{-1/(2b_0 \bar{g}_s^2)} \exp \left[- \int_0^{\bar{g}_s} dx \left(\frac{1}{\beta(x)} + \frac{1}{b_0 x^3} - \frac{b_1}{b_0^2 x} \right) \right], \end{aligned} \quad (320)$$

where $\beta(\bar{g}_s) = \mu \frac{\partial \bar{g}_s(\mu)}{\partial \mu}$ is the full renormalization group function in the scheme which defines \bar{g}_s , and b_0 and b_1 are the first two scheme-independent coefficients of the perturbative expansion

$$\beta(x) \sim -b_0 x^3 - b_1 x^5 + \dots, \quad (321)$$

with

$$b_0 = \frac{1}{(4\pi)^2} \left(11 - \frac{2}{3}N_f \right), \quad b_1 = \frac{1}{(4\pi)^4} \left(102 - \frac{38}{3}N_f \right). \quad (322)$$

Thus the Λ parameter is renormalization-scheme-dependent but in an exactly computable way, and lattice gauge theory is an ideal method to relate it to the low-energy properties of QCD. In the $\overline{\text{MS}}$ scheme presently b_{n_l} up to $n_l = 4$ are known [13–17].

The change in the coupling from one scheme S to another (taken here to be the $\overline{\text{MS}}$ scheme) is perturbative,

$$g_{\overline{\text{MS}}}^2(\mu) = g_S^2(\mu)(1 + c_g^{(1)}g_S^2(\mu) + \dots), \quad (323)$$

where $c_g^{(i)}$, $i \geq 1$ are finite renormalization coefficients. The scale μ must be taken high enough for the error in keeping only the first few terms in the expansion to be small. On the other hand, the conversion to the Λ parameter in the $\overline{\text{MS}}$ scheme is given exactly by

$$\Lambda_{\overline{\text{MS}}} = \Lambda_S \exp \left[c_g^{(1)}/(2b_0) \right]. \quad (324)$$

The fact that $\Lambda_{\overline{\text{MS}}}$ can be obtained exactly from Λ_S in any scheme S where $c_g^{(1)}$ is known together with the high-order knowledge (5-loop by now) of $\beta_{\overline{\text{MS}}}$ means that the errors in $\alpha_{\overline{\text{MS}}}(m_Z)$ are dominantly due to the errors of Λ_S . We will therefore mostly discuss them in that way. Starting from Eq. (320), we have to consider (i) the error of $\bar{g}_S^2(\mu)$ (denoted as $(\frac{\Delta\Lambda}{\Lambda})_{\Delta\alpha_S}$) and (ii) the truncation error in β_S (denoted as $(\frac{\Delta\Lambda}{\Lambda})_{\text{trunc}}$). Concerning (ii), note that knowledge of $c_g^{(n_l)}$ for the scheme S means that β_S is known to $n_l + 1$ loop order; b_{n_l} is known. We thus see that in the region where perturbation theory can be applied, the following errors of Λ_S (or consequently $\Lambda_{\overline{\text{MS}}}$) have to be considered

$$\left(\frac{\Delta\Lambda}{\Lambda} \right)_{\Delta\alpha_S} = \frac{\Delta\alpha_S(\mu)}{8\pi b_0 \alpha_S^2(\mu)} \times [1 + \mathcal{O}(\alpha_S(\mu))], \quad (325)$$

$$\left(\frac{\Delta\Lambda}{\Lambda} \right)_{\text{trunc}} = k\alpha_S^{n_l}(\mu) + \mathcal{O}(\alpha_S^{n_l+1}(\mu)), \quad (326)$$

where k depends on b_{n_l+1} and in typical good schemes such as $\overline{\text{MS}}$ it is numerically of order one. Statistical and systematic errors such as discretization effects contribute to $\Delta\alpha_S(\mu)$. In the above we dropped a scheme subscript for the Λ -parameters because of Eq. (324).

By convention $\alpha_{\overline{\text{MS}}}$ is usually quoted at a scale $\mu = M_Z$ where the appropriate effective coupling is the one in the 5-flavour theory: $\alpha_{\overline{\text{MS}}}^{(5)}(M_Z)$. In order to obtain it from a result with fewer flavours, one connects effective theories with different number of flavours as discussed by Bernreuther and Wetzel [18]. For example, one considers the $\overline{\text{MS}}$ scheme, matches the 3-flavour theory to the 4-flavour theory at a scale given by the charm-quark mass [19–21], runs with the 5-loop β -function [13–17] of the 4-flavour theory to a scale given by the b -quark mass, and there matches to the 5-flavour theory, after which one runs up to $\mu = M_Z$ with the 5-loop β function. For the matching relation at a given quark threshold we use the mass m_\star which satisfies $m_\star = \bar{m}_{\overline{\text{MS}}}(m_\star)$, where \bar{m} is the running mass (analogous to the running coupling). Then

$$\bar{g}_{N_f-1}^2(m_\star) = \bar{g}_{N_f}^2(m_\star) \times [1 + 0 \times \bar{g}_{N_f}^2(m_\star) + \sum_{n \geq 2} t_n \bar{g}_{N_f}^{2n}(m_\star)] \quad (327)$$

with [19, 21, 22]

$$t_2 = \frac{1}{(4\pi^2)^2} \frac{11}{72}, \quad (328)$$

$$t_3 = \frac{1}{(4\pi^2)^3} \left[-\frac{82043}{27648} \zeta_3 + \frac{564731}{124416} - \frac{2633}{31104} (N_f - 1) \right], \quad (329)$$

$$t_4 = \frac{1}{(4\pi^2)^4} [5.170347 - 1.009932(N_f - 1) - 0.021978(N_f - 1)^2], \quad (330)$$

(where ζ_3 is the Riemann zeta-function) provides the matching at the thresholds in the $\overline{\text{MS}}$ scheme. Often the package `RunDec` is used for quark-threshold matching and running in the $\overline{\text{MS}}$ -scheme [23, 24].

While t_2, t_3, t_4 are numerically small coefficients, the charm-threshold scale is also relatively low and so there are nonperturbative uncertainties in the matching procedure, which are difficult to estimate but which we assume here to be negligible. Obviously there is no perturbative matching formula across the strange “threshold”; here matching is entirely non-perturbative. Model dependent extrapolations of $\bar{g}_{N_f}^2$ from $N_f = 0, 2$ to $N_f = 3$ were done in the early days of lattice gauge theory. We will include these in our listings of results but not in our estimates, since such extrapolations are based on untestable assumptions.

9.1.2 Overview of the review of α_s

We begin by explaining lattice-specific difficulties in Sec. 9.2.1 and the FLAG criteria designed to assess whether the associated systematic uncertainties can be controlled and estimated in a reasonable manner. These criteria are taken over unchanged from the FLAG 19 report, as there has not yet been sufficiently broad progress to make these criteria more stringent. We would also like to point to a recent review [25] of lattice methodology and systematic uncertainties for α_s . There, a systematic scale variation is advocated to assess systematic errors due to the truncation of the perturbative series and such a procedure may indeed be incorporated into future FLAG criteria, as it can be applied without change to most lattice approaches.

We then discuss, in Sec. 9.3 – Sec. 9.9, the various lattice approaches and results from calculations with $N_f = 0, 2, 2+1$, and $2+1+1$ flavours.

Besides new results and upgrades of previous works, a new strategy of nonperturbative renormalization by decoupling has been proposed by the ALPHA collaboration [26], which shifts the perspective on results with unphysical flavour numbers, in particular for $N_f = 0$. As these can be nonperturbatively related to $N_f > 0$ results by a nonperturbative matching calculation, it becomes very important to obtain precise and controlled $N_f = 0$ results, with obvious implications for this and future FLAG reports. A short account of the decoupling strategy is given in Sec. 9.4.

In Sec. 9.11, we present averages together with our best estimates for $\alpha_{\overline{\text{MS}}}^{(5)}$. These are currently determined from 3- and 4-flavour QCD simulations only, however, in the near future the decoupling strategy is expected to link e.g. 3-flavour simulations with the pure gauge theory simulations. Therefore, for the Λ parameter, we also give results for other numbers of flavours, including $N_f = 0$ and $N_f = 2$.

9.1.3 Additions with respect to the FLAG 19 report

The additional papers since the FLAG 19 report are:

Dalla Brida 19 [27] and Nada 20 [28] from step-scaling methods (Sec. 9.3).

ALPHA 19A [26] from the decoupling method (Sec. 9.4).

TUMQCD 19 [29] and Ayala 20 [30] and Husung 20 [31] from the static quark potential (Sec. 9.5).

Cali 20 [32] from (light-quark) vacuum polarization in position space (Sec. 9.6).

Petreczky 20 [33], Petreczky 19 [34], and Boito 20 [35, 36] from heavy-quark current two-point functions (Sec. 9.8).

Zafeiropoulos 19 [37] from QCD vertices (Sec. 9.9).

9.2 General issues

9.2.1 Discussion of criteria for computations entering the averages

As in the PDG review, we only use calculations of α_s published in peer-reviewed journals, and that use NNLO or higher-order perturbative expansions, to obtain our final range in Sec. 9.11. We also, however, introduce further criteria designed to assess the ability to control important systematics, which we describe here. Some of these criteria, e.g., that for the continuum extrapolation, are associated with lattice-specific systematics and have no continuum analogue. Other criteria, e.g., that for the renormalization scale, could in principle be applied to nonlattice determinations. Expecting that lattice calculations will continue to improve significantly in the near future, our goal in reviewing the state-of-the-art here is to be conservative and avoid prematurely choosing an overly small range.

In lattice calculations, we generally take \mathcal{Q} to be some combination of physical amplitudes or Euclidean correlation functions which are free from UV and IR divergences and have a well-defined continuum limit. Examples include the force between static quarks and two-point functions of quark-bilinear currents.

In comparison to values of observables \mathcal{Q} determined experimentally, those from lattice calculations require two more steps. The first step concerns setting the scale μ in GeV, where one needs to use some experimentally measurable low-energy scale as input. Ideally one employs a hadron mass. Alternatively convenient intermediate scales such as $\sqrt{t_0}$, w_0 , r_0 , r_1 , [38–41] can be used if their relation to an experimental dimensionful observable is established. The low-energy scale needs to be computed at the same bare parameters where \mathcal{Q} is determined, at least as long as one does not use the step-scaling method (see below). This induces a practical difficulty given present computing resources. In the determination of the low-energy reference scale the volume needs to be large enough to avoid finite-size effects. On the other hand, in order for the perturbative expansion of Eq. (318) to be reliable, one has to reach sufficiently high values of μ , i.e., short enough distances. To avoid uncontrollable discretization effects the lattice spacing a has to be accordingly small. This means

$$L \gg \text{hadron size} \sim \Lambda_{\text{QCD}}^{-1} \quad \text{and} \quad 1/a \gg \mu, \quad (331)$$

(where L is the box size) and therefore

$$L/a \ggg \mu/\Lambda_{\text{QCD}}. \quad (332)$$

The currently available computer power, however, limits L/a , typically to $L/a = 32 - 96$. Unless one accepts compromises in controlling discretization errors or finite-size effects, this means one needs to set the scale μ according to

$$\mu \lll L/a \times \Lambda_{\text{QCD}} \sim 10 - 30 \text{ GeV}. \quad (333)$$

(Here \lll or \ggg means at least one order of magnitude smaller or larger.) Therefore, μ can be $1 - 3 \text{ GeV}$ at most. This raises the concern whether the asymptotic perturbative expansion truncated at 1-loop, 2-loop, or 3-loop in Eq. (318) is sufficiently accurate. There is a finite-size scaling method, usually called step-scaling method, which solves this problem by identifying $\mu = 1/L$ in the definition of $\mathcal{Q}(\mu)$, see Sec. 9.3.

For the second step after setting the scale μ in physical units (GeV), one should compute \mathcal{Q} on the lattice, $\mathcal{Q}_{\text{lat}}(a, \mu)$ for several lattice spacings and take the continuum limit to obtain the left hand side of Eq. (318) as

$$\mathcal{Q}(\mu) \equiv \lim_{a \rightarrow 0} \mathcal{Q}_{\text{lat}}(a, \mu) \text{ with } \mu \text{ fixed}. \quad (334)$$

This is necessary to remove the discretization error.

Here it is assumed that the quantity \mathcal{Q} has a continuum limit, which is regularization-independent. The method discussed in Sec. 9.7, which is based on the perturbative expansion of a lattice-regulated, divergent short-distance quantity $W_{\text{lat}}(a)$ differs in this respect and must be treated separately.

In summary, a controlled determination of α_s needs to satisfy the following:

1. The determination of α_s is based on a comparison of a short-distance quantity \mathcal{Q} at scale μ with a well-defined continuum limit without UV and IR divergences to a perturbative expansion formula in Eq. (318).
2. The scale μ is large enough so that the perturbative expansion in Eq. (318) is precise to the order at which it is truncated, i.e., it has good *asymptotic* convergence.
3. If \mathcal{Q} is defined by physical quantities in infinite volume, one needs to satisfy Eq. (332).

Nonuniversal quantities need a separate discussion, see Sec. 9.7.

Conditions 2. and 3. give approximate lower and upper bounds for μ respectively. It is important to see whether there is a window to satisfy 2. and 3. at the same time. If it exists, it remains to examine whether a particular lattice calculation is done inside the window or not.

Obviously, an important issue for the reliability of a calculation is whether the scale μ that can be reached lies in a regime where perturbation theory can be applied with confidence. However, the value of μ does not provide an unambiguous criterion. For instance, the Schrödinger Functional, or SF-coupling (Sec. 9.3) is conventionally taken at the scale $\mu = 1/L$, but one could also choose $\mu = 2/L$. Instead of μ we therefore define an effective α_{eff} . For schemes such as SF (see Sec. 9.3) or qq (see Sec. 9.5) this is directly the coupling

of the scheme. For other schemes such as the vacuum polarization we use the perturbative expansion Eq. (318) for the observable \mathcal{Q} to define

$$\alpha_{\text{eff}} = \mathcal{Q}/c_1. \quad (335)$$

If there is an α_s -independent term it should first be subtracted. Note that this is nothing but defining an effective, regularization-independent coupling, a physical renormalization scheme.

Let us now comment further on the use of the perturbative series. Since it is only an asymptotic expansion, the remainder $R_n(\mathcal{Q}) = \mathcal{Q} - \sum_{i \leq n} c_i \alpha_s^i$ of a truncated perturbative expression $\mathcal{Q} \sim \sum_{i \leq n} c_i \alpha_s^i$ cannot just be estimated as a perturbative error $k \alpha_s^{n+1}$. The error is nonperturbative. Often one speaks of “nonperturbative contributions”, but nonperturbative and perturbative cannot be strictly separated due to the asymptotic nature of the series (see, e.g., Ref. [42]).

Still, we do have some general ideas concerning the size of nonperturbative effects. The known ones such as instantons or renormalons decay for large μ like inverse powers of μ and are thus roughly of the form

$$\exp(-\gamma/\alpha_s), \quad (336)$$

with some positive constant γ . Thus we have, loosely speaking,

$$\mathcal{Q} = c_1 \alpha_s + c_2 \alpha_s^2 + \dots + c_n \alpha_s^n + \mathcal{O}(\alpha_s^{n+1}) + \mathcal{O}(\exp(-\gamma/\alpha_s)). \quad (337)$$

For small α_s , the $\exp(-\gamma/\alpha_s)$ is negligible. Similarly the perturbative estimate for the magnitude of relative errors in Eq. (337) is small; as an illustration for $n = 3$ and $\alpha_s = 0.2$ the relative error is $\sim 0.8\%$ (assuming coefficients $|c_{n+1}/c_1| \sim 1$).

For larger values of α_s nonperturbative effects can become significant in Eq. (337). An instructive example comes from the values obtained from τ decays, for which $\alpha_s \approx 0.3$. Here, different applications of perturbation theory (fixed order and contour improved) each look reasonably asymptotically convergent² but the difference does not seem to decrease much with the order (see, e.g., the contribution of Pich in Ref. [44]). In addition nonperturbative terms in the spectral function may be nonnegligible even after the integration up to m_τ (see, e.g., Refs. [45], [46]). All of this is because α_s is not really small.

Since the size of the nonperturbative effects is very hard to estimate one should try to avoid such regions of the coupling. In a fully controlled computation one would like to verify the perturbative behaviour by changing α_s over a significant range instead of estimating the errors as $\sim \alpha_s^{n+1}$. Some computations try to take nonperturbative power ‘corrections’ to the perturbative series into account by including such terms in a fit to the μ -dependence. We note that this is a delicate procedure, both because the separation of nonperturbative and perturbative is theoretically not well defined and because in practice a term like, e.g., $\alpha_s(\mu)^3$ is hard to distinguish from a $1/\mu^2$ term when the μ -range is restricted and statistical and systematic errors are present. We consider it safer to restrict the fit range to the region where the power corrections are negligible compared to the estimated perturbative error.

The above considerations lead us to the following special criteria for the determination of α_s :

- Renormalization scale

²See, however, the recent discussion in [43].

- ★ all points relevant in the analysis have $\alpha_{\text{eff}} < 0.2$
 - all points have $\alpha_{\text{eff}} < 0.4$ and at least one $\alpha_{\text{eff}} \leq 0.25$
 - otherwise
- Perturbative behaviour
 - ★ verified over a range of a factor 4 change in $\alpha_{\text{eff}}^{n_1}$ without power corrections or alternatively $\alpha_{\text{eff}}^{n_1} \leq \frac{1}{2}\Delta\alpha_{\text{eff}}/(8\pi b_0\alpha_{\text{eff}}^2)$ is reached
 - agreement with perturbation theory over a range of a factor $(3/2)^2$ in $\alpha_{\text{eff}}^{n_1}$ possibly fitting with power corrections or alternatively $\alpha_{\text{eff}}^{n_1} \leq \Delta\alpha_{\text{eff}}/(8\pi b_0\alpha_{\text{eff}}^2)$ is reached
 - otherwise

Here $\Delta\alpha_{\text{eff}}$ is the accuracy cited for the determination of α_{eff} and n_1 is the loop order to which the connection of α_{eff} to the $\overline{\text{MS}}$ scheme is known. Recall the discussion around Eqs. (325,326); the β -function of α_{eff} is then known to $n_1 + 1$ loop order.³

- Continuum extrapolation

At a reference point of $\alpha_{\text{eff}} = 0.3$ (or less) we require

- ★ three lattice spacings with $\mu a < 1/2$ and full $\mathcal{O}(a)$ improvement, or three lattice spacings with $\mu a \leq 1/4$ and 2-loop $\mathcal{O}(a)$ improvement, or $\mu a \leq 1/8$ and 1-loop $\mathcal{O}(a)$ improvement
- three lattice spacings with $\mu a < 3/2$ reaching down to $\mu a = 1$ and full $\mathcal{O}(a)$ improvement, or three lattice spacings with $\mu a \leq 1/4$ and 1-loop $\mathcal{O}(a)$ improvement
- otherwise

We also need to specify what is meant by μ . Here are our choices:

$$\begin{aligned}
 \text{step-scaling} & : \mu = 1/L, \\
 \text{heavy quark-antiquark potential} & : \mu = 2/r, \\
 \text{observables in position space} & : \mu = 1/|x|, \\
 \text{observables in momentum space} & : \mu = q, \\
 \text{moments of heavy-quark currents} & : \mu = 2\bar{m}_c, \\
 \text{eigenvalues of the Dirac operator} & : \mu = \lambda_{\overline{\text{MS}}}
 \end{aligned} \tag{338}$$

where $|x|$ is the Euclidean norm of the 4-vector x , q is the magnitude of the momentum, \bar{m}_c is the heavy-quark mass (in the $\overline{\text{MS}}$ scheme) and usually taken around the charm-quark mass and $\lambda_{\overline{\text{MS}}}$ is the eigenvalue of the Dirac operator, see Sec. 9.10. We note again that the above criteria cannot be applied when regularization dependent quantities $W_{\text{lat}}(a)$ are used instead of $\mathcal{Q}(\mu)$. These cases are specifically discussed in Sec. 9.7.

³Once one is in the perturbative region with α_{eff} , the error in extracting the Λ parameter due to the truncation of perturbation theory scales like $\alpha_{\text{eff}}^{n_1}$, as discussed around Eq. (326). In order to detect/control such corrections properly, one needs to change the correction term significantly; we require a factor of four for a ★ and a factor $(3/2)^2$ for a ○. An exception to the above is the situation where the correction terms are small anyway, i.e., $\alpha_{\text{eff}}^{n_1} \approx (\Delta\Lambda/\Lambda)_{\text{trunc}} < (\Delta\Lambda/\Lambda)_{\Delta\alpha} \approx \Delta\alpha_{\text{eff}}/(8\pi b_0\alpha_{\text{eff}}^2)$ is reached.

In principle one should also account for electro-weak radiative corrections. However, both in the determination of α_s at intermediate scales μ and in the running to high scales, we expect electro-weak effects to be much smaller than the presently reached precision. Such effects are therefore not further discussed.

The attentive reader will have noticed that bounds such as $\mu a < 3/2$ or at least one value of $\alpha_{\text{eff}} \leq 0.25$ which we require for a \circ are not very stringent. There is a considerable difference between \circ and \star . We have chosen the above bounds, unchanged as compared to FLAG 16 and FLAG 19, since not too many computations would satisfy more stringent ones at present. Nevertheless, we believe that the \circ criteria already give reasonable bases for estimates of systematic errors. An exception may be Cal3 20, which is discussed in detail in Sec. 9.6. In the future, we expect that we will be able to tighten our criteria for inclusion in the average, and that many more computations will reach the present \star rating in one or more categories.

In addition to our explicit criteria, the following effects may influence the precision of results:

Topology sampling: In principle a good way to improve the quality of determinations of α_s is to push to very small lattice spacings thus enabling large μ . It is known that the sampling of field space becomes very difficult for the HMC algorithm when the lattice spacing is small and one has the standard periodic boundary conditions. In practice, for all known discretizations the topological charge slows down dramatically for $a \approx 0.05$ fm and smaller [47–53]. Open boundary conditions solve the problem [54] but are not frequently used. Since the effect of the freezing on short distance observables is not known, we also do need to pay attention to this issue. Remarks are added in the text when appropriate.

Quark-mass effects: We assume that effects of the finite masses of the light quarks (including strange) are negligible in the effective coupling itself where large, perturbative, μ is considered.

Scale setting: The scale does not need to be very precise, since using the lowest-order β -function shows that a 3% error in the scale determination corresponds to a $\sim 0.5\%$ error in $\alpha_s(M_Z)$. As long as systematic errors from chiral extrapolation and finite-volume effects are well below 3% we do not need to be concerned about those at the present level of precision in $\alpha_s(M_Z)$. This may change in the future.

9.2.2 Physical scale

Since FLAG 19, a new FLAG working group on scale setting has been established. We refer to Sec. 11 for definitions and the current status. Note that the error from scale setting is sub-dominant for current α_s determinations.

A popular scale choice has been the intermediate r_0 scale, and its variant r_1 , which both derive from the force between static quarks, see Eq.(358). One should bear in mind that their determination from physical observables also has to be taken into account. The phenomenological value of r_0 was originally determined as $r_0 \approx 0.49$ fm through potential models describing quarkonia [40]. Of course the quantity is precisely defined, independently of such model considerations. But a lattice computation with the correct sea-quark content is needed to determine a completely sharp value. When the quark content is not quite realistic, the value of r_0 may depend to some extent on which experimental input is used to determine (actually define) it.

The latest determinations from two-flavour QCD are $r_0 = 0.420(14)\text{--}0.450(14)$ fm by the

ETM collaboration [55, 56], using as input f_π and f_K and carrying out various continuum extrapolations. On the other hand, the ALPHA collaboration [57] determined $r_0 = 0.503(10)$ fm with input from f_K , and the QCDSF collaboration [58] cites $0.501(10)(11)$ fm from the mass of the nucleon (no continuum limit). Recent determinations from three-flavour QCD are consistent with $r_1 = 0.313(3)$ fm and $r_0 = 0.472(5)$ fm [59–61]. Due to the uncertainty in these estimates, and as many results are based directly on r_0 to set the scale, we shall often give both the dimensionless number $r_0\Lambda_{\overline{\text{MS}}}$, as well as $\Lambda_{\overline{\text{MS}}}$. In the cases where no physical r_0 scale is given in the original papers or we convert to the r_0 scale, we use the value $r_0 = 0.472$ fm. In case $r_1\Lambda_{\overline{\text{MS}}}$ is given in the publications, we use $r_0/r_1 = 1.508$ [61], to convert, which remains well consistent with the update [52] neglecting the error on this ratio. In some, mostly early, computations the string tension, $\sqrt{\sigma}$ was used. We convert to r_0 using $r_0^2\sigma = 1.65 - \pi/12$, which has been shown to be an excellent approximation in the relevant pure gauge theory [62, 63].

The new scales t_0, w_0 based on the gradient flow are very attractive alternatives to r_0 but their discretization errors are still under discussion [64–67] and their values at the physical point are not yet determined with great precision. We remain with r_0 as our main reference scale for now. A general discussion of the various scales is given in [68] and in the scale-setting section of this FLAG report, cf. Sec. 11.

9.2.3 Studies of truncation errors of perturbation theory

As discussed previously, we have to determine α_s in a region where the perturbative expansion for the β -function, Eq. (321) in the integral Eq. (320), is reliable. In principle this must be checked, however, this is difficult to achieve as we need to reach up to a sufficiently high scale. A frequently used recipe to estimate the size of truncation errors of the perturbative series is to vary the renormalization-scale dependence around the chosen ‘optimal’ scale μ_* , of an observable evaluated at a fixed order in the coupling from $\mu = \mu_*/2$ to $2\mu_*$. For examples, see Ref. [25].

Alternatively, or in addition, the renormalization scheme chosen can be varied, which investigates the perturbative conversion of the chosen scheme to the perturbatively defined $\overline{\text{MS}}$ scheme and in particular ‘fastest apparent convergence’ when the ‘optimal’ scale is chosen so that the $\mathcal{O}(\alpha_s^2)$ coefficient vanishes.

The ALPHA collaboration in Ref. [69] and ALPHA 17 [70], within the SF approach defined a set of ν -schemes for which the 3-loop (scheme-dependent) coefficient of the β -function for $N_f = 2 + 1$ flavours was computed to be $b_2^\nu = -(0.064(27) + 1.259(1)\nu)/(4\pi)^3$. The standard SF scheme has $\nu = 0$. For comparison, $b_2^{\overline{\text{MS}}} = 0.324/(4\pi)^3$. A range of scales from about 4 GeV to 128 GeV was investigated. It was found that while the procedure of varying the scale by a factor 2 up and down gave a correct estimate of the residual perturbative error for $\nu \approx 0 \dots 0.3$, for negative values, e.g., $\nu = -0.5$, the estimated perturbative error is much too small to account for the mismatch in the Λ -parameter of $\approx 8\%$ at $\alpha_s = 0.15$. This mismatch, however, did, as expected, still scale with $\alpha_s^{n_l}$ with $n_l = 2$. In the schemes with negative ν , the coupling α_s has to be quite small for scale-variations of a factor 2 to correctly signal the perturbative errors.

For a systematic study of renormalization scale variations as a measure of perturbative truncation errors in various lattice determinations of α_s we refer to the recent review by Del Debbio and Ramos [25].

9.3 α_s from Step-Scaling Methods

9.3.1 General considerations

The method of step-scaling functions avoids the scale problem, Eq. (331). It is in principle independent of the particular boundary conditions used and was first developed with periodic boundary conditions in a two-dimensional model [71].

The essential idea of the step-scaling strategy is to split the determination of the running coupling at large μ and of a hadronic scale into two lattice calculations and connect them by ‘step-scaling’. In the former part, we determine the running coupling constant in a finite-volume scheme in which the renormalization scale is set by the inverse lattice size $\mu = 1/L$. In this calculation, one takes a high renormalization scale while keeping the lattice spacing sufficiently small as

$$\mu \equiv 1/L \sim 10 \dots 100 \text{ GeV}, \quad a/L \ll 1. \quad (339)$$

In the latter part, one chooses a certain $\bar{g}_{\text{max}}^2 = \bar{g}^2(1/L_{\text{max}})$, typically such that L_{max} is around 0.5–1 fm. With a common discretization, one then determines L_{max}/a and (in a large volume $L \geq 2\text{--}3$ fm) a hadronic scale such as a hadron mass, $\sqrt{t_0}/a$ or r_0/a at the same bare parameters. In this way one gets numbers for, e.g., L_{max}/r_0 and by changing the lattice spacing a carries out a continuum limit extrapolation of that ratio.

In order to connect $\bar{g}^2(1/L_{\text{max}})$ to $\bar{g}^2(\mu)$ at high μ , one determines the change of the coupling in the continuum limit when the scale changes from L to L/s , starting from $L = L_{\text{max}}$ and arriving at $\mu = s^k/L_{\text{max}}$. This part of the strategy is called step-scaling. Combining these results yields $\bar{g}^2(\mu)$ at $\mu = s^k (r_0/L_{\text{max}}) r_0^{-1}$, where r_0 stands for the particular chosen hadronic scale. Most applications use a scale factor $s = 2$.

At present most applications in QCD use Schrödinger functional boundary conditions [72, 73] and we discuss this below in a little more detail. (However, other boundary conditions are also possible, such as twisted boundary conditions and the discussion also applies to them.) An important reason is that these boundary conditions avoid zero modes for the quark fields and quartic modes [74] in the perturbative expansion in the gauge fields. Furthermore the corresponding renormalization scheme is well studied in perturbation theory [75–77] with the 3-loop β -function and 2-loop cutoff effects (for the standard Wilson regularization) known.

In order to have a perturbatively well-defined scheme, the SF scheme uses Dirichlet boundary conditions at time $t = 0$ and $t = T$. These break translation invariance and permit $\mathcal{O}(a)$ counter terms at the boundary through quantum corrections. Therefore, the leading discretization error is $\mathcal{O}(a)$. Improving the lattice action is achieved by adding counter terms at the boundaries whose coefficients are denoted as c_t, \tilde{c}_t . In practice, these coefficients are computed with 1-loop or 2-loop perturbative accuracy. A better precision in this step yields a better control over discretization errors, which is important, as can be seen, e.g., in Refs. [62, 78].

Also computations with Dirichlet boundary conditions do in principle suffer from the insufficient change of topology in the HMC algorithm at small lattice spacing. However, in a small volume the weight of nonzero charge sectors in the path integral is exponentially suppressed [79]⁴ and in a Monte Carlo run of typical length very few configurations with nontrivial topology should appear. Considering the issue quantitatively Ref. [80] finds a

⁴We simplify here and assume that the classical solution associated with the used boundary conditions has charge zero. In practice this is the case.

strong suppression below $L \approx 0.8$ fm. Therefore the lack of topology change of the HMC is not a serious issue for the high energy regime in step-scaling studies. However, the matching to hadronic observables requires volumes where the problem cannot be ignored. Therefore, Ref. [81] includes a projection to zero topology into the *definition* of the coupling. We note also that a mix of Dirichlet and open boundary conditions is expected to remove the topology issue entirely [82] and may be considered in the future.

Apart from the boundary conditions, the very definition of the coupling needs to be chosen. We briefly discuss in turn, the two schemes used at present, namely, the ‘Schrödinger Functional’ (SF) and ‘Gradient Flow’ (GF) schemes.

The SF scheme is the first one, which was used in step-scaling studies in gauge theories [72]. Inhomogeneous Dirichlet boundary conditions are imposed in time,

$$A_k(x)|_{x_0=0} = C_k, \quad A_k(x)|_{x_0=L} = C'_k, \quad (340)$$

for $k = 1, 2, 3$. Periodic boundary conditions (up to a phase for the fermion fields) with period L are imposed in space. The matrices

$$\begin{aligned} LC_k &= i \operatorname{diag}(\eta - \pi/3, -\eta/2, -\eta/2 + \pi/3), \\ LC'_k &= i \operatorname{diag}(-(\eta + \pi), \eta/2 + \pi/3, \eta/2 + 2\pi/3), \end{aligned}$$

just depend on the dimensionless parameter η . The coupling \bar{g}_{SF} is obtained from the η -derivative of the effective action,

$$\langle \partial_\eta S |_{\eta=0} \rangle = \frac{12\pi}{\bar{g}_{\text{SF}}^2}. \quad (341)$$

For this scheme, the finite $c_g^{(i)}$, Eq. (323), are known for $i = 1, 2$ [76, 77].

More recently, gradient-flow couplings have been used frequently because of their small statistical errors at large couplings (in contrast to \bar{g}_{SF} , which has small statistical errors at small couplings). The gradient flow is introduced as follows [38, 83]. Consider the flow gauge field $B_\mu(t, x)$ with the flow time t , which is a one parameter deformation of the bare gauge field $A_\mu(x)$, where $B_\mu(t, x)$ is the solution to the gradient-flow equation

$$\begin{aligned} \partial_t B_\mu(t, x) &= D_\nu G_{\nu\mu}(t, x), \\ G_{\mu\nu} &= \partial_\mu B_\nu - \partial_\nu B_\mu + [B_\mu, B_\nu], \end{aligned} \quad (342)$$

with initial condition $B_\mu(0, x) = A_\mu(x)$. The renormalized coupling is defined by [38]

$$\bar{g}_{\text{GF}}^2(\mu) = \mathcal{N} t^2 \langle E(t, x) \rangle |_{\mu=1/\sqrt{8t}}, \quad (343)$$

with $\mathcal{N} = 16\pi^2/3 + \mathcal{O}((a/L)^2)$ and where $E(t, x)$ is the action density given by

$$E(t, x) = \frac{1}{4} G_{\mu\nu}^a(t, x) G_{\mu\nu}^a(t, x). \quad (344)$$

In a finite volume, one needs to specify additional conditions. In order not to introduce two independent scales one sets

$$\sqrt{8t} = cL, \quad (345)$$

for some fixed number c [84]. Schrödinger functional boundary conditions [85] or twisted boundary conditions [86, 87] have been employed. Matching of the GF coupling to the $\overline{\text{MS}}$ -scheme coupling is known to 1-loop for twisted boundary conditions with zero quark flavours and $SU(3)$ group [87] and to 2-loop with SF boundary conditions with zero quark flavours [88]. The former is based on a MC evaluation at small couplings⁵ and the latter on numerical stochastic perturbation theory.

9.3.2 Discussion of computations

In Tab. 60 we give results from various determinations of the Λ parameter. For a clear assessment of the N_f -dependence, the last column also shows results that refer to a common hadronic scale, r_0 . As discussed above, the renormalization scale can be chosen large enough such that $\alpha_s < 0.2$ and the perturbative behaviour can be verified. Consequently only \star is present for these criteria except for early work where the $n_l = 2$ loop correction to $\overline{\text{MS}}$ was not yet known and we assigned a \blacksquare concerning the renormalization scale. With dynamical fermions, results for the step-scaling functions are always available for at least $a/L = \mu a = 1/4, 1/6, 1/8$. All calculations have a nonperturbatively $\mathcal{O}(a)$ improved action in the bulk. For the discussed boundary $\mathcal{O}(a)$ terms this is not so. In most recent calculations 2-loop $\mathcal{O}(a)$ improvement is employed together with at least three lattice spacings.⁶ This means a \star for the continuum extrapolation. In other computations only 1-loop c_t was available and we arrive at \circ . We note that the discretization errors in the step-scaling functions of the SF coupling are usually found to be very small, at the percent level or below. However, the overall desired precision is very high as well, and the results in CP-PACS 04 [78] show that discretization errors at the below percent level cannot be taken for granted. In particular with staggered fermions (unimproved except for boundary terms) few percent effects are seen in Perez 10 [91].

In the work by PACS-CS 09A [93], the continuum extrapolation in the scale setting is performed using a constant function in a and with a linear function. Potentially the former leaves a considerable residual discretization error. We here use, as discussed with the collaboration, the continuum extrapolation linear in a , as given in the second line of PACS-CS 09A [93] results in Tab. 60. After perturbative conversion from a three-flavour result to five flavours (see Sec. 9.2.1), they obtain

$$\alpha_{\overline{\text{MS}}}^{(5)}(M_Z) = 0.118(3). \quad (346)$$

In Ref. [92], the ALPHA collaboration determined $\Lambda_{\overline{\text{MS}}}^{(3)}$ combining step-scaling in \bar{g}_{GF}^2 in the lower scale region $\mu_{\text{had}} \leq \mu \leq \mu_0$, and step-scaling in \bar{g}_{SF}^2 for higher scales $\mu_0 \leq \mu \leq \mu_{\text{PT}}$. Both schemes are defined with SF boundary conditions. For \bar{g}_{GF}^2 a projection to the sector of zero topological charge is included, Eq. (344) is restricted to the magnetic components, and $c = 0.3$. The scales μ_{had} , μ_0 , and μ_{PT} are defined by $\bar{g}_{\text{GF}}^2(\mu_{\text{had}}) = 11.3$, $\bar{g}_{\text{SF}}^2(\mu_0) = 2.012$, and $\mu_{\text{PT}} = 16\mu_0$ which are roughly estimated as

$$1/L_{\text{max}} \equiv \mu_{\text{had}} \approx 0.2 \text{ GeV}, \quad \mu_0 \approx 4 \text{ GeV}, \quad \mu_{\text{PT}} \approx 70 \text{ GeV}. \quad (347)$$

⁵For a variant of the twisted periodic finite volume scheme the 1-loop matching has been computed analytically [89].

⁶With 2-loop $\mathcal{O}(a)$ improvement we here mean c_t including the g_0^4 term and \tilde{c}_t with the g_0^2 term. For gluonic observables such as the running coupling this is sufficient for cutoff effects being suppressed to $\mathcal{O}(g^6 a)$.

Collaboration	Ref.	N_f	publication status	renormalization scale	perturbative behaviour	continuum extrapolation	scale	$\Lambda_{\overline{\text{MS}}}[\text{MeV}]$	$r_0\Lambda_{\overline{\text{MS}}}$
ALPHA 10A	[90]	4	A	★	★	★	only running of α_s in Fig. 4		
Perez 10	[91]	4	C	★	★	○	only step-scaling function in Fig. 4		
ALPHA 17	[92]	2+1	A	★	★	★	$\sqrt{8t_0} = 0.415 \text{ fm}$	341(12)	0.816(29)
PACS-CS 09A	[93]	2+1	A	★	★	○	m_ρ	371(13)(8)($^{+0}_{-27}$) [#]	0.888(30)(18)($^{+0}_{-65}$) [†]
			A	★	★	○	m_ρ	345(59) ^{##}	0.824(141) [†]
ALPHA 12*	[57]	2	A	★	★	★	f_K	310(20)	0.789(52)
ALPHA 04	[94]	2	A	■	★	★	$r_0 = 0.5 \text{ fm}^\S$	245(16)(16) [§]	0.62(2)(2) [§]
ALPHA 01A	[95]	2	A	★	★	★	only running of α_s in Fig. 5		
Nada 20	[28]	0	A	★	★	★	consistency checks for [27], same gauge configurations		
Dalla Brida 19	[27]	0	A	★	★	★	$r_0 = 0.5 \text{ fm}$	260.5(4.4)	0.660(11)
Ishikawa 17	[87]	0	A	★	★	★	$r_0, [\sqrt{\sigma}]$	253(4)($^{+13}_{-2}$) [†]	0.606(9)($^{+31}_{-5}$) [†]
CP-PACS 04 ^{&}	[78]	0	A	★	★	○	only tables of g_{SF}^2		
ALPHA 98 ^{††}	[96]	0	A	★	★	○	$r_0 = 0.5 \text{ fm}$	238(19)	0.602(48)
Lüscher 93	[75]	0	A	★	○	○	$r_0 = 0.5 \text{ fm}$	233(23)	0.590(60) ^{§§}

[#] Result with a constant (in a) continuum extrapolation of the combination $L_{\text{max}}m_\rho$.

[†] In conversion from $\Lambda_{\overline{\text{MS}}}$ to $r_0\Lambda_{\overline{\text{MS}}}$ and vice versa, r_0 is taken to be 0.472 fm.

^{##} Result with a linear continuum extrapolation in a of the combination $L_{\text{max}}m_\rho$.

^{*} Supersedes ALPHA 04.

[§] The $N_f = 2$ results were based on values for r_0/a which have later been found to be too small by [57]. The effect will be of the order of 10–15%, presumably an increase in Λr_0 . We have taken this into account by a ■ in the renormalization scale.

[&] This investigation was a precursor for PACS-CS 09A and confirmed two step-scaling functions as well as the scale setting of ALPHA 98.

^{††} Uses data of Lüscher 93 and therefore supersedes it.

^{§§} Converted from $\alpha_{\overline{\text{MS}}}(37r_0^{-1}) = 0.1108(25)$.

⁺ Also $\Lambda_{\overline{\text{MS}}}/\sqrt{\sigma} = 0.532(8)($^{+27}_{-5}$)$ is quoted.

Table 60: Results for the Λ parameter from computations using step-scaling of the SF-coupling. Entries without values for Λ computed the running and established perturbative behaviour at large μ .

Step-scaling is carried out with an $\mathcal{O}(a)$ -improved Wilson quark action [97] and Lüscher-Weisz gauge action [98] in the low-scale region and an $\mathcal{O}(a)$ -improved Wilson quark action [99] and Wilson gauge action in the high-energy part. For the step-scaling using steps of $L/a \rightarrow 2L/a$, three lattice sizes $L/a = 8, 12, 16$ were simulated for \bar{g}_{GF}^2 and four lattice sizes $L/a = (4,)6, 8, 12$ for \bar{g}_{SF}^2 . The final results do not use the small lattices given in parenthesis.

The parameter $\Lambda_{\overline{\text{MS}}}^{(3)}$ is then obtained via

$$\Lambda_{\overline{\text{MS}}}^{(3)} = \underbrace{\frac{\Lambda_{\overline{\text{MS}}}^{(3)}}{\mu_{\text{PT}}}}_{\text{perturbation theory}} \times \underbrace{\frac{\mu_{\text{PT}}}{\mu_{\text{had}}}}_{\text{step-scaling}} \times \underbrace{\frac{\mu_{\text{had}}}{f_{\pi K}}}_{\text{large volume simulation}} \times \underbrace{f_{\pi K}}_{\text{experimental data}}, \quad (348)$$

where the hadronic scale $f_{\pi K}$ is $f_{\pi K} = \frac{1}{3}(2f_K + f_\pi) = 147.6(5)$ MeV. The first factor on the right hand side of Eq. (348) is obtained from $\alpha_{\text{SF}}(\mu_{\text{PT}})$ which is the output from SF step-scaling using Eq. (320) with $\alpha_{\text{SF}}(\mu_{\text{PT}}) \approx 0.1$ and the 3-loop β -function and the exact conversion to the $\overline{\text{MS}}$ -scheme. The second factor is essentially obtained from step-scaling in the GF scheme and the measurement of $\bar{g}_{\text{SF}}^2(\mu_0)$ (except for the trivial scaling factor of 16 in the SF running). The third factor is obtained from a measurement of the hadronic quantity at large volume.

A large-volume simulation is done for three lattice spacings with sufficiently large volume and reasonable control over the chiral extrapolation so that the scale determination is precise enough. The step-scaling results in both schemes satisfy renormalization criteria, perturbation theory criteria, and continuum limit criteria just as previous studies using step-scaling. So we assign green stars for these criteria.

The dependence of Λ , Eq. (320) with 3-loop β -function, on α_s and on the chosen scheme is discussed in [69]. This investigation provides a warning on estimating the truncation error of perturbative series. Details are explained in Sec. 9.2.3.

The result for the Λ parameter is $\Lambda_{\overline{\text{MS}}}^{(3)} = 341(12)$ MeV, where the dominant error comes from the error of $\alpha_{\text{SF}}(\mu_{\text{PT}})$ after step-scaling in the SF scheme. Using 4-loop matching at the charm and bottom thresholds and 5-loop running one finally obtains

$$\alpha_{\overline{\text{MS}}}^{(5)}(M_Z) = 0.11852(84). \quad (349)$$

Several other results do not have a sufficient number of quark flavours or do not yet contain the conversion of the scale to physical units (ALPHA 10A [90], Perez 10 [91]). Thus no value for $\alpha_{\overline{\text{MS}}}^{(5)}(M_Z)$ is quoted.

The computation of Ishikawa et al. [87] is based on the gradient flow coupling with twisted boundary conditions [86] (TGF coupling) in the pure gauge theory. Again they use $c = 0.3$. Step-scaling with a scale factor $s = 3/2$ is employed, covering a large range of couplings from $\alpha_s \approx 0.5$ to $\alpha_s \approx 0.1$ and taking the continuum limit through global fits to the step-scaling function on $L/a = 12, 16, 18$ lattices with between 6 and 8 parameters. Systematic errors due to variations of the fit functions are estimated. Two physical scales are considered: r_0/a is taken from [62] and σa^2 from [100] and [101]. As the ratio $\Lambda_{\text{TGF}}/\Lambda_{\overline{\text{MS}}}$ has not yet been computed analytically, Ref. [87] determines the 1-loop relation between \bar{g}_{SF} and \bar{g}_{TGF} from MC simulations performed in the weak coupling region and then uses the known $\Lambda_{\text{SF}}/\Lambda_{\overline{\text{MS}}}$. Systematic errors due to variations of the fit functions dominate the overall uncertainty.

Since FLAG 19 two new and quite extensive $N_f = 0$ step-scaling studies have been carried out in Dalla Brida 19 [27] and by Nada and Ramos [28]. They use different strategies for the running from mid to high energies, but use the same gauge configurations and share the running at low energies and matching to the hadronic scales. These results are therefore correlated. However, given the comparatively high value for $r_0\Lambda_{\overline{\text{MS}}}$, it is re-assuring that these conceptually different approaches yield perfectly compatible results within errors of similar size of around 1.5% for $\sqrt{8t_0}\Lambda_{\overline{\text{MS}}} = 0.6227(98)$, or, alternatively $r_0\Lambda_{\overline{\text{MS}}} = 0.660(11)$.

In Dalla Brida 19 [27] two GF-coupling definitions with SF-boundary conditions are considered, corresponding to (colour-) magnetic and electric components of the action density respectively. The coupling definitions include the projection to $Q = 0$, as was also done in [92]. The flow time parameter is set to $c = 0.3$, and both Zeuthen and Wilson flow are measured. Lattice sizes range from $L/a = 8$ to $L/a = 48$, covering up to a factor of 3 in lattice spacings for the step-scaling function, where both L/a and $2L/a$ are needed. Lattice effects in the step-scaling function are visible but can be extrapolated using global fits with a^2 errors. Some remnant $\mathcal{O}(a)$ effects from the boundaries are expected, as their perturbative cancellation is incomplete. These $\mathcal{O}(a)$ contaminations are treated as a systematic error on the data, following [92] and are found to be subdominant. An intermediate reference scale μ_{ref} is defined where $\alpha = 0.2$, and the scales above and below are analyzed separately. Again this is similar to [92], except that here GF coupling data is available also at high energy scales. The GF β -functions are then obtained by fitting to the continuum extrapolated data for the step-scaling functions. In addition, a nonperturbative matching to the standard SF coupling is performed above μ_{ref} for a range of couplings covering a factor 2. The nonperturbative β -function for the SF scheme can thus be inferred from the GF β -function. It turns out that GF schemes are very slow to reach the perturbative regime. Particularly the Λ -parameter for the magnetic GF coupling shows a large slope in α^2 , which is the parametric uncertainty with known 3-loop β -function. Also, convincing contact with the 3-loop β -function is barely seen down to $\alpha = 0.08$. This is likely to be related to the rather large 3-loop β -function coefficients, especially for the magnetic GF scheme [88]. In contrast, once the GF couplings are matched nonperturbatively to the SF scheme the contact to perturbative running can be safely made. It is also re-assuring that in all cases the extrapolations (linear in α^2) to $\alpha = 0$ for the Λ -parameters agree very well, and the authors argue in favour of such extrapolations. Their data confirms that this procedure yields consistent results with the SF scheme for $\nu = 0$, where such an extrapolation is not required.

The low energy regime between μ_{ref} and a hadronic scale μ_{had} is covered again using the nonperturbative step-scaling function and the derived β -function. Finally, contact between μ_{had} and hadronic scales t_0 and r_0 is established using 5 lattice spacings covering a factor up to 2.7. The multitude of cross checks of both continuum limit and perturbative truncation errors make this a study which passes all current FLAG criteria by some margin. The comparatively high value for $r_0\Lambda_{\overline{\text{MS}}}$ found in this study must therefore be taken very seriously.

In Nada 20 [28], Nada and Ramos provide further consistency checks of [27] for scales larger than μ_{ref} . The step scaling function for $c = 0.2$ is constructed in 2 steps, by determining first the relation between couplings for $c = 0.2$ and $c = 0.4$ at the same L and then increasing L to $2L$ keeping the flow time fixed (in units of the lattice spacing), so that one arrives again at $c = 0.2$ on the $2L$ volume. The authors demonstrate that the direct construction of the step-scaling function for $c = 0.2$ would require much larger lattices in order to control the continuum limit at the same level of precision. The consistency with [27] for the Λ -parameter is therefore a highly non-trivial check on the systematic effects of the continuum extrapolations. The study obtains results for the Λ -parameter (again extrapolating to $\alpha = 0$) with a similar error as in [27]. using the low-energy running and matching to the hadronic scale from that reference. For this reason and since gauge configurations are shared between both papers, these results are not independent of [27], so Dalla Brida 19 will be taken as representative for both works.

9.4 The decoupling method

The ALPHA collaboration has proposed a new strategy to compute the Λ parameter in QCD with $N_f \geq 3$ flavours based on simultaneous decoupling of $N_f \geq 3$ heavy quarks with RGI mass M [26]. We refer to [102] for a pedagogical introduction and to [103] for recent results. Generically, a running coupling in a mass-dependent renormalization scheme

$$\bar{g}^2(\mu, M)^{(N_f)} = \bar{g}^2(\mu)^{(N_f=0)} + \mathcal{O}(M^{-k}) \quad (350)$$

can be represented by the corresponding $N_f = 0$ coupling, up to power corrections in $1/M$. The leading power is usually $k = 2$, however renormalization schemes in finite volume may have $k = 1$, depending on the set-up. For example, this is the case with standard SF or open boundary conditions in combination with a standard mass term. In practice one may try to render such boundary contributions numerically small by a careful choice of the scheme's parameters. In principle, power corrections can be either $(\mu/M)^k$ or $(\Lambda/M)^k$. Fixing $\mu = \mu_{\text{dec}}$, e.g. by prescribing a value for the mass-independent coupling, such that $\mu_{\text{dec}}/\Lambda = \mathcal{O}(1)$ thus helps to reduce the need for very large M . Defining $\bar{g}^2(\mu_{\text{dec}}, M) = u_M$ at fixed $\bar{g}^2(\mu_{\text{dec}}, M = 0)$, Eq. (350) translates to a relation between Λ -parameters, which can be cast in the form,

$$\frac{\Lambda_{\overline{\text{MS}}}^{(N_f)}}{\mu_{\text{dec}}} P \left(\frac{M}{\mu_{\text{dec}}} \frac{\mu_{\text{dec}}}{\Lambda_{\overline{\text{MS}}}^{(N_f)}} \right) = \frac{\Lambda_{\overline{\text{MS}}}^{(0)}}{\Lambda_s^{(0)}} \varphi_s^{(N_f=0)}(\sqrt{u_M}) + \mathcal{O}(M^{-k}), \quad (351)$$

with the function φ_s as defined in Eq. (320), for scheme s and $N_f = 0$. A crucial observation is that the function P , which gives the ratios of Λ -parameters $\Lambda_{\overline{\text{MS}}}^{(0)}/\Lambda_{\overline{\text{MS}}}^{(N_f)}$, can be evaluated perturbatively to a very good approximation [104, 105]. Eq. (350) also implies a relation between the couplings in mass-independent schemes, in the theories with N_f and zero flavours, respectively. In the $\overline{\text{MS}}$ scheme this relation is analogous to Eq. (327),

$$\bar{g}_{\overline{\text{MS}}}^2(m_\star)^{(N_f=0)} = \bar{g}_{\overline{\text{MS}}}^2(m_\star)^{(N_f)} \times C \left(\bar{g}_{\overline{\text{MS}}}^2(m_\star)^{(N_f)} \right) \quad (352)$$

and the function $C(g)$ is also known up to 4-loop order [19–22, 106]. The function $P(y)$, with $y \equiv M/\Lambda_{\overline{\text{MS}}}^{(N_f)}$ can therefore be evaluated perturbatively in the $\overline{\text{MS}}$ scheme, as the ratio

$$P(y) = \frac{\varphi_{\overline{\text{MS}}}^{(N_f=0)} \left(g^\star(y) \sqrt{C(g^\star(y))} \right)}{\varphi_{\overline{\text{MS}}}^{(N_f)}(g^\star(y))}, \quad g^\star(y) = \bar{g}_{\overline{\text{MS}}}^2(m_\star)^{(N_f)}. \quad (353)$$

Hence, perturbation theory is only required at the scale set by the heavy-quark mass, which works the better the larger M can be chosen. Once P is known, the LHS of (351) can be inferred from a $N_f = 0$ computation of the RHS in the scheme s , assuming the ratio $\Lambda_{\overline{\text{MS}}}/\Lambda_s$ is known from a 1-loop calculation.

To put the decoupling strategy into practice, the ALPHA collaboration uses $N_f = 3$, so that information from [92] can be used. Using the massless GF coupling in finite volume from this project, μ_{dec} is defined through $\bar{g}_{\text{GF}}^2(\mu_{\text{dec}}) = 3.95$, and thus known in physical units, $\mu_{\text{dec}} = 789(15)$ MeV. Varying L/a between 12 and 32 (five lattice spacings) defines a range of values for the bare coupling along a line of constant μ_{dec} and for vanishing quark mass. Next, a mass-dependent GF coupling is defined at constant μ_{dec} , using the available information

on nonperturbative mass renormalization [107] and $\mathcal{O}(a)$ improvement. In order to obtain a larger suppression of the leading $1/M$ boundary correction term, the time extent T is here set to $2L$, so as to maximize the distance to the time boundaries. Choosing 4 values of $z = M/\mu_{\text{dec}}$ within the range from 2 to 8, with up to 5 lattice spacings⁷ and using precision results for $N_f = 0$ from [27] then leads to the result for $\Lambda_{\overline{\text{MS}}}^{(N_f=3)}$, up to power corrections in $1/z$, expected to be predominantly of order $1/z^2$. Figure 39, taken from [26] shows the

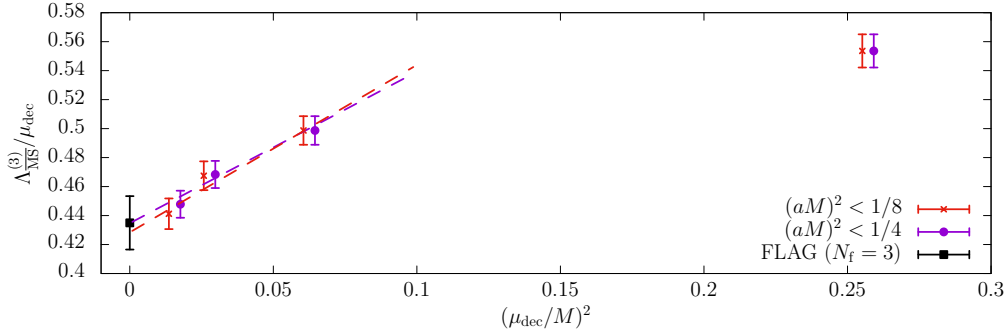


Figure 39: Illustration of the decoupling method, taken from ref. [26].

continuum extrapolated results obtained for $\Lambda_{\overline{\text{MS}}}^{(3)}/\mu_{\text{dec}}$ at different values of z , together with the FLAG 19 average for three-flavour QCD. While the authors of [26] stopped short of quoting an extrapolated value for the three-flavour Λ -parameter, the result $\Lambda_{\overline{\text{MS}}}^{(3)} = 332(10)(2)$ MeV is now given in the 2021 lattice conference proceedings [103], compatible with ALPHA 17 albeit with a somewhat smaller error. Despite some common elements with ALPHA 17, the authors emphasize that the decoupling method is largely independent, with the overlap in squared error amounting to ca. 40 percent. This is due to the fact that the error in ALPHA 17 is dominated by the $N_f = 3$ step scaling procedure at *high* energy, and this part is completely replaced by the $N_f = 0$ result by Dalla Brida 19 [27]. The decoupling method thus seems to offer scope for a further error reduction, the major challenges being the continuum extrapolation for the GF coupling at fixed and large RGI masses, followed by the large M limit.

It is important to note that this new method relies on new precision results for $N_f = 0$ which have appeared in the last two years [27, 28]. Therefore, the pure gauge theory acquires new relevance for α_s results, beyond its traditional rôle as a test bed for the study of systematic errors. FLAG will take account of this development by continuing to carefully monitor $N_f = 0$ results. It is hoped that this will encourage more groups to undertake precision studies with $N_f = 0$.

9.5 α_s from the potential at short distances

9.5.1 General considerations

The basic method was introduced in Ref. [108] and developed in Ref. [109]. The force or potential between an infinitely massive quark and antiquark pair defines an effective coupling

⁷At the largest mass, $z = 8$, only the 2-3 finest lattice spacings are useful in a linear extrapolation in a^2 .

constant via

$$F(r) = \frac{dV(r)}{dr} = C_F \frac{\alpha_{\text{qq}}(r)}{r^2}. \quad (354)$$

The coupling can be evaluated nonperturbatively from the potential through a numerical differentiation, see below. In perturbation theory one also defines couplings in different schemes $\alpha_{\bar{V}}$, α_V via

$$V(r) = -C_F \frac{\alpha_{\bar{V}}(r)}{r}, \quad \text{or} \quad \tilde{V}(Q) = -C_F \frac{\alpha_V(Q)}{Q^2}, \quad (355)$$

where one fixes the unphysical constant in the potential by $\lim_{r \rightarrow \infty} V(r) = 0$ and $\tilde{V}(Q)$ is the Fourier transform of $V(r)$. Nonperturbatively, the subtraction of a constant in the potential introduces an additional renormalization constant, the value of $V(r_{\text{ref}})$ at some distance r_{ref} . Perturbatively, it is believed to entail a renormalon ambiguity. In perturbation theory, the different definitions are all simply related to each other, and their perturbative expansions are known including the α_s^4 , $\alpha_s^4 \log \alpha_s$ and $\alpha_s^5 \log \alpha_s$, $\alpha_s^5 (\log \alpha_s)^2$ terms [110–117].

The potential $V(r)$ is determined from ratios of Wilson loops, $W(r, t)$, which behave as

$$\langle W(r, t) \rangle = |c_0|^2 e^{-V(r)t} + \sum_{n \neq 0} |c_n|^2 e^{-V_n(r)t}, \quad (356)$$

where t is taken as the temporal extension of the loop, r is the spatial one and V_n are excited-state potentials. To improve the overlap with the ground state, and to suppress the effects of excited states, t is taken large. Also various additional techniques are used, such as a variational basis of operators (spatial paths) to help in projecting out the ground state. Furthermore some lattice-discretization effects can be reduced by averaging over Wilson loops related by rotational symmetry in the continuum.

In order to reduce discretization errors it is of advantage to define the numerical derivative giving the force as

$$F(r_{\text{I}}) = \frac{V(r) - V(r - a)}{a}, \quad (357)$$

where r_{I} is chosen so that at tree level the force is the continuum force. $F(r_{\text{I}})$ is then a ‘tree-level improved’ quantity and similarly the tree-level improved potential can be defined [118].

Lattice potential results are in position space, while perturbation theory is naturally computed in momentum space at large momentum. Usually, the Fourier transform of the perturbative expansion is then matched to lattice data.

Finally, as was noted in Sec. 9.2.1, a determination of the force can also be used to determine the scales r_0 , r_1 , by defining them from the static force by

$$r_0^2 F(r_0) = 1.65, \quad r_1^2 F(r_1) = 1. \quad (358)$$

9.5.2 Discussion of computations

In Tab. 61, we list results of determinations of $r_0 \Lambda_{\overline{\text{MS}}}$ (together with $\Lambda_{\overline{\text{MS}}}$ using the scale determination of the authors).

Collaboration	Ref.	N_f		publication status	renormalization scale	perturbative behaviour	continuum extrapolation	scale	$\Lambda_{\overline{\text{MS}}}[\text{MeV}]$	$r_0\Lambda_{\overline{\text{MS}}}$
Ayala 20	[30]	2+1	A	○	★	○		$r_1 = 0.3106(17) \text{ fm}^c$	338(13)	0.802(31)
TUMQCD 19	[29]	2+1	A	○	★	○		$r_1 = 0.3106(17) \text{ fm}^c$	314_{-8}^{+16}	$0.745_{(-19)}^{(+38)}$
Takaura 18	[119, 120]	2+1	A	■	○	○		$\sqrt{t_0} = 0.1465(25) \text{ fm}^a$	$334(10)_{(-18)}^{(+20)b}$	$0.799(51)^+$
Bazavov 14	[121]	2+1	A	○	★	○		$r_1 = 0.3106(17) \text{ fm}^c$	$315_{(-12)}^{(+18)d}$	$0.746_{(-27)}^{(+42)}$
Bazavov 12	[122]	2+1	A	○ [†]	○	○ [#]		$r_0 = 0.468 \text{ fm}$	$295(30)^*$	$0.70(7)^{**}$
Karbstein 18	[123]	2	A	○	○	○		$r_0 = 0.420(14) \text{ fm}^e$	302(16)	0.643(34)
Karbstein 14	[124]	2	A	○	○	○		$r_0 = 0.42 \text{ fm}$	331(21)	0.692(31)
ETM 11C	[125]	2	A	○	○	○		$r_0 = 0.42 \text{ fm}$	$315(30)^\S$	0.658(55)
Husung 20	[31]	0	C	○	★	★		no quoted value for $\Lambda_{\overline{\text{MS}}}$		
Husung 17	[126]	0	C	○	★	★		$r_0 = 0.50 \text{ fm}$	232(6)	0.590(16)
Brambilla 10	[127]	0	A	○	★	○ ^{††}			$266(13)^+$	$0.637_{(-30)}^{(+32)\dagger\dagger}$
UKQCD 92	[109]	0	A	★	○ ⁺⁺	■		$\sqrt{\sigma} = 0.44 \text{ GeV}$	256(20)	0.686(54)
Bali 92	[128]	0	A	★	○ ⁺⁺	■		$\sqrt{\sigma} = 0.44 \text{ GeV}$	247(10)	0.661(27)

^a Scale determined from t_0 in Ref. [39].

^b $\alpha_{\overline{\text{MS}}}^{(5)}(M_Z) = 0.1179(7)_{(-12)}^{(+13)}$.

^c Determination on lattices with $m_\pi L = 2.2 - 2.6$. Scale from r_1 [52] as determined from f_π in Ref. [60].

^d $\alpha_{\overline{\text{MS}}}^{(3)}(1.5 \text{ GeV}) = 0.336_{(-8)}^{(+12)}$, $\alpha_{\overline{\text{MS}}}^{(5)}(M_Z) = 0.1166_{(-8)}^{(+12)}$.

^e Scale determined from f_π , see [55].

[†] Since values of α_{eff} within our designated range are used, we assign a ○ despite values of α_{eff} up to $\alpha_{\text{eff}} = 0.5$ being used.

[#] Since values of $2a/r$ within our designated range are used, we assign a ○ although only values of $2a/r \geq 1.14$ are used at $\alpha_{\text{eff}} = 0.3$.

^{*} Using results from Ref. [61].

^{**} $\alpha_{\overline{\text{MS}}}^{(3)}(1.5 \text{ GeV}) = 0.326(19)$, $\alpha_{\overline{\text{MS}}}^{(5)}(M_Z) = 0.1156_{(-22)}^{(+21)}$.

[§] Both potential and r_0/a are determined on a small ($L = 3.2r_0$) lattice.

^{††} Uses lattice results of Ref. [62], some of which have very small lattice spacings where according to more recent investigations a bias due to the freezing of topology may be present.

⁺ Our conversion using $r_0 = 0.472 \text{ fm}$.

⁺⁺ We give a ○ because only a NLO formula is used and the error bars are very large; our criterion does not apply well to these very early calculations.

Table 61: Short-distance potential results.

Since the last review, FLAG 19, there have been three new publications, namely, TUMQCD 19 [29], Ayala 20 [30] and Husung 20 [31].

The first determinations in the three-colour Yang Mills theory are by UKQCD 92 [109] and Bali 92 [128] who used α_{qq} as explained above, but not in the tree-level improved form. Rather a phenomenologically determined lattice-artifact correction was subtracted from the lattice potentials. The comparison with perturbation theory was on a more qualitative level

on the basis of a 2-loop β -function ($n_l = 1$) and a continuum extrapolation could not be performed as yet. A much more precise computation of α_{qq} with continuum extrapolation was performed in Refs. [62, 118]. Satisfactory agreement with perturbation theory was found [118] but the stability of the perturbative prediction was not considered sufficient to be able to extract a Λ parameter.

In Brambilla 10 [127] the same quenched lattice results of Ref. [118] were used and a fit was performed to the continuum potential, instead of the force. Perturbation theory to $n_l = 3$ loop was used including a resummation of terms $\alpha_s^3(\alpha_s \ln \alpha_s)^n$ and $\alpha_s^4(\alpha_s \ln \alpha_s)^n$. Close agreement with perturbation theory was found when a renormalon subtraction was performed. Note that the renormalon subtraction introduces a second scale into the perturbative formula which is absent when the force is considered.

Bazavov 14 [121] updates Bazavov 12 [122] and modifies this procedure somewhat. They consider the perturbative expansion for the force. They set $\mu = 1/r$ to eliminate logarithms and then integrate the force to obtain an expression for the potential. The resulting integration constant is fixed by requiring the perturbative potential to be equal to the nonperturbative one exactly at a reference distance r_{ref} and the two are then compared at other values of r . As a further check, the force is also used directly.

For the quenched calculation of Brambilla 10 [127] very small lattice spacings, $a \sim 0.025$ fm, were available from Ref. [118]. For ETM 11C [125], Bazavov 12 [122], Karbstein 14 [124] and Bazavov 14 [121] using dynamical fermions such small lattice spacings are not yet realized (Bazavov 14 reaches down to $a \sim 0.041$ fm). They all use the tree-level improved potential as described above. We note that the value of $\Lambda_{\overline{\text{MS}}}$ in physical units by ETM 11C [125] is based on a value of $r_0 = 0.42$ fm. This is at least 10% smaller than the large majority of other values of r_0 . Also the values of r_0/a on the finest lattices in ETM 11C [125] and r_1/a for Bazavov 14 [121] come from rather small lattices with $m_\pi L \approx 2.4, 2.2$ respectively.

Instead of the procedure discussed previously, Karbstein 14 [124] reanalyzes the data of ETM 11C [125] by first estimating the Fourier transform $\tilde{V}(p)$ of $V(r)$ and then fitting the perturbative expansion of $\tilde{V}(p)$ in terms of $\alpha_{\overline{\text{MS}}}(p)$. Of course, the Fourier transform requires some modelling of the r -dependence of $V(r)$ at short and at large distances. The authors fit a linearly rising potential at large distances together with string-like corrections of order r^{-n} and define the potential at large distances by this fit.⁸ Recall that for observables in momentum space we take the renormalization scale entering our criteria as $\mu = q$, Eq. (338). The analysis (as in ETM 11C [125]) is dominated by the data at the smallest lattice spacing, where a controlled determination of the overall scale is difficult due to possible finite-size effects. Karbstein 18 [123] is a reanalysis of Karbstein 14 and supersedes it. Some data with a different discretization of the static quark is added (on the same configurations) and the discrete lattice results for the static potential in position space are first parameterized by a continuous function, which then allows for an analytical Fourier transformation to momentum space.

Similarly also for Takaura 18 [119, 120] the momentum space potential $\tilde{V}(Q)$ is the central object. Namely, they assume that renormalon/power-law effects are absent in $\tilde{V}(Q)$ and only come in through the Fourier transformation. They provide evidence that renormalon effects (both $u = 1/2$ and $u = 3/2$) can be subtracted and arrive at a nonperturbative term $k \Lambda_{\overline{\text{MS}}}^3 r^2$. Two different analyses are carried out with the final result taken from ‘‘Analysis II’’. Our

⁸Note that at large distances, where string breaking is known to occur, this is not any more the ground state potential defined by Eq. (356).

numbers including the evaluation of the criteria refer to it. Together with the perturbative 3-loop (including the $\alpha_s^4 \log \alpha_s$ term) expression, this term is fitted to the nonperturbative results for the potential in the region $0.04 \text{ fm} \leq r \leq 0.35 \text{ fm}$, where 0.04 fm is $r = a$ on the finest lattice. The nonperturbative potential data originates from JLQCD ensembles (Symanzik-improved gauge action and Möbius domain-wall quarks) at three lattice spacings with a pion mass around 300 MeV. Since at the maximal distance in the analysis we find $\alpha_{\overline{\text{MS}}}(2/r) = 0.43$, the renormalization scale criterion yields a \blacksquare . The perturbative behaviour is \circ because of the high orders in perturbation theory known. The continuum-limit criterion yields a \circ .

One of the main issues for all these computations is whether the perturbative running of the coupling constant has been reached. While for $N_f = 0$ fermions Brambilla 10 [127] reports agreement with perturbative behaviour at the smallest distances, Husung 17 (which goes to shorter distances) finds relatively large corrections beyond the 3-loop α_{qq} . For dynamical fermions, Bazavov 12 [122] and Bazavov 14 [121] report good agreement with perturbation theory after the renormalon is subtracted or eliminated.

A second issue is the coverage of configuration space in some of the simulations, which use very small lattice spacings with periodic boundary conditions. Affected are the smallest two lattice spacings of Bazavov 14 [121] where very few tunnelings of the topological charge occur [52]. With present knowledge, it also seems possible that the older data by Refs. [62, 118] used by Brambilla 10 [127] are partially obtained with (close to) frozen topology.

The computation in Husung 17 [126], for $N_f = 0$ flavours, first determines the coupling $\bar{g}_{\text{qq}}^2(r, a)$ from the force and then performs a continuum extrapolation on lattices down to $a \approx 0.015 \text{ fm}$, using a step-scaling method at short distances, $r/r_0 \lesssim 0.5$. Using the 4-loop β^{qq} function this allows $r_0 \Lambda_{\text{qq}}$ to be estimated, which is then converted to the $\overline{\text{MS}}$ scheme. $\alpha_{\text{eff}} = \alpha_{\text{qq}}$ ranges from ~ 0.17 to large values; we give \circ for renormalization scale and \star for perturbative behaviour. The range $a\mu = 2a/r \approx 0.37\text{--}0.14$ leads to a \star in the continuum extrapolation. Recently these calculations have been extended in Husung 20 [31]. A finer lattice spacing of $a = 0.01 \text{ fm}$ (scale from $r_0 = 0.5 \text{ fm}$) is reached and lattice volumes up to $L/a = 192$ are simulated (in Ref. [126] the smallest lattice spacing is 0.015 fm). The Wilson action is used despite its significantly larger cutoff effects compared to Symanzik-improved actions; this avoids unitarity violations, thus allowing for a clean ground state extraction via a generalized eigenvalue problem. Open boundary conditions are used to avoid the topology-freezing problem. Furthermore, new results for the continuum approach are employed, which determine the cutoff dependence at $\mathcal{O}(a^2)$ including the exact coupling-dependent terms, in the asymptotic region where the Symanzik effective theory is applicable [129]. An ansatz for the remaining higher order cutoff effects at $\mathcal{O}(a^4)$ is propagated as a systematic error to the data, which effectively discards data for $r/a < 3.5$. The large volume step-scaling function with step factor $3/4$ is computed and compared to perturbation theory. For $\alpha_{\text{qq}} > 0.2$ there is a noticeable difference between the 2-loop and 3-loop results. Furthermore, the ultra-soft contributions at 4-loop level give a significant contribution to the static $Q\bar{Q}$ force. While this study is for $N_f = 0$ flavours it does raise the question whether the weak coupling expansion for the range of r -values used in present analyses of α_s is sufficiently reliable. Around $\alpha_{\text{qq}} \approx 0.21$ the differences get smaller but the error increases significantly, mainly due to the propagated lattice artifacts. The dependence of $\Lambda_{\overline{\text{MS}}}^{n_f=0} \sqrt{8t_0}$ on α_{qq}^3 is very similar to the one observed in the previous study but no value for its $\alpha_{\text{qq}} \rightarrow 0$ limit is quoted. Husung 20 [31] is more pessimistic about the error on the Λ parameter stating the relative error has to be 5% or

larger, while Husung 17 quotes a relative error of 3%.

In 2+1-flavor QCD two new papers appeared on the determination of the strong coupling constant from the static quark anti-quark potential after the FLAG 19 report [29, 30]. In TUMQCD 19 [29]⁹ the 2014 analysis of Bazavov 14 [121] has been extended by including three finer lattices with lattice spacing $a = 0.035, 0.030$ and 0.025 fm as well as lattice results on the free energy of static quark anti-quark pair at non-zero temperature. On the new fine lattices the effect of freezing topology has been observed, however, it was verified that this does not affect the potential within the estimated errors [130, 131]. The comparison of the lattice result on the static potential has been performed in the interval $r = [r_{\min}, r_{\max}]$, with $r_{\max} = 0.131, 0.121, 0.098, 0.073$ and 0.055 fm. The main result quoted in the paper is based on the analysis with $r_{\max} = 0.073$ fm [29]. Since the new study employs a much wider range in r than the previous one [121] we give it a ★ for the perturbative behaviour. Since $\alpha_{\text{eff}} = \alpha_{qq}$ varies in the range 0.2–0.4 for the r values used in the main analysis we give ○ for the renormalization scale. Several values of r_{\min} have been used in the analysis, the largest being $r_{\min}/a = \sqrt{8} \simeq 2.82$, which corresponds to $a\mu \simeq 0.71$. Therefore, we give a ○ for continuum extrapolation in this case. An important difference compared to the previous study [121] is the variation of the renormalization scale. In Ref. [121] the renormalization scale was varied by a factor of $\sqrt{2}$ around the nominal value of $\mu = 1/r$, in order to exclude very low scales, for which the running of the strong coupling constant is no longer perturbative. In the new analysis the renormalization scale was varied by a factor of two. As the result, despite the extended data set and shorter distances used in the new study the perturbative error did not decrease [29]. We also note that the scale dependence turned out to be non-monotonic in the range $\mu = 1/(2r) - 2/r$ [29]. The final result reads (“us” stands for “ultra-soft”),

$$\begin{aligned} \Lambda_{\overline{\text{MS}}}^{N_f=3} &= 314.0 \pm 5.8(\text{stat}) \pm 3.0(\text{lat}) \pm 1.7(\text{scale})_{-1.8}^{+13.4}(\text{pert}) \pm 4.0(\text{pert. us}) \text{ MeV} \\ &= 314_{-08}^{+16} \text{ MeV}, \end{aligned} \quad (359)$$

where all errors were combined in quadrature. This is in very good agreement with the previous determination [121].

The analysis was also applied to the singlet static quark anti-quark free energy at short distances. At short distances the free energy is expected to be the same as the static potential. This is verified numerically in the lattice calculations TUMQCD 19 [29] for $rT < 1/4$ with T being the temperature. Furthermore, this is confirmed by the perturbative calculations at $T > 0$ at NLO [132]. The advantage of using the free energy is that it gives access to much shorter distances. On the other hand, one has fewer data points because the condition $rT < 1/4$ has to be satisfied. The analysis based on the free energy gives

$$\begin{aligned} \Lambda_{\overline{\text{MS}}}^{N_f=3} &= 310.9 \pm 11.3(\text{stat}) \pm 3.0(\text{lat}) \pm 1.7(\text{scale})_{-0.8}^{+5.6}(\text{pert}) \pm 2.1(\text{pert. us}) \text{ MeV} \\ &= 311(13) \text{ MeV}, \end{aligned} \quad (360)$$

in good agreement with the above result and thus, providing additional confirmation of it.

The analysis of Ayala 20 [30] uses a subset of data presented in TUMQCD 19 [29] with the same correction of the lattice effects. For this reason the continuum extrapolation gets ○, too. They match to perturbation theory for $1/r > 2$ GeV, which corresponds to $\alpha_{\text{eff}} = \alpha_{qq} = 0.2$ –0.4. Therefore, we give ○ for the renormalization scale. They verify the perturbative

⁹The majority of authors are the same as in [121].

behaviour in the region $1 \text{ GeV} < 1/r < 2.9 \text{ GeV}$, which corresponds to variation of α_{eff}^3 by a factor of 3.34. However, the relative error on the final result has $\delta\Lambda/\Lambda \simeq 0.035$ which is larger than $\alpha_{\text{eff}}^3 = 0.011$. Therefore, we give a \star for the perturbative behaviour in this case. The final result for the Λ -parameter reads:

$$\Lambda_{\overline{\text{MS}}}^{N_f=3} = 338 \pm 2(\text{stat}) \pm 8(\text{matching}) \pm 10(\text{pert}) \text{ MeV} = 338(13) \text{ MeV}. \quad (361)$$

This is quite different from the above result. This difference is mostly due to the organization of the perturbative series. The authors use ultra-soft (log) resummation, i.e. they resum the terms $\alpha_s^{3+n} \ln^n \alpha_s$ to all orders instead of using fixed-order perturbation theory. They also include what is called the terminant of the perturbative series associated to the leading renormalon of the force [30]. When they use fixed order perturbation theory they obtain very similar results to Refs. [29, 121]. It has been argued that log resummation cannot be justified since for the distance range available in the lattice studies α_s is not small enough and the logarithmic and non-logarithmic higher-order terms are of a similar size [121]. On the other hand, the resummation of ultra-soft logs does not lead to any anomalous behaviour of the perturbative expansion like large scale dependence or bad convergence [30].

To obtain the value of $\Lambda_{\overline{\text{MS}}}^{N_f=3}$ from the static potential we combine the results in Eqs. (359) and (361) using the weighted average with the weight given by the perturbative error and using the difference in the central value as the error estimate. This leads to

$$\Lambda_{\overline{\text{MS}}}^{N_f=3} = 330(24) \text{ MeV}, \quad (362)$$

from the static potential determination. In the case of TUMQCD 19, where the perturbative error is very asymmetric we used the larger upper error for the calculation of the corresponding weight.

9.6 α_s from the light-quark vacuum polarization in momentum/position space

9.6.1 General considerations

Except for the new calculation Cali 20 [32], where position space is used (see below), the light-flavour-current 2-point function is usually evaluated in momentum space, in terms of the vacuum-polarization function. For the flavour-nonsinglet currents J_μ^a ($a = 1, 2, 3$) in the momentum representation this is parametrized as

$$\langle J_\mu^a J_\nu^b \rangle = \delta^{ab} [(\delta_{\mu\nu} Q^2 - Q_\mu Q_\nu) \Pi_J^{(1)}(Q) - Q_\mu Q_\nu \Pi_J^{(0)}(Q)], \quad (363)$$

where Q_μ is a space-like momentum and $J_\mu \equiv V_\mu$ for a vector current and $J_\mu \equiv A_\mu$ for an axial-vector current. Defining $\Pi_J(Q) \equiv \Pi_J^{(0)}(Q) + \Pi_J^{(1)}(Q)$, the operator product expansion (OPE) of $\Pi_{V/A}(Q)$ is given by

$$\begin{aligned} & \Pi_{V/A}|_{\text{OPE}}(Q^2, \alpha_s) \\ &= c + C_1^{V/A}(Q^2) + C_m^{V/A}(Q^2) \frac{\bar{m}^2(Q)}{Q^2} + \sum_{q=u,d,s} C_{\bar{q}q}^{V/A}(Q^2) \frac{\langle m_q \bar{q}q \rangle}{Q^4} \\ & \quad + C_{GG}^{V/A}(Q^2) \frac{\langle \alpha_s GG \rangle}{Q^4} + \mathcal{O}(Q^{-6}), \end{aligned} \quad (364)$$

for large Q^2 . The perturbative coefficient functions $C_X^{V/A}(Q^2)$ for the operators X ($X = 1, \bar{q}q, GG$) are given as $C_X^{V/A}(Q^2) = \sum_{i \geq 0} \left(C_X^{V/A}\right)^{(i)} \alpha_s^i(Q^2)$ and \bar{m} is the running mass of the mass-degenerate up and down quarks. $C_1^{V/A}$ is known including α_s^4 in a continuum renormalization scheme such as the $\overline{\text{MS}}$ scheme [133–136]. Nonperturbatively, there are terms in $C_X^{V/A}$ that do not have a series expansion in α_s . For an example for the unit operator see Ref. [137]. The term c is Q -independent and divergent in the limit of infinite ultraviolet cutoff. However the Adler function defined as

$$D(Q^2) \equiv -Q^2 \frac{d\Pi(Q^2)}{dQ^2}, \quad (365)$$

is a scheme-independent finite quantity. Therefore one can determine the running-coupling constant in the $\overline{\text{MS}}$ scheme from the vacuum-polarization function computed by a lattice-QCD simulation. Of course, there is the choice whether to use the vector or the axial vector channel, or both, the canonical choice being $\Pi_{V+A} = \Pi_V + \Pi_A$. While perturbation theory does not distinguish between these channels, the nonperturbative contributions are different, and the quality of lattice data may differ, too. For a given choice, the lattice data of the vacuum polarization is fitted with the perturbative formula Eq. (364) with fit parameter $\Lambda_{\overline{\text{MS}}}$ parameterizing the running coupling $\alpha_{\overline{\text{MS}}}(Q^2)$.

While there is no problem in discussing the OPE at the nonperturbative level, the ‘condensates’ such as $\langle \alpha_s GG \rangle$ are ambiguous, since they mix with lower-dimensional operators including the unity operator. Therefore one should work in the high- Q^2 regime where power corrections are negligible within the given accuracy. Thus setting the renormalization scale as $\mu \equiv \sqrt{Q^2}$, one should seek, as always, the window $\Lambda_{\text{QCD}} \ll \mu \ll a^{-1}$.

9.6.2 Definitions in position space

The 2-point current correlation functions in position space contain the same physical information as in momentum space, but the technical details are sufficiently different to warrant a separate discussion. The (Euclidean) current-current correlation function for $J_{ff'}^\mu$ (with flavour indices f, f') is taken to be either the flavour non-diagonal vector or axial vector current, with the Lorentz indices contracted,

$$C_{A,V}(x) = - \sum_{\mu} \left\langle J_{ff'A,V}^\mu(x) J_{ff'A,V}^\mu(0) \right\rangle = \frac{6}{\pi^4(x^2)^3} \left(1 + \frac{\alpha_s}{\pi} + \mathcal{O}(\alpha_s^2) \right). \quad (366)$$

In the chiral limit, the perturbative expansion is known to α_s^4 [138], and is identical for vector and axial vector correlators. The only scale is set by the Euclidean distance $\mu = 1/|x|$ and the effective coupling can thus be defined as

$$\alpha_{\text{eff}}(\mu = 1/|x|) = \pi \left[(x^2)^3 (\pi^4/6) C_{A,V}(x) - 1 \right]. \quad (367)$$

As communicated to us by the authors of [32], there is a typo in Eq. (35) of [138]. For future reference, the numerical coefficients for the 3-loop conversion

$$\alpha_{\text{eff}}(\mu) = \alpha_{\overline{\text{MS}}}(\mu) + c_1 \alpha_{\overline{\text{MS}}}^2(\mu) + c_2 \alpha_{\overline{\text{MS}}}^3(\mu) + c_3 \alpha_{\overline{\text{MS}}}^4(\mu), \quad (368)$$

should read

$$c_1 = -1.4346, \quad c_2 = 0.16979, \quad c_3 = 3.21120. \quad (369)$$

9.6.3 Discussion of computations

Results using this method in momentum space are, to date, only available using overlap fermions or domain-wall fermions. Since the last review, FLAG 19, there has been one new computation, Cali 20 [32], which uses the vacuum polarization in position space, using $\mathcal{O}(a)$ improved Wilson fermions. The results are collected in Tab. 62 for $N_f = 2$, JLQCD/TWQCD 08C [139] and for $N_f = 2 + 1$, JLQCD 10 [140], Hudspith 18 [141] and Cali 20 [32].

Collaboration	Ref.	N_f	publication status	renormalization scale	perturbative behaviour	continuum extrapolation	scale	$\Lambda_{\overline{\text{MS}}}[\text{MeV}]$	$r_0\Lambda_{\overline{\text{MS}}}$
Cali 20	[32]	2+1	A	○	★	★	m_Υ^\S	342(17)	0.818(41) ^a
Hudspith 18	[141]	2+1	P	○	○	■	m_Ω^*	337(40)	0.806(96) ^b
Hudspith 15	[142]	2+1	C	○	○	■	m_Ω^*	300(24) ⁺	0.717(58)
JLQCD 10	[140]	2+1	A	■	○	■	$r_0 = 0.472 \text{ fm}$	247(5) [†]	0.591(12)
JLQCD/TWQCD 08C [139]		2	A	○	○	■	$r_0 = 0.49 \text{ fm}$	234(9)($^{+16}_-0$)	0.581(22)($^{+40}_-0$)

[§] via t_0/a^2 , still unpublished. We use $r_0 = 0.472 \text{ fm}$

* Determined in [143].

^a Evaluates to $\alpha_{\overline{\text{MS}}}^{(5)}(M_Z) = 0.11864(114)$

In conversion to $r_0\Lambda$ we used $r_0 = 0.472 \text{ fm}$.

^b $\alpha_{\overline{\text{MS}}}^{(5)}(M_Z) = 0.1181(27)(^{+8}_{-22})$. $\Lambda_{\overline{\text{MS}}}$ determined by us from $\alpha_{\overline{\text{MS}}}^{(3)}(2 \text{ GeV}) = 0.2961(185)$. In conversion to $r_0\Lambda$ we used $r_0 = 0.472 \text{ fm}$.

⁺ Determined by us from $\alpha_{\overline{\text{MS}}}^{(3)}(2 \text{ GeV}) = 0.279(11)$. Evaluates to $\alpha_{\overline{\text{MS}}}^{(5)}(M_Z) = 0.1155(18)$.

[†] $\alpha_{\overline{\text{MS}}}^{(5)}(M_Z) = 0.1118(3)(^{+16}_{-17})$.

Table 62: Results from the vacuum polarization in both momentum and position space

We first discuss the results of JLQCD/TWQCD 08C [139] and JLQCD 10 [140]. The fit to Eq. (364) is done with the 4-loop relation between the running coupling and $\Lambda_{\overline{\text{MS}}}$. It is found that without introducing condensate contributions, the momentum scale where the perturbative formula gives good agreement with the lattice results is very narrow, $aQ \simeq 0.8\text{--}1.0$. When a condensate contribution is included the perturbative formula gives good agreement with the lattice results for the extended range $aQ \simeq 0.6\text{--}1.0$. Since there is only a single lattice spacing $a \approx 0.11 \text{ fm}$ there is a ■ for the continuum limit. The renormalization scale μ is in the range of $Q = 1.6\text{--}2 \text{ GeV}$. Approximating $\alpha_{\text{eff}} \approx \alpha_{\overline{\text{MS}}}(Q)$, we estimate that $\alpha_{\text{eff}} = 0.25\text{--}0.30$ for $N_f = 2$ and $\alpha_{\text{eff}} = 0.29\text{--}0.33$ for $N_f = 2 + 1$. Thus we give a ○ and ■ for $N_f = 2$ and $N_f = 2 + 1$, respectively, for the renormalization scale and a ■ for the

perturbative behaviour.

A further investigation of this method was initiated in Hudspith 15 [142] and completed by Hudspith 18 [141] (see also [144]) based on domain-wall fermion configurations at three lattice spacings, $a^{-1} = 1.78, 2.38, 3.15$ GeV, with three different light-quark masses on the two coarser lattices and one on the fine lattice. An extensive discussion of condensates, using continuum finite-energy sum rules was employed to estimate where their contributions might be negligible. It was found that even up to terms of $O((1/Q^2)^8)$ (a higher order than depicted in Eq. (364) but with constant coefficients) no single condensate dominates and apparent convergence was poor for low Q^2 due to cancellations between contributions of similar size with alternating signs. (See, e.g., the list given by Hudspith 15 [142].) Choosing Q^2 to be at least $\sim 3.8 \text{ GeV}^2$ mitigated the problem, but then the coarsest lattice had to be discarded, due to large lattice artefacts. So this gives a ■ for continuum extrapolation. With the higher Q^2 the quark-mass dependence of the results was negligible, so ensembles with different quark masses were averaged over. A range of Q^2 from 3.8–16 GeV^2 gives $\alpha_{\text{eff}} = 0.31\text{--}0.22$, so there is a ○ for the renormalization scale. The value of α_{eff}^3 reaches $\Delta\alpha_{\text{eff}}/(8\pi b_0\alpha_{\text{eff}})$ and thus gives a ○ for perturbative behaviour. In Hudspith 15 [142] (superseded by Hudspith 18 [141]) about a 20% difference in $\Pi_V(Q^2)$ was seen between the two lattice spacings and a result is quoted only for the smaller a .

9.6.4 Vacuum polarization in position space

Cali 20 [32] evaluate the light-current 2-point function in position space. The 2-point functions for the nonperturbatively renormalized (non-singlet) flavour currents is computed for distances $|x|$ between 0.1 and 0.25 fm and extrapolated to the chiral limit. The available CLS configurations are used for this work, with lattice spacings between 0.039 and 0.086 fm. Despite fully nonperturbative renormalization and $\mathcal{O}(a)$ improvement, the remaining $\mathcal{O}(a^2)$ effects, as measured by $O(4)$ symmetry violations, are very large, even after subtraction of tree-level lattice effects. Therefore the authors performed a numerical stochastic perturbation theory (NSPT) simulation in order to determine the lattice artifacts at $\mathcal{O}(g^2)$. Only after subtraction of these effects the constrained continuum extrapolations from 3 different lattice directions to the same continuum limit are characterized by reasonable χ^2 -values, so the feasibility of the study crucially depends on this step. Interestingly, there is no subtraction performed of nonperturbative effects. For instance, chiral-symmetry breaking would manifest itself in a difference between the vector and the axial vector 2-point functions, and is invisible to perturbation theory, where these 2-point functions are known to α_s^4 [138]. According to the authors, phenomenological estimates suggest that a difference of 1.5% between the continuum correlators would occur around 0.3 fm and this difference would not be resolvable by their lattice data. Equality within their errors is confirmed for shorter distances. We note, however, that chiral symmetry breaking effects are but one class of nonperturbative effects, and their smallness does not allow for the conclusion that such effects are generally small. In fact, the need for explicit subtractions in momentum space analyses may lead one to suspect that such effects are not negligible at the available distance scales. For the determination of $\Lambda_{\overline{\text{MS}}}^{N_f=3}$ the authors limit the range of distances to 0.13–0.19 fm, where $\alpha_{\text{eff}} \in [0.2354, 0.3075]$ (private communication by the authors). These effective couplings are converted to $\overline{\text{MS}}$ couplings at the same scales $\mu = 1/|x|$ by solving Eq. (368) numerically. Central values for the Λ -parameter thus obtained are in the range 325–370 MeV (using the β -function at 5-loop order) and a weighted average yields the quoted result 342(17) MeV, where the average emphasizes

the data around $|x| = 0.16$ fm, or $\mu = 1.3$ GeV.

Applying the FLAG criteria the range of lattice spacings yields \star for the continuum extrapolation. However, the FLAG criterion implicitly assumes that the remaining cutoff effects after non-perturbative $\mathcal{O}(a)$ improvement are small, which is not the case here. Some hypercubic lattice artefacts are still rather large even after 1-loop subtraction, but these are not used for the analysis. As for the renormalization scale, the lowest effective coupling entering the analysis is $0.235 < 0.25$, so we give \circ . As for perturbative behaviour, for the range of couplings in the above interval α_{eff}^3 changes by $(0.308/0.235)^3 \approx 2.2$, marginally reaching $(3/2)^2 = 2.25$. The errors $\Delta\alpha_{\text{eff}}$ after continuum and chiral extrapolations are 4–6% (private communication by the authors) and the induced uncertainty in Λ is comfortably above $2\alpha_{\text{eff}}^3$, which gives a \star according to FLAG criteria.

Although the current FLAG criteria are formally passed by this result, the quoted error of 5% for Λ seems very optimistic. We have performed a simple test, converting to the $\overline{\text{MS}}$ scheme by inverting Eq. (368) perturbatively (instead of solving the fixed-order equation numerically). The differences between the couplings are of order α_s^5 and thus indicative of the sensitivity to perturbative truncation errors. The resulting Λ -parameter estimates are now in the range 409–468 MeV, i.e. ca. 15–30% larger than before. While the difference between both estimates decreases proportionally to the expected α_{eff}^3 , an extraction of the Λ -parameter in this energy range is a priori affected by systematic uncertainties corresponding to such differences. The FLAG criterion might fail to capture this e.g. if the assumption of an $\mathcal{O}(1)$ coefficient for the asymptotic α_{eff}^3 behaviour is not correct. Some indication for a problematic behaviour is indeed seen when perturbatively inverting Eq. (368) to order α_s^3 . The resulting $\overline{\text{MS}}$ couplings are then closer to the values used in CalI 20, although the difference is formally $\mathcal{O}(\alpha_s^4)$ rather than $\mathcal{O}(\alpha_s^5)$.

9.7 α_s from observables at the lattice spacing scale

9.7.1 General considerations

The general method is to evaluate a short-distance quantity \mathcal{Q} at the scale of the lattice spacing $\sim 1/a$ and then determine its relationship to $\alpha_{\overline{\text{MS}}}$ via a perturbative expansion.

This is epitomized by the strategy of the HPQCD collaboration [145, 146], discussed here for illustration, which computes and then fits to a variety of short-distance quantities

$$Y = \sum_{n=1}^{n_{\text{max}}} c_n \alpha_{V'}^n(q^*). \quad (370)$$

The quantity Y is taken as the logarithm of small Wilson loops (including some nonplanar ones), Creutz ratios, ‘tadpole-improved’ Wilson loops and the tadpole-improved or ‘boosted’ bare coupling ($\mathcal{O}(20)$ quantities in total). The perturbative coefficients c_n (each depending on the choice of Y) are known to $n = 3$ with additional coefficients up to n_{max} being fitted numerically. The running coupling $\alpha_{V'}$ is related to α_V from the static-quark potential (see Sec. 9.5).¹⁰

The coupling constant is fixed at a scale $q^* = d/a$. The latter is chosen as the mean value of $\ln q$ with the one-gluon loop as measure [147, 148]. (Thus a different result for d is found for every short-distance quantity.) A rough estimate yields $d \approx \pi$, and in general the renormalization scale is always found to lie in this region.

¹⁰ $\alpha_{V'}$ is defined by $\Lambda_{V'} = \Lambda_V$ and $b_i^{V'} = b_i^V$ for $i = 0, 1, 2$ but $b_i^{V'} = 0$ for $i \geq 3$.

For example, for the Wilson loop $W_{mn} \equiv \langle W(ma, na) \rangle$ we have

$$\ln \left(\frac{W_{mn}}{u_0^{2(m+n)}} \right) = c_1 \alpha_{V'}(q^*) + c_2 \alpha_{V'}^2(q^*) + c_3 \alpha_{V'}^3(q^*) + \dots, \quad (371)$$

for the tadpole-improved version, where c_1, c_2, \dots are the appropriate perturbative coefficients and $u_0 = W_{11}^{1/4}$. Substituting the nonperturbative simulation value in the left hand side, we can determine $\alpha_{V'}(q^*)$, at the scale q^* . Note that one finds empirically that perturbation theory for these tadpole-improved quantities have smaller c_n coefficients and so the series has a faster apparent convergence compared to the case without tadpole improvement.

Using the β -function in the V' scheme, results can be run to a reference value, chosen as $\alpha_0 \equiv \alpha_{V'}(q_0)$, $q_0 = 7.5 \text{ GeV}$. This is then converted perturbatively to the continuum $\overline{\text{MS}}$ scheme

$$\alpha_{\overline{\text{MS}}}(q_0) = \alpha_0 + d_1 \alpha_0^2 + d_2 \alpha_0^3 + \dots, \quad (372)$$

where d_1, d_2 are known 1- and 2-loop coefficients.

Other collaborations have focused more on the bare ‘boosted’ coupling constant and directly determined its relationship to $\alpha_{\overline{\text{MS}}}$. Specifically, the boosted coupling is defined by

$$\alpha_P(1/a) = \frac{1}{4\pi} \frac{g_0^2}{u_0^4}, \quad (373)$$

again determined at a scale $\sim 1/a$. As discussed previously, since the plaquette expectation value in the boosted coupling contains the tadpole-diagram contributions to all orders, which are dominant contributions in perturbation theory, there is an expectation that the perturbation theory using the boosted coupling has smaller perturbative coefficients [147], and hence smaller perturbative errors.

9.7.2 Continuum limit

Lattice results always come along with discretization errors, which one needs to remove by a continuum extrapolation. As mentioned previously, in this respect the present method differs in principle from those in which α_s is determined from physical observables. In the general case, the numerical results of the lattice simulations at a value of μ fixed in physical units can be extrapolated to the continuum limit, and the result can be analyzed as to whether it shows perturbative running as a function of μ in the continuum. For observables at the cutoff-scale ($q^* = d/a$), discretization effects cannot easily be separated out from perturbation theory, as the scale for the coupling comes from the lattice spacing. Therefore the restriction $a\mu \ll 1$ (the ‘continuum-extrapolation’ criterion) is not applicable here. Discretization errors of order a^2 are, however, present. Since $a \sim \exp(-1/(2b_0 g_0^2)) \sim \exp(-1/(8\pi b_0 \alpha(q^*)))$, these errors now appear as power corrections to the perturbative running, and have to be taken into account in the study of the perturbative behaviour, which is to be verified by changing a . One thus usually fits with power corrections in this method.

In order to keep a symmetry with the ‘continuum-extrapolation’ criterion for physical observables and to remember that discretization errors are, of course, relevant, we replace it here by one for the lattice spacings used:

- Lattice spacings

- ★ 3 or more lattice spacings, at least 2 points below $a = 0.1$ fm
- 2 lattice spacings, at least 1 point below $a = 0.1$ fm
- otherwise

9.7.3 Discussion of computations

Note that due to $\mu \sim 1/a$ being relatively large the results easily have a ★ or ○ in the rating on renormalization scale.

The work of El-Khadra 92 [158] employs a 1-loop formula to relate $\alpha_{\overline{\text{MS}}}^{(0)}(\pi/a)$ to the boosted coupling for three lattice spacings $a^{-1} = 1.15, 1.78, 2.43$ GeV. (The lattice spacing is determined from the charmonium 1S-1P splitting.) They obtain $\Lambda_{\overline{\text{MS}}}^{(0)} = 234$ MeV, corresponding to $\alpha_{\text{eff}} = \alpha_{\overline{\text{MS}}}^{(0)}(\pi/a) \approx 0.15\text{--}0.2$. The work of Aoki 94 [155] calculates $\alpha_V^{(2)}$ and $\alpha_{\overline{\text{MS}}}^{(2)}$ for a single lattice spacing $a^{-1} \sim 2$ GeV, again determined from charmonium 1S-1P splitting in two-flavour QCD. Using 1-loop perturbation theory with boosted coupling, they obtain $\alpha_V^{(2)} = 0.169$ and $\alpha_{\overline{\text{MS}}}^{(2)} = 0.142$. Davies 94 [154] gives a determination of α_V from the expansion

$$-\ln W_{11} \equiv \frac{4\pi}{3} \alpha_V^{(N_f)}(3.41/a) \times [1 - (1.185 + 0.070N_f)\alpha_V^{(N_f)}], \quad (374)$$

neglecting higher-order terms. They compute the Υ spectrum in $N_f = 0, 2$ QCD for single lattice spacings at $a^{-1} = 2.57, 2.47$ GeV and obtain $\alpha_V(3.41/a) \simeq 0.15, 0.18$, respectively. Extrapolating the inverse coupling linearly in N_f , a value of $\alpha_V^{(3)}(8.3 \text{ GeV}) = 0.196(3)$ is obtained. SESAM 99 [152] follows a similar strategy, again for a single lattice spacing. They linearly extrapolated results for $1/\alpha_V^{(0)}, 1/\alpha_V^{(2)}$ at a fixed scale of 9 GeV to give $\alpha_V^{(3)}$, which is then perturbatively converted to $\alpha_{\overline{\text{MS}}}^{(3)}$. This finally gave $\alpha_{\overline{\text{MS}}}^{(5)}(M_Z) = 0.1118(17)$. Wingate 95 [153] also follows this method. With the scale determined from the charmonium 1S-1P splitting for single lattice spacings in $N_f = 0, 2$ giving $a^{-1} \simeq 1.80$ GeV for $N_f = 0$ and $a^{-1} \simeq 1.66$ GeV for $N_f = 2$, they obtain $\alpha_V^{(0)}(3.41/a) \simeq 0.15$ and $\alpha_V^{(2)} \simeq 0.18$, respectively. Extrapolating the inverse coupling linearly in N_f , they obtain $\alpha_V^{(3)}(6.48 \text{ GeV}) = 0.194(17)$.

The QCDSF/UKQCD collaboration, QCDSF/UKQCD 05 [151], [159–161], use the 2-loop relation (re-written here in terms of α)

$$\frac{1}{\alpha_{\overline{\text{MS}}}(\mu)} = \frac{1}{\alpha_P(1/a)} + 4\pi(2b_0 \ln a\mu - t_1^P) + (4\pi)^2(2b_1 \ln a\mu - t_2^P)\alpha_P(1/a), \quad (375)$$

where t_1^P and t_2^P are known. (A 2-loop relation corresponds to a 3-loop lattice β -function.) This was used to directly compute $\alpha_{\overline{\text{MS}}}$, and the scale was chosen so that the $\mathcal{O}(\alpha_P^0)$ term vanishes, i.e.,

$$\mu^* = \frac{1}{a} \exp[t_1^P/(2b_0)] \approx \begin{cases} 2.63/a & N_f = 0 \\ 1.4/a & N_f = 2 \end{cases}. \quad (376)$$

The method is to first compute $\alpha_P(1/a)$ and from this, using Eq. (375) to find $\alpha_{\overline{\text{MS}}}(\mu^*)$. The RG equation, Eq. (320), then determines $\mu^*/\Lambda_{\overline{\text{MS}}}$ and hence using Eq. (376) leads to the result for $r_0\Lambda_{\overline{\text{MS}}}$. This avoids giving the scale in MeV until the end. In the $N_f = 0$ case seven lattice spacings were used [62], giving a range $\mu^*/\Lambda_{\overline{\text{MS}}} \approx 24\text{--}72$ (or $a^{-1} \approx 2\text{--}7$ GeV) and $\alpha_{\text{eff}} = \alpha_{\overline{\text{MS}}}(\mu^*) \approx 0.15\text{--}0.10$. Neglecting higher-order perturbative terms (see discussion

Collaboration	Ref.	N_f	publication status	renormalization scale	perturbative behaviour	lattice spacings	scale	$\Lambda_{\overline{\text{MS}}}[\text{MeV}]$	$r_0\Lambda_{\overline{\text{MS}}}$
HPQCD 10 ^a §	[149]	2+1	A	○	★	★	$r_1 = 0.3133(23)$ fm	340(9)	0.812(22)
HPQCD 08A ^a	[146]	2+1	A	○	★	★	$r_1 = 0.321(5)$ fm ^{††}	338(12) [*]	0.809(29)
Maltman 08 ^a	[150]	2+1	A	○	○	★	$r_1 = 0.318$ fm	352(17) [†]	0.841(40)
HPQCD 05A ^a	[145]	2+1	A	○	○	○	r_1 ^{††}	319(17) ^{**}	0.763(42)
QCDSF/UKQCD 05	[151]	2	A	★	■	★	$r_0 = 0.467(33)$ fm	261(17)(26)	0.617(40)(21) ^b
SESAM 99 ^c	[152]	2	A	○	■	■	$c\bar{c}(1S-1P)$		
Wingate 95 ^d	[153]	2	A	★	■	■	$c\bar{c}(1S-1P)$		
Davies 94 ^e	[154]	2	A	★	■	■	Υ		
Aoki 94 ^f	[155]	2	A	★	■	■	$c\bar{c}(1S-1P)$		
Kitazawa 16	[156]	0	A	★	★	★	w_0	260(5) ^j	0.621(11) ^j
FlowQCD 15	[157]	0	P	★	★	★	$w_{0.4}$ ⁱ	258(6) ⁱ	0.618(11) ⁱ
QCDSF/UKQCD 05	[151]	0	A	★	○	★	$r_0 = 0.467(33)$ fm	259(1)(20)	0.614(2)(5) ^b
SESAM 99 ^c	[152]	0	A	★	■	■	$c\bar{c}(1S-1P)$		
Wingate 95 ^d	[153]	0	A	★	■	■	$c\bar{c}(1S-1P)$		
Davies 94 ^e	[154]	0	A	★	■	■	Υ		
El-Khadra 92 ^g	[158]	0	A	★	■	○	$c\bar{c}(1S-1P)$	234(10)	0.560(24) ^h

^a The numbers for Λ have been converted from the values for $\alpha_s^{(5)}(M_Z)$.

§ $\alpha_{\overline{\text{MS}}}^{(3)}(5 \text{ GeV}) = 0.2034(21)$, $\alpha_{\overline{\text{MS}}}^{(5)}(M_Z) = 0.1184(6)$, only update of intermediate scale and c -, b -quark masses, supersedes HPQCD 08A.

† $\alpha_{\overline{\text{MS}}}^{(5)}(M_Z) = 0.1192(11)$.

* $\alpha_V^{(3)}(7.5 \text{ GeV}) = 0.2120(28)$, $\alpha_{\overline{\text{MS}}}^{(5)}(M_Z) = 0.1183(8)$, supersedes HPQCD 05.

†† Scale is originally determined from Υ mass splitting. r_1 is used as an intermediate scale. In conversion to $r_0\Lambda_{\overline{\text{MS}}}$, r_0 is taken to be 0.472 fm.

** $\alpha_V^{(3)}(7.5 \text{ GeV}) = 0.2082(40)$, $\alpha_{\overline{\text{MS}}}^{(5)}(M_Z) = 0.1170(12)$.

^b This supersedes Refs. [159–161]. $\alpha_{\overline{\text{MS}}}^{(5)}(M_Z) = 0.112(1)(2)$. The $N_f = 2$ results were based on values for r_0/a which have later been found to be too small [57]. The effect will be of the order of 10–15%, presumably an increase in Λr_0 .

^c $\alpha_{\overline{\text{MS}}}^{(5)}(M_Z) = 0.1118(17)$.

^d $\alpha_V^{(3)}(6.48 \text{ GeV}) = 0.194(7)$ extrapolated from $N_f = 0, 2$. $\alpha_{\overline{\text{MS}}}^{(5)}(M_Z) = 0.107(5)$.

^e $\alpha_P^{(3)}(8.2 \text{ GeV}) = 0.1959(34)$ extrapolated from $N_f = 0, 2$. $\alpha_{\overline{\text{MS}}}^{(5)}(M_Z) = 0.115(2)$.

^f Estimated $\alpha_{\overline{\text{MS}}}^{(5)}(M_Z) = 0.108(5)(4)$.

^g This early computation violates our requirement that scheme conversions are done at the 2-loop level. $\Lambda_{\overline{\text{MS}}}^{(4)} = 160_{(-37)}^{(+47)} \text{ MeV}$, $\alpha_{\overline{\text{MS}}}^{(4)}(5 \text{ GeV}) = 0.174(12)$. We converted this number to give $\alpha_{\overline{\text{MS}}}^{(5)}(M_Z) = 0.106(4)$.

^h We used $r_0 = 0.472$ fm to convert to $r_0\Lambda_{\overline{\text{MS}}}$.

ⁱ Reference scale $w_{0.4}$ where w_x is defined by $t\partial_t[t^2\langle E(t)\rangle]_{t=w_x^2} = x$ in terms of the action density $E(t)$ at positive flow time t [157]. Our conversion to r_0 scale using [157] $r_0/w_{0.4} = 2.587(45)$ and $r_0 = 0.472$ fm.

^j Our conversion from $w_0\Lambda_{\overline{\text{MS}}} = 0.2154(12)$ to r_0 scale using $r_0/w_0 = (r_0/w_{0.4}) \cdot (w_{0.4}/w_0) = 2.885(50)$ with the factors cited by the collaboration [157] and with $r_0 = 0.472$ fm.

Table 63: Wilson loop results. Some early results for $N_f = 0, 2$ did not determine $\Lambda_{\overline{\text{MS}}}$.

after Eq. (377) below) in Eq. (375) this is sufficient to allow a continuum extrapolation of $r_0\Lambda_{\overline{\text{MS}}}$. A similar computation for $N_f = 2$ by QCDSF/UKQCD 05 [151] gave $\mu^*/\Lambda_{\overline{\text{MS}}} \approx 12\text{--}17$ (or roughly $a^{-1} \approx 2\text{--}3$ GeV) and $\alpha_{\text{eff}} = \alpha_{\overline{\text{MS}}}(\mu^*) \approx 0.20\text{--}0.18$. The $N_f = 2$ results of QCDSF/UKQCD 05 [151] are affected by an uncertainty which was not known at the time of publication: It has been realized that the values of r_0/a of Ref. [151] were significantly too low [57]. As this effect is expected to depend on a , it influences the perturbative behaviour leading us to assign a ■ for that criterion.

Since FLAG 13, there has been one new result for $N_f = 0$ by FlowQCD 15 [157], later updated and published in Kitazawa 16 [156]. They also use the techniques as described in Eqs. (375), (376), but together with the gradient flow scale w_0 (rather than the r_0 scale) leading to a determination of $w_0\Lambda_{\overline{\text{MS}}}$. The continuum limit is estimated by extrapolating the data at 6 lattice spacings linearly in a^2 . The data range used is $\mu^*/\Lambda_{\overline{\text{MS}}} \approx 50\text{--}120$ (or $a^{-1} \approx 5\text{--}11$ GeV) and $\alpha_{\overline{\text{MS}}}(\mu^*) \approx 0.12\text{--}0.095$. Since a very small value of $\alpha_{\overline{\text{MS}}}$ is reached, there is a ★ in the perturbative behaviour. Note that our conversion to the common r_0 scale unfortunately leads to a significant increase of the error of the Λ parameter compared to using w_0 directly [68]. Again we note that the results of QCDSF/UKQCD 05 [151] ($N_f = 0$) and Kitazawa 16 [156] may be affected by frozen topology as they have lattice spacings significantly below $a = 0.05$ fm. Kitazawa 16 [156] investigate this by evaluating w_0/a in a fixed topology and estimate any effect at about $\sim 1\%$.

The work of HPQCD 05A [145] (which supersedes the original work [162]) uses three lattice spacings $a^{-1} \approx 1.2, 1.6, 2.3$ GeV for $2 + 1$ flavour QCD. Typically the renormalization scale $q \approx \pi/a \approx 3.50\text{--}7.10$ GeV, corresponding to $\alpha_{V'} \approx 0.22\text{--}0.28$.

In the later update HPQCD 08A [146] twelve data sets (with six lattice spacings) are now used reaching up to $a^{-1} \approx 4.4$ GeV, corresponding to $\alpha_{V'} \approx 0.18$. The values used for the scale r_1 were further updated in HPQCD 10 [149]. Maltman 08 [150] uses most of the same lattice ensembles as HPQCD 08A [146], but not the one at the smallest lattice spacing, $a \approx 0.045$ fm. Maltman 08 [150] also considers a much smaller set of quantities (three versus 22) that are less sensitive to condensates. They also use different strategies for evaluating the condensates and for the perturbative expansion, and a slightly different value for the scale r_1 . The central values of the final results from Maltman 08 [150] and HPQCD 08A [146] differ by 0.0009 (which would be decreased to 0.0007 taking into account a reduction of 0.0002 in the value of the r_1 scale used by Maltman 08 [150]).

As mentioned before, the perturbative coefficients are computed through 3-loop order [163], while the higher-order perturbative coefficients c_n with $n_{\text{max}} \geq n > 3$ (with $n_{\text{max}} = 10$) are numerically fitted using the lattice-simulation data for the lattice spacings with the help of Bayesian methods. It turns out that corrections in Eq. (371) are of order $|c_i/c_1|\alpha^i = 5\text{--}15\%$ and $3\text{--}10\%$ for $i = 2, 3$, respectively. The inclusion of a fourth-order term is necessary to obtain a good fit to the data, and leads to a shift of the result by 1 – 2 sigma. For all but one of the 22 quantities, central values of $|c_4/c_1| \approx 2\text{--}4$ were found, with errors from the fits of ≈ 2 . It should be pointed out that the description of lattice results for the short distance quantities does not require Bayesian priors, once the term proportional to c_4 is included [150]. We also stress that different short distance quantities have quite different nonperturbative contributions [164]. Hence the fact that different observables lead to consistent α_s values is a nontrivial check of the approach.

An important source of uncertainty is the truncation of perturbation theory. In HPQCD 08A [146], 10 [149] it is estimated to be about 0.4% of $\alpha_{\overline{\text{MS}}}(M_Z)$. In FLAG 13 we included a rather detailed discussion of the issue with the result that we prefer for the time being a

more conservative error based on the above estimate $|c_4/c_1| = 2$. From Eq. (370) this gives an estimate of the uncertainty in α_{eff} of

$$\Delta\alpha_{\text{eff}}(\mu_1) = \left| \frac{c_4}{c_1} \right| \alpha_{\text{eff}}^4(\mu_1), \quad (377)$$

at the scale μ_1 where α_{eff} is computed from the Wilson loops. This can be used with a variation in Λ at lowest order of perturbation theory and also applied to α_s evolved to a different scale μ_2 ,¹¹

$$\frac{\Delta\Lambda}{\Lambda} = \frac{1}{8\pi b_0\alpha_s} \frac{\Delta\alpha_s}{\alpha_s}, \quad \frac{\Delta\alpha_s(\mu_2)}{\Delta\alpha_s(\mu_1)} = \frac{\alpha_s^2(\mu_2)}{\alpha_s^2(\mu_1)}. \quad (378)$$

With $\mu_2 = M_Z$ and $\alpha_s(\mu_1) = 0.2$ (a typical value extracted from Wilson loops in HPQCD 10 [149], HPQCD 08A [146] at $\mu = 5$ GeV) we have

$$\Delta\alpha_{\overline{\text{MS}}}(m_Z) = 0.0012, \quad (379)$$

which we shall later use as the typical perturbative uncertainty of the method with $2 + 1$ fermions.

Tab. 63 summarizes the results. Within the errors of 3–5% $N_f = 3$ determinations of $r_0\Lambda$ nicely agree.

9.8 α_s from heavy-quark current two-point functions

9.8.1 General considerations

The method has been introduced in HPQCD 08, Ref. [165], and updated in HPQCD 10, Ref. [149], see also Ref. [166]. In addition there is a 2+1+1-flavour result, HPQCD 14A [167].

The basic observable is constructed from a current,

$$J(x) = iam_c \bar{\psi}_c(x) \gamma_5 \psi_{c'}(x), \quad (380)$$

of two mass-degenerate heavy-valence quarks, c, c' , usually taken to be at or around the charm-quark mass. The pre-factor m_c denotes the bare mass of the quark. When the lattice discretization respects chiral symmetry, $J(x)$ is a renormalization group invariant local field, i.e., it requires no renormalization. Staggered fermions and twisted-mass fermions have such a residual chiral symmetry. The (Euclidean) time-slice correlation function

$$G(x_0) = a^6 \sum_{\vec{x}} \langle J^\dagger(x) J(0) \rangle, \quad (381)$$

$(J^\dagger(x) = iam_c \bar{\psi}_{c'}(x) \gamma_5 \psi_c(x))$ has a $\sim x_0^{-3}$ singularity at short distances and moments

$$G_n = a \sum_{x_0=-(T/2-a)}^{T/2-a} x_0^n G(x_0) \quad (382)$$

are nonvanishing for even n and furthermore finite for $n \geq 4$. Here T is the time extent of the lattice. The moments are dominated by contributions at x_0 of order $1/m_c$. For large mass m_c

¹¹From Eq. (327) we see that at low order in PT the coupling α_s is continuous and differentiable across the mass thresholds (at the same scale). Therefore to leading order α_s and $\Delta\alpha_s$ are independent of N_f .

these are short distances and the moments become increasingly perturbative for decreasing n . Denoting the lowest-order perturbation theory moments by $G_n^{(0)}$, one defines the normalized moments

$$R_n = \begin{cases} G_4/G_4^{(0)} & \text{for } n = 4, \\ \frac{am_{\eta_c}}{2am_c} \left(\frac{G_n}{G_n^{(0)}} \right)^{1/(n-4)} & \text{for } n \geq 6, \end{cases} \quad (383)$$

of even order n . Note that Eq. (380) contains the variable (bare) heavy-quark mass m_c . The normalization $G_n^{(0)}$ is introduced to help in reducing lattice artifacts. In addition, one can also define moments with different normalizations,

$$\tilde{R}_n = 2R_n/m_{\eta_c} \quad \text{for } n \geq 6. \quad (384)$$

While \tilde{R}_n also remains renormalization-group invariant, it now also has a scale which might introduce an additional ambiguity [168].

The normalized moments can then be parameterized in terms of functions

$$R_n \equiv \begin{cases} r_4(\alpha_s(\mu)) & \text{for } n = 4, \\ \frac{m_{\eta_c}}{2\tilde{m}_c(\mu_m)} r_n(\alpha_s(\mu)) & \text{for } n \geq 6, \end{cases} \quad (385)$$

with $\tilde{m}_c(\mu_m)$ being the renormalized heavy-quark mass. The scale μ_m at which the heavy-quark mass is defined could be different from the scale μ at which α_s is defined [169]. The HPQCD collaboration, however, used the choice $\mu = \mu_m = 3m_c(\mu)$. This ensures that the renormalization scale is never too small. The reduced moments r_n have a perturbative expansion

$$r_n = 1 + r_{n,1}\alpha_s + r_{n,2}\alpha_s^2 + r_{n,3}\alpha_s^3 + \dots, \quad (386)$$

where the written terms $r_{n,i}(\mu/\tilde{m}_c(\mu))$, $i \leq 3$ are known for low n from Refs. [170–174]. In practice, the expansion is performed in the $\overline{\text{MS}}$ scheme. Matching nonperturbative lattice results for the moments to the perturbative expansion, one determines an approximation to $\alpha_{\overline{\text{MS}}}(\mu)$ as well as $\tilde{m}_c(\mu)$. With the lattice spacing (scale) determined from some extra physical input, this calibrates μ . As usual suitable pseudoscalar masses determine the bare-quark masses, here in particular the charm mass, and then through Eq. (385) the renormalized charm-quark mass.

A difficulty with this approach is that large masses are needed to enter the perturbative domain. Lattice artifacts can then be sizeable and have a complicated form. The ratios in Eq. (383) use the tree-level lattice results in the usual way for normalization. This results in unity as the leading term in Eq. (386), suppressing some of the kinematical lattice artifacts. We note that in contrast to, e.g., the definition of α_{qq} , here the cutoff effects are of order $a^k\alpha_s$, while there the tree-level term defines α_s and therefore the cutoff effects after tree-level improvement are of order $a^k\alpha_s^2$. To obtain the continuum results for the moments it is important to perform fits with high powers of a . This implies many fit parameters. To deal with this problem the HPQCD collaboration used Bayesian fits of their lattice results. More recent analyses of the moments, however, did not rely on Bayesian fits [33, 34, 168, 175].

Finite-size effects (FSE) due to the omission of $|x_0| > T/2$ in Eq. (382) grow with n as $(m_{\eta_c} T/2)^n \exp(-m_{\eta_c} T/2)$. In practice, however, since the (lower) moments are short-distance dominated, the FSE are expected to be small at the present level of precision. Possible exception could be the ratio R_8/R_{10} , where the finite-volume effects could be significant as discussed below.

Moments of correlation functions of the quark's electromagnetic current can also be obtained from experimental data for e^+e^- annihilation [176, 177]. This enables a nonlattice determination of α_s using a similar analysis method. In particular, the same continuum perturbation-theory computation enters both the lattice and the phenomenological determinations.

9.8.2 Discussion of computations

The determination of the strong-coupling constant from the moments of quarkonium correlators by HPQCD collaboration have been discussed in detail in the FLAG 2016 and 2019 reports. Therefore, we only give the summary of these determinations in Table 64.

Two additional computations have appeared between the FLAG 16 and the FLAG 19 reports. We re-discuss them here (see also the summary section), as the assessment in FLAG 19 was partially based on an inconsistent use of the FLAG criteria and has now been changed. Maezawa and Petreczky, [175] computed the two-point functions of the $c\bar{c}$ pseudoscalar operator and obtained R_4 , R_6/R_8 and R_8/R_{10} based on the HotQCD collaboration HISQ staggered ensembles, [52]. The scale is set by measuring $r_1 = 0.3106(18)$ fm. Continuum limits are taken fitting the lattice-spacing dependence with $a^2 + a^4$ form as the best fit. For R_4 , they also employ other forms for fit functions such as a^2 , $\alpha_s^{\text{boosted}} a^2 + a^4$, etc., the results agreeing within errors. Matching R_4 with the 3-loop formula Eq. (386) through order $\alpha_{\overline{\text{MS}}}^3$ [170], where μ is fixed to m_c , they obtain $\alpha_{\overline{\text{MS}}}^{(3)}(\mu = m_c) = 0.3697(54)(64)(15)$. The first error is statistical, the second is the uncertainty in the continuum extrapolation, and the third is the truncation error in the perturbative approximation of r_4 . This last error is estimated by the ‘‘typical size’’ of the missing 4-loop contribution, which they assume to be $\alpha_{\overline{\text{MS}}}^4(\mu)$ multiplied by 2 times the 3-loop coefficient $2 \times r_{4,3} \times \alpha_{\overline{\text{MS}}}^4(\mu) = 0.2364 \times \alpha_{\overline{\text{MS}}}^4(\mu)$. The result is converted to

$$\alpha_{\overline{\text{MS}}}^{(5)}(M_Z) = 0.11622(84). \quad (387)$$

Since $\alpha_{\text{eff}} = 0.38$ we assign \blacksquare for the criterion of the renormalization scale. As $\Delta\Lambda/\Lambda < \alpha_{\text{eff}}^2$, we assign \blacksquare for the criterion of perturbative behaviour. The lattice cutoff ranges as $a^{-1} = 1.42\text{--}4.89$ GeV with $\mu = 2m_c \sim 2.6$ GeV so that we assign \circ for continuum extrapolation.

JLQCD 16 [168] also computed the two-point functions of the $c\bar{c}$ pseudoscalar operator and obtained R_6 , R_8 , R_{10} and their ratios based on 2+1-flavour QCD with Möbius domain-wall quark for three lattice cutoff $a^{-1} = 2.5, 3.6, 4.5$ GeV. The scale is set by $\sqrt{t_0} = 0.1465(21)(13)$ fm. The continuum limit is taken assuming linear dependence on a^2 . They find a sizeable lattice-spacing dependence of R_4 , which is therefore not used in their analysis, but for R_6, R_8, R_{10} the dependence is mild giving reasonable control over the continuum limit. They use the perturbative formulae for the vacuum polarization in the pseudoscalar channel Π_{PS} through order $\alpha_{\overline{\text{MS}}}^3$ in the $\overline{\text{MS}}$ scheme [172, 173] to obtain $\alpha_{\overline{\text{MS}}}^{(4)}$. Combining the matching of lattice results with continuum perturbation theory for $R_6, R_6/R_8$ and R_{10} , they obtain $\alpha_{\overline{\text{MS}}}^{(4)}(\mu = 3 \text{ GeV}) = 0.2528(127)$, where the error is dominated by the perturbative truncation error. To estimate the truncation error they study the dependence of the final

Collaboration	Ref.	N_f		publication status	renormalization scale	perturbative behaviour	continuum extrapolation	scale	$\Lambda_{\overline{\text{MS}}}[\text{MeV}]$	$r_0\Lambda_{\overline{\text{MS}}}$
HPQCD 14A	[167]	2+1+1	A	○	★	○		$w_0 = 0.1715(9) \text{ fm}^a$	$294(11)^{bc}$	$0.703(26)$
Petreczky 20	[33]	2+1	P	○	○	★		$r_1 = 0.3106(18) \text{ fm}$	$332(17)^h$	$0.792(41)^g$
Boito 20	[36]	2+1	A	■	■	○		$m_c(m_c) = 1.28(2) \text{ GeV}$	$328(30)^h$	$0.785(72)$
Petreczky 19, $m_h=m_c$	[34]	2+1	A	■	■	★		$r_1 = 0.3106(18) \text{ fm}^g$	$314(10)$	$0.751(24)^g$
Petreczky 19, $\frac{m_h}{m_c}=1.5$	[34]	2+1	A	■	■	○		$r_1 = 0.3106(18) \text{ fm}^g$	$310(10)$	$0.742(24)^g$
Maezawa 16	[175]	2+1	A	■	■	○		$r_1 = 0.3106(18) \text{ fm}^d$	$309(10)^e$	$0.739(24)^e$
JLQCD 16	[168]	2+1	A	■	○	○		$\sqrt{t_0} = 0.1465(25) \text{ fm}$	$331(38)^f$	$0.792(89)^f$
HPQCD 10	[149]	2+1	A	○	★	○		$r_1 = 0.3133(23) \text{ fm}^\dagger$	$338(10)^*$	$0.809(25)$
HPQCD 08B	[165]	2+1	A	■	■	■		$r_1 = 0.321(5) \text{ fm}^\dagger$	$325(18)^+$	$0.777(42)$

^a Scale determined in [178] using f_π .

^b $\alpha_{\overline{\text{MS}}}^{(4)}(5 \text{ GeV}) = 0.2128(25)$, $\alpha_{\overline{\text{MS}}}^{(5)}(M_Z) = 0.11822(74)$.

^c We evaluated $\Lambda_{\overline{\text{MS}}}^{(4)}$ from $\alpha_{\overline{\text{MS}}}^{(4)}$. We also used $r_0 = 0.472 \text{ fm}$.

^d Scale is determined from f_π .

^e $\alpha_{\overline{\text{MS}}}^{(3)}(m_c = 1.267 \text{ GeV}) = 0.3697(85)$, $\alpha_{\overline{\text{MS}}}^{(5)}(M_Z) = 0.11622(84)$. Our conversion with $r_0 = 0.472 \text{ fm}$.

^f We evaluated $\Lambda_{\overline{\text{MS}}}^{(3)}$ from the given $\alpha_{\overline{\text{MS}}}^{(4)}(3 \text{ GeV}) = 0.2528(127)$. $\alpha_{\overline{\text{MS}}}^{(5)}(M_Z) = 0.1177(26)$. We also used $r_0 = 0.472 \text{ fm}$ to convert.

^g We used $r_0 = 0.472 \text{ fm}$ to convert.

^h We back-engineered from $\alpha_{\overline{\text{MS}}}^{(5)}(M_Z) = 0.1177(20)$. We used $r_0 = 0.472 \text{ fm}$ to convert.

^{*} $\alpha_{\overline{\text{MS}}}^{(3)}(5 \text{ GeV}) = 0.2034(21)$, $\alpha_{\overline{\text{MS}}}^{(5)}(M_Z) = 0.1183(7)$.

[†] Scale is determined from Υ mass splitting.

⁺ We evaluated $\Lambda_{\overline{\text{MS}}}^{(3)}$ from the given $\alpha_{\overline{\text{MS}}}^{(4)}(3 \text{ GeV}) = 0.251(6)$. $\alpha_{\overline{\text{MS}}}^{(5)}(M_Z) = 0.1174(12)$.

Table 64: Heavy-quark current two-point function results. Note that all analysis using $2+1$ flavour simulations perturbatively add a dynamical charm quark. Partially they then quote results in $N_f = 4$ -flavour QCD, which we converted back to $N_f = 3$, corresponding to the nonperturbative sea quark content.

result on the choice of the renormalization scales μ , μ_m which are used as renormalization scales for α_s and the quark mass. Independently [169] the two scales are varied in the range of 2 GeV to 4 GeV. The above result is converted to $\alpha_{\overline{\text{MS}}}^{(5)}(M_Z)$ as

$$\alpha_{\overline{\text{MS}}}^{(5)}(M_Z) = 0.1177(26). \quad (388)$$

Since $\alpha_{\text{eff}} \simeq 0.37$, they have ■ for the renormalization scale criterion. Since $\Delta\Lambda/\Lambda \simeq \alpha_{\text{eff}}^2$, we also assign ○ for the criterion of perturbative behaviour. The lattice cutoff ranges over $a^{-1} = 2.5\text{--}4.5 \text{ GeV}$ with $\mu = 3 \text{ GeV}$ so we also give them a ○ for continuum extrapolation. We note, however, that the χ^2/dof of the a^2 extrapolation was quite bad, namely between 2.1 and 5.1 [168]. Please note that the 2019 FLAG review mistakenly took $\alpha_{\overline{\text{MS}}}^{(5)}(2m_c)$ for α_{eff} . This resulted in a ○ rating for the renormalization scale for both Maezawa 16 and

JLQCD 16. With the consistent definition of α_{eff} both determinations now have ■ for the renormalization scale.

Three new determinations of α_s from the moments of quarkonium correlators appeared since the 2019 FLAG review [33, 34, 36]. Petreczky 19 [34] extended the calculation of [175] by considering heavy-quark masses larger than the charm-quark mass, namely, $m_h = 1.5m_c$, $2m_c$ and $3m_c$. Also three additional lattice spacings, $a = 0.025$, 0.03 and 0.035 fm have been added to the analysis. Another improvement compared to Maezawa 16 was the use of random-colour wall sources which greatly reduced the statistical errors. In fact, the statistical errors on the moments were completely negligible compared to other sources of errors. The lattices corresponding to the three smallest lattice spacings have been generated for the calculations of the QCD equation of state at high temperature [130] at light sea-quark masses corresponding to the pion mass of 300 MeV in the continuum limit, instead of the pion mass of 160 MeV as in the previous calculations. However, it has been checked that the effect of the larger light sea-quark masses is very small, about the size of the statistical errors [34]. Therefore, the calculations at the two light sea-quark masses have been combined into a single analysis [34]. For each value of the heavy-quark mass the continuum extrapolations have been performed using various fit ansätze, some of which included high powers of a . Due to availability of many lattice spacing it was possible to perform such fits without using Bayesian priors. The variation of the continuum-extrapolated values with the variation of the fit range in a^2 and the fit forms has been investigated and included as the systematic error of the continuum results. The renormalization scale μ was fixed to the heavy-quark mass, and $\alpha_s(\mu = m_h)$ and the corresponding $\Lambda_{\overline{MS}}^{N_f=3}$ has been determined for each value of m_h using continuum results for R_4 , R_6/R_8 and R_8/R_{10} . The perturbative error was estimated as in Maezawa 16 but with the coefficient of the 4-loop term being 1.6 times the coefficient of the 3-loop term. The values of $\Lambda_{\overline{MS}}^{N_f=3}$ obtained for $m_h = m_c$ and $m_h = 1.5m_c$ were consistent with each other, $\Lambda_{\overline{MS}}^{N_f=3} = 314(10)$ MeV for $m_h = m_c$ and $\Lambda_{\overline{MS}}^{N_f=3} = 310(10)$ MeV for $m_h = 1.5m_c$. However, the $\Lambda_{\overline{MS}}^{N_f=3}$ values turned out to be significantly lower for $m_h = 2m_c$ and $3m_c$. In Petreczky 20 [33], it has been argued that reliable continuum extrapolations of R_4 , R_6/R_8 and R_8/R_{10} are not possible for $m_h \geq 2m_c$. Therefore, we only review the results obtained for $m_h = m_c$ and $m_h = 1.5m_c$. There are many lattice spacings available for analysis, including three lattice spacings $a \leq 0.035$ fm, implying that $a\mu < 0.5$. Therefore, we assign ★ for the continuum extrapolation. The value of α_{eff} is 0.38 and 0.31 for $m_h = m_c$ and $m_h = 1.5m_c$, respectively. So we assign ■ for the renormalization scale. Since $(\Delta\Lambda/\Lambda)_{\Delta\alpha} < \alpha_{\text{eff}}^2$ we assign ■ for the perturbative behaviour.

Petreczky 20 [33] used the same raw lattice data as Petreczky 19 but a different strategy for continuum extrapolation and α_s extraction. The lattice spacing dependence of the results of R_4 at different quark masses was fitted simultaneously in a similar manner as in the HPQCD 10 and HPQCD 14 analyses, but without using Bayesian priors. In extracting α_s several choices of the renormalization scale μ in the range $2/3m_h - 3m_h$ have been considered. The perturbative error was estimated as in Petreczky 19 but the variation of the results due to the scale variation was larger than the estimated perturbative error. The final error of the result $\Lambda_{\overline{MS}}^{N_f=3} = 331(17)$ MeV comes mostly from the scale variation [33]. Since there are three lattice spacing available with $a\mu < 0.5$ we give ★ for continuum extrapolation. Because $\alpha_{\text{eff}} = 0.22 - 0.38$ we give ○ for the renormalization scale. Finally, since $(\Delta\Lambda/\Lambda)_{\Delta\alpha} > \alpha_{\text{eff}}^2$ for the smallest α_{eff} value we give ○ for the perturbative behaviour. In addition to R_4 Petreczky 20 also considered using R_6/R_8 and R_8/R_{10} for the α_s determination. It was pointed out

that the lattice spacing dependence of R_6/R_8 is quite subtle and therefore reliable continuum extrapolations for this ratio are not possible for $m_h \geq 2m_c$ [33]. For $m_h = m_c$ and $1.5m_c$ the ratio R_6/R_8 leads to α_s values that are consistent with the ones from R_4 . Furthermore, it was argued that finite-volume effects in the case of R_8/R_{10} are large for $m_h = m_c$ and therefore the corresponding data are not suitable for extracting α_s . This observation may explain why the central values of α_s extracted from R_8/R_{10} in some previous studies were systematically lower [34, 165, 175]. On the other hand for $m_h \geq 1.5m_c$ the finite-volume effects are sufficiently small in the continuum extrapolated results if some small-volume lattice data are excluded from the analysis [33]. The α_s obtained from R_8/R_{10} with $m_h \geq 1.5m_c$ were consistent with the ones obtained from R_4 .

Boito 20 [36] use published continuum extrapolated lattice results on R_4 , R_6/R_8 and R_8/R_{10} from various groups combined with experimental results on e^+e^- annihilation. They quote a separate result for each lattice determinations of R_4 , R_6/R_8 and R_8/R_{10} for $m_h = m_c$ from different lattice groups. They vary the scale μ and μ_m independently in the region between m_c and 4 GeV. As the typical value they quote $\alpha_s(M_Z) = 0.1177(20)$. The error is dominated by the perturbative uncertainty. Since the effective coupling is around 0.38 we give \blacksquare for the renormalization scale. Because $(\Delta\Lambda/\Lambda)_{\Delta\alpha} < \alpha_{\text{eff}}^2$ we give this determination \blacksquare for perturbative behaviour. The continuum results used in the analysis were rated as \circ with the exception of HPQCD 08B, which however, does not affect the quoted α_s value. Therefore we give them \circ for the continuum extrapolation. An interesting point of the Boito 20 analysis is that the α_s values extracted from R_8/R_{10} are systematically lower than the ones extracted from R_4 . This confirms the above assertion that finite volume effects are significant for R_8/R_{10} at $m_h = m_c$.

Aside from the final results for $\alpha_s(m_Z)$ obtained by matching with perturbation theory, it is interesting to make a comparison of the short distance quantities in the continuum limit R_n which are available from HPQCD 08 [165], JLQCD 16 [168], Maezawa 16 [175], Petreczky 19 [34] and Petreczky 20 [33] (all using 2 + 1 flavours). This comparison is shown in Tab. 65. The results are in quite good agreement with each other. For future studies it is

	HPQCD 08	HPQCD 10	Maezawa 16	JLQCD 16	Petreczky 19	Petreczky 20
R_4	1.272(5)	1.282(4)	1.265(7)	-	1.279(4)	1.278(2)
R_6	1.528(11)	1.527(4)	1.520(4)	1.509(7)	1.521(3)	1.522(2)
R_8	1.370(10)	1.373(3)	1.367(8)	1.359(4)	1.369(3)	1.368(3)
R_{10}	1.304(9)	1.304(2)	1.302(8)	1.297(4)	1.311(7)	1.301(3)
R_6/R_8	1.113(2)	-	1.114(2)	1.111(2)	1.1092(6)	1.10895(32)
R_8/R_{10}	1.049(2)	-	1.0495(7)	1.0481(9)	1.0485(8)	-

Table 65: Moments and the ratios of the moments from $N_f = 3$ simulations at the charm mass.

of course interesting to check agreement of these numbers before turning to the more involved determination of α_s .

9.9 α_s from QCD vertices

9.9.1 General considerations

The most intuitive and in principle direct way to determine the coupling constant in QCD is to compute the appropriate three- or four-point gluon vertices or alternatively the quark-quark-gluon vertex or ghost-ghost-gluon vertex (i.e., $q\bar{q}A$ or $c\bar{c}A$ vertex, respectively). A suitable combination of renormalization constants then leads to the relation between the bare (lattice) and renormalized coupling constant. This procedure requires the implementation of a nonperturbative renormalization condition and the fixing of the gauge. For the study of nonperturbative gauge fixing and the associated Gribov ambiguity, we refer to Refs. [179–181] and references therein. In practice the Landau gauge is used and the renormalization constants are defined by requiring that the vertex is equal to the tree-level value at a certain momentum configuration. The resulting renormalization schemes are called ‘MOM’ scheme (symmetric momentum configuration) or ‘ $\widetilde{\text{MOM}}$ ’ (one momentum vanishes), which are then converted perturbatively to the $\overline{\text{MS}}$ scheme.

A pioneering work to determine the three-gluon vertex in the $N_f = 0$ theory is Alles 96 [182] (which was followed by Ref. [183] for two flavour QCD); a more recent $N_f = 0$ computation was Ref. [184] in which the three-gluon vertex as well as the ghost-ghost-gluon vertex was considered. (This requires a computation of the propagator of the Faddeev–Popov ghost on the lattice.) The latter paper concluded that the resulting $\Lambda_{\overline{\text{MS}}}$ depended strongly on the scheme used, the order of perturbation theory used in the matching and also on nonperturbative corrections [185].

Subsequently in Refs. [186, 187] a specific $\widetilde{\text{MOM}}$ scheme with zero ghost momentum for the ghost-ghost-gluon vertex was used. In this scheme, dubbed the ‘MM’ (Minimal MOM) or ‘Taylor’ (T) scheme, the vertex is not renormalized, and so the renormalized coupling reduces to

$$\alpha_T(\mu) = D_{\text{lat}}^{\text{gluon}}(\mu, a) D_{\text{lat}}^{\text{ghost}}(\mu, a)^2 \frac{g_0^2}{4\pi}, \quad (389)$$

where $D_{\text{lat}}^{\text{ghost}}$ and $D_{\text{lat}}^{\text{gluon}}$ are the (bare lattice) dressed ghost and gluon ‘form factors’ of these propagator functions in the Landau gauge,

$$D^{ab}(p) = -\delta^{ab} \frac{D^{\text{ghost}}(p)}{p^2}, \quad D_{\mu\nu}^{ab}(p) = \delta^{ab} \left(\delta_{\mu\nu} - \frac{p_\mu p_\nu}{p^2} \right) \frac{D^{\text{gluon}}(p)}{p^2}, \quad (390)$$

and we have written the formula in the continuum with $D^{\text{ghost}/\text{gluon}}(p) = D_{\text{lat}}^{\text{ghost}/\text{gluon}}(p, 0)$. Thus there is now no need to compute the ghost-ghost-gluon vertex, just the ghost and gluon propagators.

9.9.2 Discussion of computations

For the calculations considered here, to match to perturbative scaling, it was first necessary to reduce lattice artifacts by an $H(4)$ extrapolation procedure (addressing $O(4)$ rotational invariance), e.g., ETM 10F [193] or by lattice perturbation theory, e.g., Sternbeck 12 [191]. To match to perturbation theory, collaborations vary in their approach. In ETM 10F [193], it was necessary to include the operator A^2 in the OPE of the ghost and gluon propagators, while in Sternbeck 12 [191] very large momenta are used and $a^2 p^2$ and $a^4 p^4$ terms are included

Collaboration	Ref.	N_f	publication status renormalization scale perturbative behaviour continuum extrapolation	scale	$\Lambda_{\overline{\text{MS}}}[\text{MeV}]$	$r_0\Lambda_{\overline{\text{MS}}}$
ETM 13D	[188]	2+1+1	A ○ ○ ■	f_π	314(7)(14)(10) ^a	0.752(18)(34)(81) [†]
ETM 12C	[189]	2+1+1	A ○ ○ ■	f_π	324(17) [§]	0.775(41) [†]
ETM 11D	[190]	2+1+1	A ○ ○ ■	f_π	316(13)(8)(⁺⁰ ₋₉) [*]	0.756(31)(19)(⁺⁰ ₋₂₂) [†]
Zafeiropoulos 19	[37]	2+1	A ■ ■ ■	m_Ω	320(4)(12) ^b	0.766(10)(29) [†]
Sternbeck 12	[191]	2+1	C	only running of α_s in Fig. 4		
Sternbeck 12	[191]	2	C	Agreement with $r_0\Lambda_{\overline{\text{MS}}}$ value of [57]		
Sternbeck 10	[192]	2	C ○ ★ ■		251(15) [#]	0.60(3)(2)
ETM 10F	[193]	2	A ○ ○ ○	f_π	330(23)(22)(⁺⁰ ₋₃₃)	0.72(5) ⁺
Boucaud 01B	[183]	2	A ○ ○ ■	$K^* - K$	264(27) ^{**}	0.669(69)
Sternbeck 12	[191]	0	C	Agreement with $r_0\Lambda_{\overline{\text{MS}}}$ value of [127]		
Sternbeck 10	[192]	0	C ★ ★ ■		259(4) [#]	0.62(1)
Ilgenfritz 10	[194]	0	A ★ ★ ■	only running of α_s in Fig. 13		
Boucaud 08	[187]	0	A ○ ★ ■	$\sqrt{\sigma} = 445 \text{ MeV}$	224(3)(⁺⁸ ₋₅)	0.59(1)(⁺² ₋₁)
Boucaud 05	[184]	0	A ■ ★ ■	$\sqrt{\sigma} = 445 \text{ MeV}$	320(32)	0.85(9)
Soto 01	[195]	0	A ○ ○ ○	$\sqrt{\sigma} = 445 \text{ MeV}$	260(18)	0.69(5)
Boucaud 01A	[196]	0	A ○ ○ ○	$\sqrt{\sigma} = 445 \text{ MeV}$	233(28) MeV	0.62(7)
Boucaud 00B	[197]	0	A ○ ○ ○	only running of α_s		
Boucaud 00A	[198]	0	A ○ ○ ○	$\sqrt{\sigma} = 445 \text{ MeV}$	237(3)(⁺⁰ ₋₁₀)	0.63(1)(⁺⁰ ₋₃)
Becirevic 99B	[199]	0	A ○ ○ ■	$\sqrt{\sigma} = 445 \text{ MeV}$	319(14)(⁺¹⁰ ₋₂₀)	0.84(4)(⁺³ ₋₅)
Becirevic 99A	[200]	0	A ○ ○ ■	$\sqrt{\sigma} = 445 \text{ MeV}$	$\lesssim 353(2)(+25-15)$	$\lesssim 0.93(+7-4)$
Boucaud 98B	[201]	0	A ■ ○ ■	$\sqrt{\sigma} = 445 \text{ MeV}$	295(5)(15)	0.78(4)
Boucaud 98A	[202]	0	A ■ ○ ■	$\sqrt{\sigma} = 445 \text{ MeV}$	300(5)	0.79(1)
Alles 96	[182]	0	A ■ ■ ■	$\sqrt{\sigma} = 440 \text{ MeV}^{++}$	340(50)	0.91(13)

^a $\alpha_{\overline{\text{MS}}}^{(5)}(M_Z) = 0.1196(4)(8)(6)$.

[†] We use the 2+1 value $r_0 = 0.472 \text{ fm}$.

[§] $\alpha_{\overline{\text{MS}}}^{(5)}(M_Z) = 0.1200(14)$.

^{*} First error is statistical; second is due to the lattice spacing and third is due to the chiral extrapolation.

$\alpha_{\overline{\text{MS}}}^{(5)}(M_Z) = 0.1198(9)(5)(⁺⁰₋₅)$.

^b $\alpha_{\overline{\text{MS}}}^{(5)}(M_Z) = 0.1172(3)(9)(5)$. The first error is the uncertainty in the determination of α_T , the second due to the condensate while the third is due to higher order nonperturbative corrections.

[#] In the paper only $r_0\Lambda_{\overline{\text{MS}}}$ is given, we converted to MeV with $r_0 = 0.472 \text{ fm}$.

⁺ The determination of r_0 from the f_π scale is found in Ref. [55].

^{**} $\alpha_{\overline{\text{MS}}}^{(5)}(M_Z) = 0.113(3)(4)$.

⁺⁺ The scale is taken from the string tension computation of Ref. [128].

Table 66: Results for the gluon-ghost vertex.

in their fit to the momentum dependence. A further later refinement was the introduction of higher nonperturbative OPE power corrections in ETM 11D [190] and ETM 12C [189].

Although the expected leading power correction, $1/p^4$, was tried, ETM finds good agreement with their data only when they fit with the next-to-leading-order term, $1/p^6$. The update ETM 13D [188] investigates this point in more detail, using better data with reduced statistical errors. They find that after again including the $1/p^6$ term they can describe their data over a large momentum range from about 1.75 GeV to 7 GeV.

In all calculations except for Sternbeck 10 [192], Sternbeck 12 [191], the matching with the perturbative formula is performed including power corrections in the form of condensates, in particular $\langle A^2 \rangle$. Three lattice spacings are present in almost all calculations with $N_f = 0, 2$, but the scales ap are rather large. This mostly results in a \blacksquare on the continuum extrapolation (Sternbeck 10 [192], Boucaud 01B [183] for $N_f = 2$. Ilgenfritz 10 [194], Boucaud 08 [187], Boucaud 05 [184], Becirevic 99B [199], Becirevic 99A [200], Boucaud 98B [201], Boucaud 98A [202], Alles 96 [182] for $N_f = 0$). A \circ is reached in the $N_f = 0$ computations Boucaud 00A [198], 00B [197], 01A [196], Soto 01 [195] due to a rather small lattice spacing, but this is done on a lattice of a small physical size. The $N_f = 2 + 1 + 1$ calculation, fitting with condensates, is carried out for two lattice spacings and with $ap > 1.5$, giving \blacksquare for the continuum extrapolation as well. In ETM 10F [193] we have $0.25 < \alpha_{\text{eff}} < 0.4$, while in ETM 11D [190], ETM 12C [189] (and ETM 13 [203]) we find $0.24 < \alpha_{\text{eff}} < 0.38$, which gives a \circ in these cases for the renormalization scale. In ETM 10F [193] the values of ap violate our criterion for a continuum limit only slightly, and we give a \circ .

In Sternbeck 10 [192], the coupling ranges over $0.07 \leq \alpha_{\text{eff}} \leq 0.32$ for $N_f = 0$ and $0.19 \leq \alpha_{\text{eff}} \leq 0.38$ for $N_f = 2$ giving \star and \circ for the renormalization scale, respectively. The fit with the perturbative formula is carried out without condensates, giving a satisfactory description of the data. In Boucaud 01A [196], depending on a , a large range of α_{eff} is used which goes down to 0.2 giving a \circ for the renormalization scale and perturbative behaviour, and several lattice spacings are used leading to \circ in the continuum extrapolation. The $N_f = 2$ computation Boucaud 01B [196], fails the continuum limit criterion because both $a\mu$ is too large and an unimproved Wilson fermion action is used. Finally in the conference proceedings Sternbeck 12 [191], the $N_f = 0, 2, 3$ coupling α_T is studied. Subtracting 1-loop lattice artifacts and subsequently fitting with $a^2 p^2$ and $a^4 p^4$ additional lattice artifacts, agreement with the perturbative running is found for large momenta ($r_0^2 p^2 > 600$) without the need for power corrections. In these comparisons, the values of $r_0 \Lambda_{\overline{MS}}$ from other collaborations are used. As no numbers are given, we have not introduced ratings for this study.

Since the previous FLAG review, there has been one new result, Zafeiropoulos 19 [37], again based on the method described in ETM 10F, [193] but now for $N_f = 3$ flavours rather than two. Again an $\langle A^2 \rangle$ condensate is included, but cannot be determined; an estimate is used from ETM 10F ($N_f = 2$) and ETM12C ($N_f = 4$). The scale Λ is determined from the largest momenta available (when a plateau appears), and the error is estimated from the larger range $p \sim 3.0\text{--}3.7$ GeV. This is used to determine $\alpha_{\overline{MS}}$. In this work there is also some emphasis on being close to the physical-quark masses, using three domain-wall fermion data sets and careful consideration of discretization effects following [204]. The disadvantage is that a lower upper bound on the momenta is now reached.

The range of effective couplings is $0.35 \lesssim \alpha_{\text{eff}} \lesssim 0.42$, and over this range we have $(\alpha_{\text{eff}}(3.0 \text{ GeV})/\alpha_{\text{eff}}(3.7 \text{ GeV}))^3 \sim 1.7$, which leads to a \blacksquare for perturbative behaviour. With no α_{eff} at or below 0.3 and only two lattice spacings, we also obtain a \blacksquare for both the renormalization scale and the continuum extrapolation.

In Tab. 66 we summarize the results. Presently there are no $N_f \geq 3$ calculations of α_s from QCD vertices that satisfy the FLAG criteria to be included in the range.

9.10 α_s from the eigenvalue spectrum of the Dirac operator

9.10.1 General considerations

Consider the spectral density of the continuum Dirac operator

$$\rho(\lambda) = \frac{1}{V} \left\langle \sum_k (\delta(\lambda - i\lambda_k) + \delta(\lambda + i\lambda_k)) \right\rangle, \quad (391)$$

where V is the volume and λ_k are the eigenvalues of the Dirac operator in a gauge background.

Its perturbative expansion

$$\rho(\lambda) = \frac{3}{4\pi^2} \lambda^3 (1 - \rho_1 \bar{g}^2 - \rho_2 \bar{g}^4 - \rho_3 \bar{g}^6 + \mathcal{O}(\bar{g}^8)), \quad (392)$$

is known including ρ_3 in the $\overline{\text{MS}}$ scheme [205, 206]. In renormalization group improved form one sets the renormalization scale μ to $\mu = s\lambda$ with $s = \mathcal{O}(1)$ and the ρ_i are pure numbers. Nakayama 18 [207] initiated a study of $\rho(\lambda)$ in the perturbative regime. They prefer to consider μ independent from λ . Then ρ_i are polynomials in $\log(\lambda/\mu)$ of degree i . One may consider

$$F(\lambda) \equiv \frac{\partial \log(\rho(\lambda))}{\partial \log(\lambda)} = 3 - F_1 \bar{g}^2 - F_2 \bar{g}^4 - F_3 \bar{g}^6 - F_4 \bar{g}^8 + \mathcal{O}(\bar{g}^{10}), \quad (393)$$

where the coefficients, F_i , which are known for $i = 1, \dots, 4$, are again polynomials of degree i in $\log(\lambda/\mu)$. Choosing the alternate renormalization-group-improved form with $\mu = s\lambda$ in Eq. (392), Eq. (393) would instead lead to

$$F(\lambda) = 3 - \bar{F}_2 \bar{g}^4(\lambda) - \bar{F}_3 \bar{g}^6(\lambda) - \bar{F}_4 \bar{g}^8(\lambda) + \mathcal{O}(\bar{g}^{10}), \quad (394)$$

with pure numbers \bar{F}_i and $\bar{F}_1 = 0$. Determinations of α_s can be carried out by a computation and continuum extrapolation of $\rho(\lambda)$ and/or $F(\lambda)$ at large λ . Such computations are made possible by the techniques of [85, 207, 208].

We note that according to our general discussions in terms of an effective coupling, we have $n_l = 2$; the 3-loop β function of a coupling defined from Eq. (392) or Eq. (394) is known.¹²

9.10.2 Discussion of computations

There is one pioneering result to date using this method by Nakayama 18 [207]. They computed the eigenmode distributions of the Hermitian operator $a^2 D_{\text{ov}}^\dagger D_{\text{ov}}$ where $D_{\text{ov}} = D_{\text{ov}}(m_f = 0, am_{\text{PV}})$ is the overlap operator and m_{PV} is the Pauli–Villars regulator on ensembles with 2+1 flavours using Möbius domain-wall quarks for three lattice cutoffs $a^{-1} = 2.5, 3.6, 4.5$ GeV, where $am_{\text{PV}} = 3$ or ∞ . The bare eigenvalues are converted to the $\overline{\text{MS}}$ scheme at $\mu = 2$ GeV by multiplying with the renormalization constant $Z_m(2 \text{ GeV})$, which is then transformed to those renormalized at $\mu = 6$ GeV using the renormalization-group equation. The scale is set by $\sqrt{t_0} = 0.1465(21)(13)$ fm. The continuum limit is taken assuming a linear dependence in a^2 , while the volume size is kept about constant: 2.6–2.8 fm. Choosing the

¹²In the present situation, Nakayama 18 [207], the effective coupling is defined by $\bar{g}_\lambda^2(\mu) = \bar{F}_2^{-1/2} (3 - F(\lambda))$ with $\mu = \lambda$. The alternative definition, Eq. (394), would give $\bar{g}_\lambda^2(\mu) = \bar{F}_2^{-1/2} (3 - F(\lambda))^{1/2}$.

renormalization scale $\mu = 6 \text{ GeV}$, Nakayama 18 [207] extracted the strong coupling constant $\alpha_{\overline{\text{MS}}}^{(3)}(6 \text{ GeV}) = 0.204(10)$. The result is converted to

$$\alpha_{\overline{\text{MS}}}^{(5)}(M_Z) = 0.1226(36). \quad (395)$$

Three lattice spacings in the range $a^{-1} = 2.5\text{--}4.5 \text{ GeV}$ with $\mu = \lambda = 0.8\text{--}1.25 \text{ GeV}$ yield quite small values $a\mu$. However, our continuum-limit criterion does not apply as it requires us to consider $\alpha_s = 0.3$. We thus deviate from the general rule and give a \circ which would result at the smallest value $\alpha_{\overline{\text{MS}}}(\mu) = 0.4$ considered by Nakayama 18 [207]. The values of $\alpha_{\overline{\text{MS}}}$ lead to a \blacksquare for the renormalization scale, while perturbative behaviour is rated \circ .

In Tab. 67 we list this result.

Collaboration	Ref.	N_f	publication status	renormalization scale	perturbative behaviour	continuum extrapolation	scale	$\Lambda_{\overline{\text{MS}}}[\text{MeV}]$	$r_0\Lambda_{\overline{\text{MS}}}$
Nakayama 18	[207]	2+1	A	\blacksquare	\circ	\circ	$\sqrt{t_0}$	409(60) *	0.978(144)

* $\alpha_{\overline{\text{MS}}}^{(5)}(M_Z) = 0.1226(36)$. $\Lambda_{\overline{\text{MS}}}$ determined by us using $\alpha_{\overline{\text{MS}}}^{(3)}(6 \text{ GeV}) = 0.204(10)$. Uses $r_0 = 0.472 \text{ fm}$

Table 67: Dirac eigenvalue result.

9.11 Summary

After reviewing the individual computations, we are now in a position to discuss the overall result. We first present the current status and for that briefly consider $r_0\Lambda$ with its flavour dependence from $N_f = 0$ to 4 flavours. Then we discuss the central $\alpha_{\overline{\text{MS}}}(M_Z)$ results, which just use $N_f \geq 3$, give ranges for each sub-group discussed previously, and give final FLAG average as well as an overall average together with the current PDG nonlattice numbers. Finally we return to $r_0\Lambda$, presenting our estimates for the various N_f .

9.11.1 The present situation

We first summarize the status of lattice-QCD calculations of the QCD scale $\Lambda_{\overline{\text{MS}}}$. Fig. 40 shows all the results for $r_0\Lambda_{\overline{\text{MS}}}$ discussed in the previous sections.

Many of the numbers are the ones given directly in the papers. However, when only $\Lambda_{\overline{\text{MS}}}$ in physical units (MeV) is available, we have converted them by multiplying with the value of r_0 in physical units. The notation used is full green squares for results used in our final average, while a lightly shaded green square indicates that there are no red squares in the previous colour coding but the computation does not enter the ranges because either it has been superseded by an update or it is not published. Red open squares mean that there is at least one red square in the colour coding.

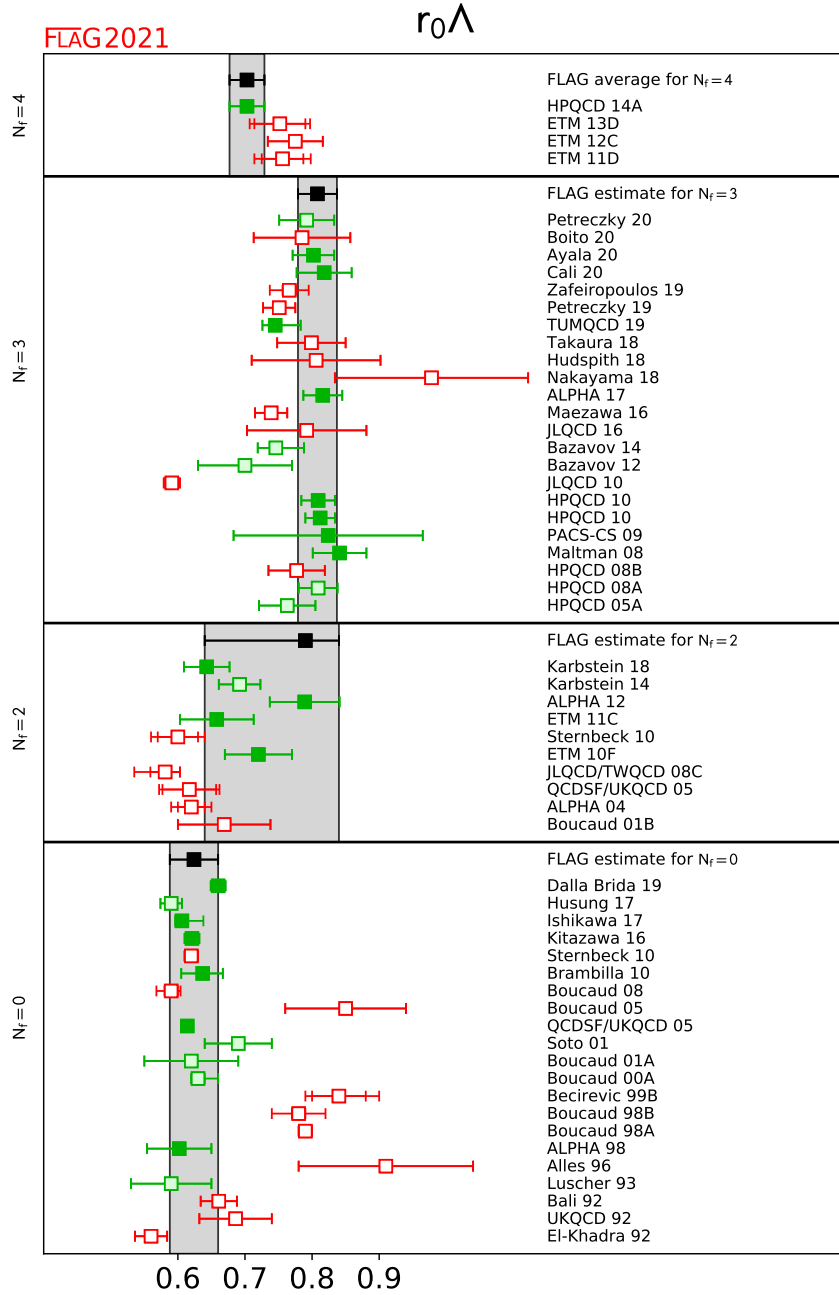


Figure 40: $r_0\Lambda_{\overline{\text{MS}}}$ estimates for $N_f = 0, 2, 3, 4$ flavours. Full green squares are used in our final ranges, pale green squares also indicate that there are no red squares in the colour coding but the computations were superseded by later more complete ones or not published, while red open squares mean that there is at least one red square in the colour coding.

For $N_f = 0$ there is now some tension: the value of the new result, Dalla Brida 19 [27] is rather high compared to the previous FLAG average and yet it passes the FLAG 19 criteria by some margin.

When two flavours of quarks are included, the numbers extracted by the various groups

show a considerable spread, as in particular older computations did not yet control the systematics sufficiently. This illustrates the difficulty of the problem and emphasizes the need for strict criteria. The agreement among the more modern calculations with three or more flavours, however, is quite good.

We now turn to the status of the essential result for phenomenology, $\alpha_{\overline{\text{MS}}}^{(5)}(M_Z)$. In Tab. 68 and the upper plot in Fig. 41 we show all the results for $\alpha_{\overline{\text{MS}}}^{(5)}(M_Z)$ (i.e., $\alpha_{\overline{\text{MS}}}$ at the Z mass)

Collaboration	Ref.	N_f	publication status	renormalization scale	perturbative behaviour	continuum extrapolation	$\alpha_{\overline{\text{MS}}}(M_Z)$	Remark	Tab.
ALPHA 17	[92]	2+1	A	★	★	★	0.11852(84)	step-scaling	60
PACS-CS 09A	[93]	2+1	A	★	★	○	0.11800(300)	step-scaling	60
pre-range (average)							0.11848(81)		
Ayala 20	[30]	2+1	A	○	★	○	0.11836(88)	Q - \bar{Q} potential	61
TUMQCD 19	[29]	2+1	A	○	★	○	0.11671($^{+110}_{-57}$)	Q - \bar{Q} potential (and free energy)	61
Takaura 18	[119, 120]	2+1	A	■	○	○	0.11790(70)($^{+130}_{-120}$)	Q - \bar{Q} potential	61
Bazavov 14	[121]	2+1	A	○	★	○	0.11660(100)	Q - \bar{Q} potential	61
Bazavov 12	[122]	2+1	A	○	○	○	0.11560($^{+210}_{-220}$)	Q - \bar{Q} potential	61
pre-range with estimated pert. error							0.11782(165)		
Cali 20	[32]	2+1	A	○	★	★	0.11863(114)	vacuum pol. (position space)	62
Hudspith 18	[141]	2+1	P	○	★	■	0.11810(270)($^{+80}_{-220}$)	vacuum polarization	62
JLQCD 10	[140]	2+1	A	■	○	■	0.11180(30)($^{+160}_{-170}$)	vacuum polarization	62
pre-range with estimated pert. error							0.11863(360)		
HPQCD 10	[149]	2+1	A	○	★	★	0.11840(60)	Wilson loops	63
Maltman 08	[150]	2+1	A	○	○	★	0.11920(110)	Wilson loops	63
pre-range with estimated pert. error							0.11871(128)		
Petreczky 20	[33]	2+1	P	○	○	★	0.11773(119).	heavy current two points	64
Boito 20	[35, 36]	2+1	A	■	■	○	0.1177(20)	use published lattice data	64
Petreczky 19	[34]	2+1	A	■	■	★	0.1159(12).	heavy current two points	64
JLQCD 16	[168]	2+1	A	■	○	○	0.11770(260)	heavy current two points	64
Maazawa 16	[175]	2+1	A	■	○	○	0.11622(84)	heavy current two points	64
HPQCD 14A	[167]	2+1+1	A	○	★	○	0.11822(74)	heavy current two points	64
HPQCD 10	[149]	2+1	A	○	★	○	0.11830(70)	heavy current two points	64
HPQCD 08B	[165]	2+1	A	■	■	■	0.11740(120)	heavy current two points	64
pre-range with estimated pert. error							0.11826(200)		
Zafeiropoulos 19	[37]	2+1	A	■	■	■	0.1172(11)	gluon-ghost vertex	66
ETM 13D	[188]	2+1+1	A	○	○	■	0.11960(40)(80)(60)	gluon-ghost vertex	66
ETM 12C	[189]	2+1+1	A	○	○	■	0.12000(140)	gluon-ghost vertex	66
ETM 11D	[190]	2+1+1	A	○	○	■	0.11980(90)(50)($^{+0}_{-50}$)	gluon-ghost vertex	66
Nakayama 18	[207]	2+1	A	★	○	■	0.12260(360)	Dirac eigenvalues	67

Table 68: Results for $\alpha_{\overline{\text{MS}}}(M_Z)$. Different methods are listed separately and they are combined to a pre-range when computations are available without any ■. A weighted average of the pre-ranges gives 0.11843(60), using the smallest pre-range uncertainty gives 0.11843(81) while the average uncertainty of the ranges used as an error gives 0.11843(187). Note that TUMQCD 19 supersedes Bazavov 14/12.

obtained from $N_f = 2 + 1$ and $N_f = 2 + 1 + 1$ simulations. The conversion from $N_f = 3$ or $N_f = 4$ to $N_f = 5$ is made by matching the coupling constant at the charm and bottom quark thresholds and using the scale as determined or used by the authors.

As can be seen from the tables and figures, at present there are several computations satisfying the criteria to be included in the FLAG average. Since FLAG 19 four new computations of $\alpha_{\overline{\text{MS}}}^{(5)}(M_Z)$ pass all our criteria with at least a \circ . The results agree quite well within the stated uncertainties, which vary significantly.

9.11.2 Our range for $\alpha_{\overline{\text{MS}}}^{(5)}$

We now explain the determination of our range. We only include those results without a red tag and that are published in a refereed journal. We also do not include any numbers that were obtained by extrapolating from theories with less than three flavours. They are not controlled and can be looked up in the previous FLAG reviews.

A general issue with most determinations of $\alpha_{\overline{\text{MS}}}$, both lattice and nonlattice, is that they are dominated by perturbative truncation errors, which are difficult to estimate. Further, all results discussed here except for those of Secs. 9.3, 9.7 are based on extractions of $\alpha_{\overline{\text{MS}}}$ that are largely influenced by data with $\alpha_{\text{eff}} \geq 0.3$. At smaller α_s the momentum scale μ quickly gets at or above a^{-1} . We have included computations using $a\mu$ up to 1.5 and α_{eff} up to 0.4, but one would ideally like to be significantly below that. Accordingly we choose to not simply perform weighted averages with the individual errors estimated by each group. Rather, we use our own more conservative estimates of the perturbative truncation errors in the weighted average.

In the following we repeat aspects of the methods and calculations that inform our estimates of the perturbative truncation errors. We also provide separate estimates for α_s obtained from step-scaling, the heavy-quark potential, Wilson loops, heavy-quark current two-point functions and vacuum polarization to enable a comparison of the different lattice approaches; these are summarized in Tab. 68.

- *Step-scaling*

The step-scaling computations of PACS-CS 09A [93] and ALPHA 17 [92] reach energies around the Z -mass where perturbative uncertainties in the three-flavour theory are negligible. Perturbative errors do enter in the conversion of the Λ -parameters from three to five flavours, but successive order contributions decrease rapidly and can be neglected. We form a weighted average of the two results and obtain $\alpha_{\overline{\text{MS}}} = 0.11848(81)$.

- *Static-quark potential computations*

Brambilla 10 [127], ETM 11C [125] and Bazavov 12 [122] give evidence that they have reached distances where perturbation theory can be used. However, in addition to Λ , a scale is introduced into the perturbative prediction by the process of subtracting the renormalon contribution. This subtraction is avoided in Bazavov 14 [121] by using the force and again agreement with perturbative running is reported. Husung 17 [126] (unpublished) studies the reliability of perturbation theory in the pure gauge theory with lattice spacings down to 0.015 fm and finds that at weak coupling there is a downwards trend in the Λ -parameter with a slope $\Delta\Lambda/\Lambda \approx 9\alpha_s^3$. The downward trend is broadly confirmed in Husung 20 [31] albeit with larger errors.

Bazavov 14 [121] satisfies all of the criteria to enter the FLAG average for α_s but has been superseded by TUMQCD 19 [29]. Moreover, there is another study, Ayala 20 [30] who use the very same data as TUMQCD 19, but treat perturbation theory differently, resulting in a rather different central value. This shows that perturbative truncation

errors are the main source of errors. We combine the results for $\Lambda_{\overline{\text{MS}}}^{N_f=3}$ from both groups as a weighted average (with the larger upward error of TUMQCD 19) and take the difference of the central values as the uncertainty of the average. We obtain $\Lambda_{\overline{\text{MS}}}^{N_f=3} = 330(24)$ MeV, which translates to $\alpha_s(m_Z) = 0.11782(165)$.

- *Small Wilson loops*

Here the situation is unchanged as compared to FLAG 16. In the determination of α_s from observables at the lattice spacing scale, there is an interplay of higher-order perturbative terms and lattice artifacts. In HPQCD 05A [145], HPQCD 08A [146] and Maltman 08 [150] both lattice artifacts (which are power corrections in this approach) and higher-order perturbative terms are fitted. We note that Maltman 08 [150] and HPQCD 08A [146] analyze largely the same data set but use different versions of the perturbative expansion and treatments of nonperturbative terms. After adjusting for the slightly different lattice scales used, the values of $\alpha_{\overline{\text{MS}}}(M_Z)$ differ by 0.0004 to 0.0008 for the three quantities considered. In fact the largest of these differences (0.0008) comes from a tadpole-improved loop, which is expected to be best behaved perturbatively. We therefore replace the perturbative-truncation errors from [150] and [149] with our estimate of the perturbative uncertainty Eq. (379). Taking the perturbative errors to be 100% correlated between the results, we obtain for the weighted average $\alpha_{\overline{\text{MS}}} = 0.11871(128)$.

- *Heavy quark current two-point functions*

Other computations with small errors are HPQCD 10 [149] and HPQCD 14A [167], where correlation functions of heavy valence quarks are used to construct short-distance quantities. Due to the large quark masses needed to reach the region of small coupling, considerable discretization errors are present, see Fig. 30 of FLAG 16. These are treated by fits to the perturbative running (a 5-loop running $\alpha_{\overline{\text{MS}}}$ with a fitted 5-loop coefficient in the β -function is used) with high-order terms in a double expansion in $a^2\Lambda^2$ and $a^2m_c^2$ supplemented by priors which limit the size of the coefficients. The priors play an especially important role in these fits given the much larger number of fit parameters than data points. We note, however, that the size of the coefficients does not prevent high-order terms from contributing significantly, since the data includes values of am_c that are rather close to 1.

We note that the result of JLQCD 16 was classified in FLAG 19 as having passed all FLAG criteria, although the scale is set by the charm-quark mass, implying $\alpha_{\text{eff}} \simeq 0.38$. We now assign a red flag for renormalization scale, as we do for Petreczky 19 and Boito 20 (see below). Since FLAG 19, there have been three new studies, Petreczky 19 [34], Petreczky 20 [33] and Boito 20 [36] (Petreczky 19/Petreczky 20 supersede Maezawa 16 [175]). While Petreczky 19/Petreczky 20 share the same lattice data for heavy quark masses in the range $m_h = m_c - 4m_c$ they use a different strategy for continuum extrapolations and a different treatment of perturbative uncertainties. Petreczky 19 [34] perform continuum extrapolation separately for each value of the valence-quark mass, while Petreczky 20 rely on joint continuum extrapolations of the lattice data at different heavy-quark masses, similar to the analysis of HPQCD, but without Bayesian priors. It is concluded that reliable continuum extrapolations for $m_h \geq 2m_c$ require a joint fit to the data. This limits the eligible α_s determinations in Petreczky 19 [34] to $m_h = m_c$ and $1.5m_c$, for which, however, the FLAG criteria are not satisfied. There is also a difference

in the choice of renormalization scale between both analyses: Petreczky 19 [34] uses $\mu = m_h$, while Petreczky 20 [33] considers several choices of μ in the range $\mu = 2/3m_h - 3m_h$, which leads to larger perturbative uncertainties in the determination of α_s [33]. Boito 20 [36] use published continuum extrapolated lattice results for $m_h = m_c$ and performs its own extraction of α_s . Limiting the choice of m_h to the charm-quark mass means that the FLAG criteria are not met ($\alpha_{\text{eff}} \simeq 0.38$). However, their analysis gives valuable insight into the perturbative error. In addition to the renormalization scale μ , Boito 20 also vary the renormalization scale μ_m at which the charm quark mass is defined. The corresponding result $\alpha_s(M_Z) = 0.1177(20)$ agrees well with previous lattice determination but has a larger error, which is dominated by the perturbative uncertainty due to the variation of both scales. This increased uncertainty suggests that the perturbative error estimated by HPQCD using a fixed scale $\mu = 3m_h$ may be too small. Therefore, we take the average of the HPQCD 10 and HPQCD 14A determinations and assign an error of 0.0020, based on the analysis of Boito 20 [36]. This results in the range $\alpha_s(M_Z) = 0.11826(200)$.

- *Light quark vacuum polarization*

Since FLAG 19 a new study, Cali 20 [32] appeared, which uses the light current two-point functions in position space, evaluated on a subset of CLS configurations for lattice spacings in the range 0.038–0.076 fm, and for Euclidean distances 0.13–0.19 fm, corresponding to renormalization scales $\mu = 1\text{--}1.5$ GeV. Both flavour nonsinglet vector and axial vector currents are considered and their difference is shown to vanish within errors. After continuum and chiral limits are taken, the effective coupling from the axial vector two-point function is converted at 3-loop order to $\alpha_{\overline{\text{MS}}}(\mu)$. The authors do this by numerical solution for $\alpha_{\overline{\text{MS}}}$ and then perform a weighted average of the Λ -parameter estimates for the available energy range, which yields $\Lambda_{\overline{\text{MS}}}^{N_f=3} = 342(17)$ MeV. Note that this is the first calculation in the vacuum polarization category that passes the current FLAG criteria. Yet the renormalization scales are rather low and one might suspect that other nonperturbative (i.e., non chiral-symmetry breaking) effects may still be sizeable. Our main issue is a rather optimistic estimate of perturbative truncation errors, based only on the variation of the Λ -parameter from the range of effective couplings considered. If the solution for the $\overline{\text{MS}}$ coupling is done by series expansion in α_{eff} , the differences in $\alpha_{\overline{\text{MS}}}$, formally of order α_{eff}^5 , are still large at the scales considered. Hence, as a measure of the systematic uncertainty we take the difference 409 – 355 MeV between $\Lambda_{\overline{\text{MS}}}^{N_f=3}$ estimates at $\mu = 1.5$ GeV as a proxy for the total error, i.e. $\Lambda_{\overline{\text{MS}}}^{N_f=3} = 342(54)$ MeV, which translates to our pre-range, $\alpha_s(m_Z) = 0.11863(360)$, from vacuum polarization.

- *Other methods*

Computations using other methods do not qualify for an average yet, predominantly due to a lacking \circ in the continuum extrapolation.

We obtain the central value for our range of α_s from the weighted average of the five pre-ranges listed in Tab. 68. The error of this weighted average is 0.0006, which is quite a bit smaller than the most precise entry. Because, however, the errors on almost all of the α_s calculations that enter the average are dominated by perturbative truncation errors, which are especially difficult to estimate, we choose instead to take a larger range for α_s of 0.0008.

This is the error on the pre-range for α_s from step-scaling, because perturbative-truncation errors are sub-dominant in this method. Our final range is then given by

$$\alpha_{\overline{\text{MS}}}^{(5)}(M_Z) = 0.1184(8). \quad (396)$$

moving up by 2 in the last given digit compared to FLAG 19 and with the same uncertainty. Of the eleven calculations that are included most are within 1σ of this range, an exception being TUMQCD 19 (which supersedes Bazavov 14 and Bazavov 12). Further, the range for $\alpha_{\overline{\text{MS}}}^{(5)}(M_Z)$ presented here is based on results with rather different systematics (apart from the matching across the charm threshold). We therefore believe that the true value is very likely to lie within this range.

All computations which enter this range, with the exception of HPQCD 14A [167], rely on a perturbative inclusion of the charm and bottom quarks. Perturbation theory for the matching of $\bar{g}_{N_f}^2$ and $\bar{g}_{N_f-1}^2$ looks very well behaved even at the mass of the charm. Worries that still there may be purely nonperturbative effects at this rather low scale have been removed by nonperturbative studies of the accuracy of perturbation theory. While the original study in Ref. [104] was not precise enough, the extended one in Ref. [105] estimates effects in the Λ -parameter to be significantly below 1% and thus negligible for the present and near future accuracy.

9.11.3 Ranges for $[r_0\Lambda]^{(N_f)}$ and $\Lambda_{\overline{\text{MS}}}$

In the present situation, we give ranges for $[r_0\Lambda]^{(N_f)}$ and $\Lambda_{\overline{\text{MS}}}$, discussing their determination case by case. We include results with $N_f < 3$ because it is interesting to see the N_f -dependence of the connection of low- and high-energy QCD. This aids our understanding of the field theory and helps in finding possible ways to tackle it beyond the lattice approach. It is also of interest in providing an impression on the size of the vacuum-polarization effects of quarks, in particular with an eye on the still difficult-to-treat heavier charm and bottom quarks. Most importantly, however, the decoupling strategy described in subsection 9.4 means that Λ -parameters at different N_f can be connected by a nonperturbative matching computation. Thus, even results at unphysical flavour numbers, in particular $N_f = 0$, may enter results for the physically interesting case. Rather than phasing out results for “unphysical flavour numbers”, continued scrutiny by FLAG will be necessary. Having said this, we emphasize that results for $[r_0\Lambda]^{(0)}$ and $[r_0\Lambda]^{(2)}$ are *not* meant to be used directly for phenomenology.

For the ranges we obtain:

$$[r_0\Lambda_{\overline{\text{MS}}}]^{(4)} = 0.70(3), \quad (397)$$

$$[r_0\Lambda_{\overline{\text{MS}}}]^{(3)} = 0.808(29), \quad (398)$$

$$[r_0\Lambda_{\overline{\text{MS}}}]^{(2)} = 0.79^{(+5)}_{(-15)}, \quad (399)$$

$$[r_0\Lambda_{\overline{\text{MS}}}]^{(0)} = 0.624(36). \quad (400)$$

No change has occurred since FLAG 19 for $N_f = 2, 4$, so we take over the respective discussion from FLAG 19.

For $N_f = 2 + 1 + 1$, we presently do not quote a range as there is a single result: HPQCD 14A [167] found $[r_0\Lambda]^{(4)} = 0.70(3)$.

For $N_f = 2 + 1$, we take as a central value the weighted average of Cali 20 [32], Ayala 20 [30], TUMQCD 19[29], ALPHA 17 [92] HPQCD 10 [149] (Wilson loops and current two-point

correlators), PACS-CS 09A [93] (with linear continuum extrapolation) and Maltman 08 [150]. Since the uncertainty in r_0 is small compared to that of Λ , we can directly propagate the error from the analog of Eq. (396) with the 2+1+1 number removed and arrive at

$$[r_0\Lambda_{\overline{\text{MS}}}]^{(3)} = 0.808(29). \quad (401)$$

(The error of the straight weighted average is 0.012.) It is in good agreement with all 2+1 results without red tags. In physical units, using $r_0 = 0.472$ fm and neglecting its error, this means¹³

$$\Lambda_{\overline{\text{MS}}}^{(3)} = 338(12) \text{ MeV}, \quad (402)$$

where the error of the straight weighted average is less than 5 MeV.

For $N_f = 2$, at present there is one computation with a ★ rating for all criteria, ALPHA 12 [57]. We adopt it as our central value and enlarge the error to cover the central values of the other three results with filled green boxes. This results in an asymmetric error. Our range is unchanged as compared to FLAG 13,

$$[r_0\Lambda_{\overline{\text{MS}}}]^{(2)} = 0.79^{(+5)}_{(-15)}, \quad (403)$$

and in physical units, using $r_0 = 0.472$ fm,

$$\Lambda_{\overline{\text{MS}}}^{(2)} = 330^{(+21)}_{(-63)} \text{ MeV}. \quad (404)$$

A weighted average of the four eligible numbers would yield $[r_0\Lambda_{\overline{\text{MS}}}]^{(2)} = 0.689(23)$, not covering the best result and in particular leading to a smaller error than we feel is justified, given the issues discussed previously in Sec. 9.5.2 (Karbstein 18 [123], ETM 11C [125]) and Sec. 9.9.2 (ETM 10F [193]). Thus we believe that our estimate is a conservative choice; the low values of ETM 11C [125] and Karbstein 18 [123] lead to a large downward error. We note that this can largely be explained by different values of r_0 between ETM 11C [125] and ALPHA 12 [57]. We still hope that future work will improve the situation.

For $N_f = 0$, the new result DallaBrida 19 [27], is quite large compared to the FLAG 19 average. We combine it with those results which entered the FLAG 19 report, namely ALPHA 98 [96], QCDSF/UKQCD 05 [151], Brambilla 10 [127], Kitazawa 16 [156] and Ishikawa 17 [87] for forming a range.¹⁴ Taking a weighted average of the six numbers, we obtain $[r_0\Lambda_{\overline{\text{MS}}}]^{(0)} = 0.624(5)$, up from 0.615(5) for FLAG 19.

Clearly the errors are dominantly systematic, mostly due to perturbative truncation errors. Since we do not change the FLAG 19 criteria for this edition, we give a range which encompasses all central values. Unfortunately, this requires to double the error of the FLAG 19 result (which was given by 0.615(18)), due to the large central value of 0.660 by DallaBrida 19. We arrive at our range for $N_f = 0$,

$$[r_0\Lambda_{\overline{\text{MS}}}]^{(0)} = 0.624(36). \quad (405)$$

¹³In the FLAG 19 report [1], an inaccurate conversion of $[r_0\Lambda_{\overline{\text{MS}}}]^{(3)}$ in Eq. (345) to physical units (using $r_0 = 0.472$ fm) led to 343 MeV in Eqs. (346,353). However, using $\text{fm} \times \text{MeV} = 1/197.3$ gives 337 MeV (Eqs. (351) and (352) are however correct). Note: Equation references in this footnote are from FLAG 19 [1].

¹⁴We have assigned a ○ for the continuum limit, in Boucaud 00A [198], 00B [197], 01A [196], Soto 01 [195] but these results are from lattices of a very small physical size with finite-size effects that are not easily quantified.

This is clearly not very satisfactory, and, despite this large error, this still means that the high quality, and statistics dominated new step-scaling result Dalla Brida 19 is more than 3 sigma away from the central value of the new FLAG average.

Converting to physical units, again using $r_0 = 0.472$ fm yields

$$\Lambda_{\overline{\text{MS}}}^{(0)} = 261(15) \text{ MeV}. \quad (406)$$

While the conversion of the Λ parameter to physical units is quite unambiguous for $N_f = 2+1$, our choice of $r_0 = 0.472$ fm also for smaller numbers of flavour amounts to a convention, in particular for $N_f = 0$. Indeed, in the Tabs. 60–66 somewhat different numbers in MeV are found.

9.11.4 Conclusions

With the present results our range for the strong coupling is
(repeating Eq. (396))

$$\alpha_{\overline{\text{MS}}}^{(5)}(M_Z) = 0.1184(8) \quad \text{Refs. [29, 30, 32, 92, 93, 149, 150, 167]},$$

and the associated Λ parameters

$$\Lambda_{\overline{\text{MS}}}^{(5)} = 214(10) \text{ MeV} \quad \text{Refs. [29, 30, 32, 92, 93, 149, 150, 167]}, \quad (407)$$

$$\Lambda_{\overline{\text{MS}}}^{(4)} = 297(12) \text{ MeV} \quad \text{Refs. [29, 30, 32, 92, 93, 149, 150, 167]}, \quad (408)$$

$$\Lambda_{\overline{\text{MS}}}^{(3)} = 339(12) \text{ MeV} \quad \text{Refs. [29, 30, 32, 92, 93, 149, 150, 167]}. \quad (409)$$

Compared with FLAG 19, the central values have moved slightly, with the errors remaining the same.

It is interesting to compare with the Particle Data Group average of nonlattice determinations of recent years,

$$\alpha_{\overline{\text{MS}}}^{(5)}(M_Z) = 0.1176(11), \quad \text{PDG 20, nonlattice [10], also appeared as Eq. (319)},$$

$$\alpha_{\overline{\text{MS}}}^{(5)}(M_Z) = 0.1174(16), \quad \text{PDG 18, nonlattice [11]}, \quad (410)$$

$$\alpha_{\overline{\text{MS}}}^{(5)}(M_Z) = 0.1174(16), \quad \text{PDG 16, nonlattice [210]}, \quad (411)$$

$$\alpha_{\overline{\text{MS}}}^{(5)}(M_Z) = 0.1175(17), \quad \text{PDG 14, nonlattice [211]}, \quad (412)$$

$$\alpha_{\overline{\text{MS}}}^{(5)}(M_Z) = 0.1183(12), \quad \text{PDG 12, nonlattice [212]}. \quad (413)$$

(there was no update in [11]). There is good agreement with Eq. (396). Despite our very conservative error estimate, the FLAG lattice average has an error that is 30% smaller than the PDG 20 nonlattice-world average and a weighted average of the two [Eq. (396) and Eq. (319)] yields

$$\alpha_{\overline{\text{MS}}}^{(5)}(M_Z) = 0.1181(7), \quad \text{FLAG 21 + PDG 20}. \quad (414)$$

In the lower plot in Fig. 41 we show as blue circles the various PDG pre-averages which lead to the PDG 20 nonlattice average. They are on a similar level as our pre-ranges (green squares) : each one corresponds to an estimate (by the PDG) of α_s determined from one set

of input quantities. Within each pre-average multiple groups did the analysis and published their results as displayed in Ref. [10].

The fact that our range for the lattice determination of $\alpha_{\overline{\text{MS}}}(M_Z)$ in Eq. (396) is in excellent agreement with the PDG 20 nonlattice average Eq. (319) is an excellent check for the subtle interplay of theory, phenomenology and experiments in the nonlattice determinations. The work done on the lattice provides an entirely independent determination, with negligible experimental uncertainty, which reaches a better precision even with our quite conservative estimate of its uncertainty.

We finish by commenting on perspectives for the future. The step-scaling methods have been shown to yield a very precise result and to satisfy all criteria easily. A downside is that dedicated simulations have to be done and the method is thus hardly used. It would be desirable to have at least one more such computation by an independent collaboration, as also requested in the review [12]. While this FLAG review does not report an error reduction compared to FLAG 19, the understanding of some systematic errors has improved. With the exception of the step-scaling result, all determinations of α_s , appear to be limited by systematic uncertainties due to perturbative truncation errors. Similar conclusions have been drawn in the recent review article [25]. In order to improve control of systematics it would be necessary to reach higher energy scales without incurring large cutoff effects. This could be achieved by applying step-scaling methods in large (infinite) volume, provided that finite volume effects are carefully controlled. Even a relatively modest increase by a scale factor 2–3 could significantly enhance the scope for some of the current approaches to determine α_s . Another hope for improvement are decoupling strategies, following the recent proposal by the ALPHA collaboration, cf. Sec. 9.4. This in turn motivates further state-of-the-art studies in the pure gauge theory ($N_f = 0$), where it would be important to resolve the current tension between results in the literature.

References

- [1] [FLAG 19] S. Aoki et al., *FLAG Review 2019: Flavour Lattice Averaging Group (FLAG)*, *Eur. Phys. J. C* **80** (2020) 113 [1902.08191].
- [2] S. Dittmaier et al., *Handbook of LHC Higgs Cross Sections: 2. Differential Distributions*, [1201.3084](#).
- [3] LHC HIGGS CROSS SECTION WORKING GROUP collaboration, *Handbook of LHC Higgs Cross Sections: 3. Higgs Properties*, [1307.1347](#).
- [4] LBNE collaboration, *Scientific Opportunities with the Long-Baseline Neutrino Experiment*, [1307.7335](#).
- [5] S. Dawson, A. Gritsan, H. Logan, J. Qian, C. Tully et al., *Higgs Working Group Report of the Snowmass 2013 Community Planning Study*, [1310.8361](#).
- [6] A. Accardi et al., *A critical appraisal and evaluation of modern PDFs*, *Eur. Phys. J. C* **76** (2016) 471 [1603.08906].
- [7] G.P. Lepage, P.B. Mackenzie and M.E. Peskin, *Expected Precision of Higgs Boson Partial Widths within the Standard Model*, [1404.0319](#).

- [8] D. Buttazzo, G. Degrossi, P.P. Giardino, G.F. Giudice, F. Sala, A. Salvio et al., *Investigating the near-criticality of the Higgs boson*, *JHEP* **12** (2013) 089 [[1307.3536](#)].
- [9] J.R. Espinosa, *Vacuum Stability and the Higgs Boson*, *PoS LATTICE2013* (2014) 010 [[1311.1970](#)].
- [10] PARTICLE DATA GROUP collaboration, *Review of Particle Physics*, *PTEP* **2020** (2020) 083C01.
- [11] PARTICLE DATA GROUP collaboration, *Review of Particle Physics*, *Phys. Rev.* **D98** (2018) 030001.
- [12] G.P. Salam, *The strong coupling: a theoretical perspective*, in *From My Vast Repertoire ...: Guido Altarelli's Legacy*, A. Levy, S. Forte and G. Ridolfi, eds., pp. 101–121 (2019), DOI [[1712.05165](#)].
- [13] T. van Ritbergen, J. A. M. Vermaseren and S. A. Larin, *The four-loop β -function in Quantum Chromodynamics*, *Phys. Lett.* **B400** (1997) 379 [[hep-ph/9701390](#)].
- [14] M. Czakon, *The Four-loop QCD beta-function and anomalous dimensions*, *Nucl. Phys.* **B710** (2005) 485 [[hep-ph/0411261](#)].
- [15] T. Luthe, A. Maier, P. Marquard and Y. Schröder, *Towards the five-loop Beta function for a general gauge group*, *JHEP* **07** (2016) 127 [[1606.08662](#)].
- [16] F. Herzog, B. Ruijl, T. Ueda, J.A.M. Vermaseren and A. Vogt, *The five-loop beta function of Yang-Mills theory with fermions*, *JHEP* **02** (2017) 090 [[1701.01404](#)].
- [17] P.A. Baikov, K.G. Chetyrkin and J.H. Kuhn, *Five-Loop Running of the QCD coupling constant*, *Phys. Rev. Lett.* **118** (2017) 082002 [[1606.08659](#)].
- [18] W. Bernreuther and W. Wetzel, *Decoupling of heavy quarks in the minimal subtraction scheme*, *Nucl.Phys.* **B197** (1982) 228.
- [19] K. Chetyrkin, J.H. Kuhn and C. Sturm, *QCD decoupling at four loops*, *Nucl.Phys.* **B744** (2006) 121 [[hep-ph/0512060](#)].
- [20] Y. Schröder and M. Steinhauser, *Four-loop decoupling relations for the strong coupling*, *JHEP* **01** (2006) 051 [[hep-ph/0512058](#)].
- [21] B.A. Kniehl, A.V. Kotikov, A.I. Onishchenko and O.L. Veretin, *Strong-coupling constant with flavor thresholds at five loops in the anti-MS scheme*, *Phys. Rev. Lett.* **97** (2006) 042001 [[hep-ph/0607202](#)].
- [22] A.G. Grozin, M. Hoeschele, J. Hoff and M. Steinhauser, *Simultaneous decoupling of bottom and charm quarks*, *JHEP* **09** (2011) 066 [[1107.5970](#)].
- [23] K.G. Chetyrkin, J.H. Kuhn and M. Steinhauser, *RunDec: A Mathematica package for running and decoupling of the strong coupling and quark masses*, *Comput. Phys. Commun.* **133** (2000) 43 [[hep-ph/0004189](#)].
- [24] F. Herren and M. Steinhauser, *Version 3 of RunDec and CRunDec*, *Comput. Phys. Commun.* **224** (2018) 333 [[1703.03751](#)].

- [25] L. Del Debbio and A. Ramos, *Lattice determinations of the strong coupling*, *Physics Reports* **920** (2021) 1 [2101.04762].
- [26] [ALPHA 19A] M. Dalla Brida, R. Höllwieser, F. Knechtli, T. Korzec, A. Ramos and R. Sommer, *Non-perturbative renormalization by decoupling*, *Phys. Lett. B* **807** (2020) 135571 [1912.06001].
- [27] M. Dalla Brida and A. Ramos, *The gradient flow coupling at high-energy and the scale of $SU(3)$ Yang–Mills theory*, *Eur. Phys. J. C* **79** (2019) 720 [1905.05147].
- [28] A. Nada and A. Ramos, *An analysis of systematic effects in finite size scaling studies using the gradient flow*, *Eur. Phys. J. C* **81** (2021) 1 [2007.12862].
- [29] [TUMQCD 19] A. Bazavov, N. Brambilla, X. Garcia i Tormo, P. Petreczky, J. Soto, A. Vairo et al., *Determination of the QCD coupling from the static energy and the free energy*, *Phys. Rev. D* **100** (2019) 114511 [1907.11747].
- [30] C. Ayala, X. Lobregat and A. Pineda, *Determination of $\alpha(M_z)$ from an hyperasymptotic approximation to the energy of a static quark-antiquark pair*, *JHEP* **09** (2020) 016 [2005.12301].
- [31] N. Husung, A. Nada and R. Sommer, *Yang Mills short distance potential and perturbation theory*, *PoS LATTICE2019* (2020) 263.
- [32] S. Cali, K. Cichy, P. Korcyl and J. Simeth, *Running coupling constant from position-space current-current correlation functions in three-flavor lattice QCD*, *Phys. Rev. Lett.* **125** (2020) 242002 [2003.05781].
- [33] P. Petreczky and J.H. Weber, *Strong coupling constant from moments of quarkonium correlators revisited*, *Eur. Phys. J. C* **82** (2022) 64 [2012.06193].
- [34] P. Petreczky and J. Weber, *Strong coupling constant and heavy quark masses in $(2+1)$ -flavor QCD*, *Phys. Rev. D* **100** (2019) 034519 [1901.06424].
- [35] D. Boito and V. Mateu, *Precise α_s determination from charmonium sum rules*, *Phys. Lett. B* **806** (2020) 135482 [1912.06237].
- [36] D. Boito and V. Mateu, *Precise determination of α_s from relativistic quarkonium sum rules*, *JHEP* **03** (2020) 094 [2001.11041].
- [37] S. Zafeiropoulos, P. Boucaud, F. De Soto, J. Rodríguez-Quintero and J. Segovia, *Strong Running Coupling from the Gauge Sector of Domain Wall Lattice QCD with Physical Quark Masses*, *Phys. Rev. Lett.* **122** (2019) 162002 [1902.08148].
- [38] M. Lüscher, *Properties and uses of the Wilson flow in lattice QCD*, *JHEP* **08** (2010) 071 [1006.4518], [Erratum: *JHEP* **03** (2014) 092].
- [39] [BMW 12A] S. Borsanyi, S. Dür, Z. Fodor, C. Hoelbling, S.D. Katz et al., *High-precision scale setting in lattice QCD*, *JHEP* **1209** (2012) 010 [1203.4469].
- [40] R. Sommer, *A new way to set the energy scale in lattice gauge theories and its applications to the static force and α_s in $SU(2)$ Yang-Mills theory*, *Nucl. Phys.* **B411** (1994) 839 [hep-lat/9310022].

- [41] C.W. Bernard et al., *The static quark potential in three flavor QCD*, *Phys. Rev.* **D62** (2000) 034503 [[hep-lat/0002028](#)].
- [42] G. Martinelli and C.T. Sachrajda, *On the difficulty of computing higher twist corrections*, *Nucl.Phys.* **B478** (1996) 660 [[hep-ph/9605336](#)].
- [43] A.H. Hoang and C. Regner, *On the Difference between FOPT and CIPT for Hadronic Tau Decays*, vol. 230, 2021, DOI [[2105.11222](#)].
- [44] S. Bethke, A.H. Hoang, S. Kluth, J. Schieck, I.W. Stewart et al., *Workshop on Precision Measurements of α_s* , [1110.0016](#).
- [45] D. Boito, M. Golterman, K. Maltman, J. Osborne and S. Peris, *Strong coupling from the revised ALEPH data for hadronic τ decays*, *Phys. Rev.* **D91** (2015) 034003 [[1410.3528](#)].
- [46] D. Boito, M. Golterman, K. Maltman and S. Peris, *Strong coupling from hadronic τ decays: A critical appraisal*, *Phys. Rev.* **D95** (2017) 034024 [[1611.03457](#)].
- [47] L. Del Debbio, H. Panagopoulos and E. Vicari, *Theta dependence of $SU(N)$ gauge theories*, *JHEP* **08** (2002) 044 [[hep-th/0204125](#)].
- [48] C. Bernard et al., *Topological susceptibility with the improved Asqtad action*, *Phys. Rev.* **D68** (2003) 114501 [[hep-lat/0308019](#)].
- [49] [ALPHA 10C] S. Schaefer, R. Sommer and F. Virotta, *Critical slowing down and error analysis in lattice QCD simulations*, *Nucl.Phys.* **B845** (2011) 93 [[1009.5228](#)].
- [50] A. Chowdhury, A. Harindranath, J. Maiti and P. Majumdar, *Topological susceptibility in lattice Yang-Mills theory with open boundary condition*, *JHEP* **02** (2014) 045 [[1311.6599](#)].
- [51] [LSD 14] R. C. Brower et al., *Maximum-Likelihood Approach to Topological Charge Fluctuations in Lattice Gauge Theory*, *Phys. Rev.* **D90** (2014) 014503 [[1403.2761](#)].
- [52] [HotQCD 14] A. Bazavov et al., *Equation of state in $(2+1)$ -flavor QCD*, *Phys.Rev.* **D90** (2014) 094503 [[1407.6387](#)].
- [53] [JLQCD 15] H. Fukaya, S. Aoki, G. Cossu, S. Hashimoto, T. Kaneko and J. Noaki, *η' meson mass from topological charge density correlator in QCD*, *Phys. Rev.* **D92** (2015) 111501 [[1509.00944](#)].
- [54] M. Lüscher and S. Schaefer, *Lattice QCD without topology barriers*, *JHEP* **1107** (2011) 036 [[1105.4749](#)].
- [55] [ETM 09C] R. Baron et al., *Light meson physics from maximally twisted mass lattice QCD*, *JHEP* **08** (2010) 097 [[0911.5061](#)].
- [56] [ETM 09] B. Blossier et al., *Pseudoscalar decay constants of kaon and D-mesons from $N_f = 2$ twisted mass lattice QCD*, *JHEP* **0907** (2009) 043 [[0904.0954](#)].
- [57] [ALPHA 12] P. Fritzsch, F. Knechtli, B. Leder, M. Marinkovic, S. Schaefer et al., *The strange quark mass and the Λ parameter of two flavor QCD*, *Nucl.Phys.* **B865** (2012) 397 [[1205.5380](#)].

- [58] [QCDSF 12] G. Bali, P. Bruns, S. Collins, M. Deka, B. Glasle et al., *Nucleon mass and sigma term from lattice QCD with two light fermion flavors*, *Nucl.Phys.* **B866** (2013) 1 [[1206.7034](#)].
- [59] [HPQCD 09B] C. T. H. Davies, E. Follana, I. Kendall, G.P. Lepage and C. McNeile, *Precise determination of the lattice spacing in full lattice QCD*, *Phys.Rev.* **D81** (2010) 034506 [[0910.1229](#)].
- [60] [MILC 10] A. Bazavov et al., *Results for light pseudoscalar mesons*, *PoS LAT2010* (2010) 074 [[1012.0868](#)].
- [61] [HotQCD 11] A. Bazavov, T. Bhattacharya, M. Cheng, C. DeTar, H. Ding et al., *The chiral and deconfinement aspects of the QCD transition*, *Phys.Rev.* **D85** (2012) 054503 [[1111.1710](#)].
- [62] S. Necco and R. Sommer, *The $N_f = 0$ heavy quark potential from short to intermediate distances*, *Nucl.Phys.* **B622** (2002) 328 [[hep-lat/0108008](#)].
- [63] M. Lüscher and P. Weisz, *Quark confinement and the bosonic string*, *JHEP* **0207** (2002) 049 [[hep-lat/0207003](#)].
- [64] S. Sint and A. Ramos, *On $O(a^2)$ effects in gradient flow observables*, *PoS LATTICE2014* (2015) 329 [[1411.6706](#)].
- [65] Z. Fodor, K. Holland, J. Kuti, S. Mondal, D. Negradi et al., *The lattice gradient flow at tree-level and its improvement*, *JHEP* **1409** (2014) 018 [[1406.0827](#)].
- [66] [MILC 15] A. Bazavov et al., *Gradient flow and scale setting on MILC HISQ ensembles*, *Phys. Rev.* **D93** (2016) 094510 [[1503.02769](#)].
- [67] [QCDSF/UKQCD 15B] V. .G. Bornyakov et al., *Wilson flow and scale setting from lattice QCD*, [1508.05916](#).
- [68] R. Sommer, *Scale setting in lattice QCD*, *PoS LATTICE2013* (2014) 015 [[1401.3270](#)].
- [69] [ALPHA 16] M. Dalla Brida, P. Fritzsche, T. Korzec, A. Ramos, S. Sint and R. Sommer, *Determination of the QCD Λ -parameter and the accuracy of perturbation theory at high energies*, *Phys. Rev. Lett.* **117** (2016) 182001 [[1604.06193](#)].
- [70] [ALPHA 18] M. Dalla Brida, P. Fritzsche, T. Korzec, A. Ramos, S. Sint and R. Sommer, *A non-perturbative exploration of the high energy regime in $N_f = 3$ QCD*, *Eur. Phys. J.* **C78** (2018) 372 [[1803.10230](#)].
- [71] M. Lüscher, P. Weisz and U. Wolff, *A numerical method to compute the running coupling in asymptotically free theories*, *Nucl.Phys.* **B359** (1991) 221.
- [72] M. Lüscher, R. Narayanan, P. Weisz and U. Wolff, *The Schrödinger functional: a renormalizable probe for non-abelian gauge theories*, *Nucl. Phys.* **B384** (1992) 168 [[hep-lat/9207009](#)].
- [73] S. Sint, *On the Schrödinger functional in QCD*, *Nucl.Phys.* **B421** (1994) 135 [[hep-lat/9312079](#)].

- [74] A. Coste, A. Gonzalez-Arroyo, J. Jurkiewicz and C. Korthals Altes, *Zero momentum contribution to Wilson loops in periodic boxes*, *Nucl.Phys.* **B262** (1985) 67.
- [75] M. Lüscher, R. Sommer, P. Weisz and U. Wolff, *A precise determination of the running coupling in the $SU(3)$ Yang-Mills theory*, *Nucl.Phys.* **B413** (1994) 481 [[hep-lat/9309005](#)].
- [76] S. Sint and R. Sommer, *The running coupling from the QCD Schrödinger functional: a one loop analysis*, *Nucl.Phys.* **B465** (1996) 71 [[hep-lat/9508012](#)].
- [77] [ALPHA 99] A. Bode, P. Weisz and U. Wolff, *Two loop computation of the Schrödinger functional in lattice QCD*, *Nucl.Phys.* **B576** (2000) 517 [[hep-lat/9911018](#)].
- [78] [CP-PACS 04] S. Takeda, S. Aoki, M. Fukugita, K.-I. Ishikawa, N. Ishizuka et al., *A scaling study of the step scaling function in $SU(3)$ gauge theory with improved gauge actions*, *Phys.Rev.* **D70** (2004) 074510 [[hep-lat/0408010](#)].
- [79] M. Lüscher, *A Semiclassical Formula for the Topological Susceptibility in a Finite Space-time Volume*, *Nucl. Phys.* **B205** (1982) 483.
- [80] P. Fritzsche, A. Ramos and F. Stollenwerk, *Critical slowing down and the gradient flow coupling in the Schrödinger functional*, *PoS Lattice2013* (2014) 461 [[1311.7304](#)].
- [81] M. Dalla Brida, P. Fritzsche, T. Korzec, A. Ramos, S. Sint and R. Sommer, *Slow running of the Gradient Flow coupling from 200 MeV to 4 GeV in $N_f = 3$ QCD*, *Phys. Rev.* **D95** (2017) 014507 [[1607.06423](#)].
- [82] M. Lüscher, *Step scaling and the Yang-Mills gradient flow*, *JHEP* **06** (2014) 105 [[1404.5930](#)].
- [83] R. Narayanan and H. Neuberger, *Infinite N phase transitions in continuum Wilson loop operators*, *JHEP* **03** (2006) 064 [[hep-th/0601210](#)].
- [84] Z. Fodor, K. Holland, J. Kuti, D. Negradi and C.H. Wong, *The Yang-Mills gradient flow in finite volume*, *JHEP* **1211** (2012) 007 [[1208.1051](#)].
- [85] P. Fritzsche and A. Ramos, *The gradient flow coupling in the Schrödinger functional*, *JHEP* **1310** (2013) 008 [[1301.4388](#)].
- [86] A. Ramos, *The gradient flow running coupling with twisted boundary conditions*, *JHEP* **11** (2014) 101 [[1409.1445](#)].
- [87] K.-I. Ishikawa, I. Kanamori, Y. Murakami, A. Nakamura, M. Okawa and R. Ueno, *Non-perturbative determination of the Λ -parameter in the pure $SU(3)$ gauge theory from the twisted gradient flow coupling*, *JHEP* **12** (2017) 067 [[1702.06289](#)].
- [88] M. Dalla Brida and M. Lüscher, *SMD-based numerical stochastic perturbation theory*, *Eur. Phys. J.* **C77** (2017) 308 [[1703.04396](#)].
- [89] E.I. Bribian and M. Garcia Perez, *The twisted gradient flow coupling at one loop*, *JHEP* **03** (2019) 200 [[1903.08029](#)].

- [90] [ALPHA 10A] F. Tekin, R. Sommer and U. Wolff, *The running coupling of QCD with four flavors*, *Nucl.Phys.* **B840** (2010) 114 [[1006.0672](#)].
- [91] P. Perez-Rubio and S. Sint, *Non-perturbative running of the coupling from four flavour lattice QCD with staggered quarks*, *PoS LAT2010* (2010) 236 [[1011.6580](#)].
- [92] [ALPHA 17] M. Bruno, M. Dalla Brida, P. Fritzsche, T. Korzec, A. Ramos, S. Schaefer et al., *QCD Coupling from a Nonperturbative Determination of the Three-Flavor Λ Parameter*, *Phys. Rev. Lett.* **119** (2017) 102001 [[1706.03821](#)].
- [93] [PACS-CS 09A] S. Aoki et al., *Precise determination of the strong coupling constant in $N_f = 2 + 1$ lattice QCD with the Schrödinger functional scheme*, *JHEP* **0910** (2009) 053 [[0906.3906](#)].
- [94] [ALPHA 04] M. Della Morte et al., *Computation of the strong coupling in QCD with two dynamical flavours*, *Nucl. Phys.* **B713** (2005) 378 [[hep-lat/0411025](#)].
- [95] [ALPHA 01A] A. Bode et al., *First results on the running coupling in QCD with two massless flavors*, *Phys.Lett.* **B515** (2001) 49 [[hep-lat/0105003](#)].
- [96] [ALPHA 98] S. Capitani, M. Lüscher, R. Sommer and H. Wittig, *Nonperturbative quark mass renormalization in quenched lattice QCD*, *Nucl.Phys.* **B544** (1999) 669 [[hep-lat/9810063](#)].
- [97] J. Bulava and S. Schaefer, *Improvement of $N_f = 3$ lattice QCD with Wilson fermions and tree-level improved gauge action*, *Nucl. Phys.* **B874** (2013) 188 [[1304.7093](#)].
- [98] M. Lüscher and P. Weisz, *On-shell improved lattice gauge theories*, *Commun. Math. Phys.* **97** (1985) 59.
- [99] [JLQCD/CP-PACS 04] N. Yamada et al., *Non-perturbative $O(a)$ -improvement of Wilson quark action in three-flavor QCD with plaquette gauge action*, *Phys.Rev.* **D71** (2005) 054505 [[hep-lat/0406028](#)].
- [100] [RBC/UKQCD 08] C. Allton et al., *Physical results from 2+1 flavor domain wall QCD and $SU(2)$ chiral perturbation theory*, *Phys. Rev.* **D78** (2008) 114509 [[0804.0473](#)].
- [101] A. Gonzalez-Arroyo and M. Okawa, *The string tension from smeared Wilson loops at large N* , *Phys. Lett.* **B718** (2013) 1524 [[1206.0049](#)].
- [102] M. Dalla Brida, *Past, present, and future of precision determinations of the QCD parameters from lattice QCD*, *Eur. Phys. J. A* **57** (2021) 66 [[2012.01232](#)].
- [103] ALPHA collaboration, *Results for α_s from the decoupling strategy*, vol. LATTICE2021, p. 492, 2022, DOI [[2112.09623](#)].
- [104] [ALPHA 14A] M. Bruno, J. Finkenrath, F. Knechtli, B. Leder and R. Sommer, *Effects of Heavy Sea Quarks at Low Energies*, *Phys. Rev. Lett.* **114** (2015) 102001 [[1410.8374](#)].
- [105] A. Athenodorou, J. Finkenrath, F. Knechtli, T. Korzec, B. Leder, M.K. Marinkovic et al., *How perturbative are heavy sea quarks?*, *Nucl. Phys.* **B943** (2019) 114612 [[1809.03383](#)].

- [106] M. Gerlach, F. Herren and M. Steinhauser, *Wilson coefficients for Higgs boson production and decoupling relations to $\mathcal{O}(\alpha_s^4)$* , *JHEP* **11** (2018) 141 [[1809.06787](#)].
- [107] [ALPHA 18C] I. Campos, P. Fritzsche, C. Pena, D. Preti, A. Ramos and A. Vladikas, *Non-perturbative quark mass renormalisation and running in $N_f = 3$ QCD*, *Eur. Phys. J. C* **78** (2018) 387 [[1802.05243](#)].
- [108] C. Michael, *The running coupling from lattice gauge theory*, *Phys.Lett.* **B283** (1992) 103 [[hep-lat/9205010](#)].
- [109] [UKQCD 92] S. P. Booth et al., *The running coupling from $SU(3)$ lattice gauge theory*, *Phys. Lett.* **B294** (1992) 385 [[hep-lat/9209008](#)].
- [110] W. Fischler, *Quark-antiquark potential in QCD*, *Nucl.Phys.* **B129** (1977) 157.
- [111] A. Billoire, *How heavy must be quarks in order to build coulombic $q\bar{q}$ bound states*, *Phys.Lett.* **B92** (1980) 343.
- [112] M. Peter, *The static potential in QCD: a full two loop calculation*, *Nucl.Phys.* **B501** (1997) 471 [[hep-ph/9702245](#)].
- [113] Y. Schröder, *The static potential in QCD to two loops*, *Phys.Lett.* **B447** (1999) 321 [[hep-ph/9812205](#)].
- [114] N. Brambilla, A. Pineda, J. Soto and A. Vairo, *The infrared behavior of the static potential in perturbative QCD*, *Phys.Rev.* **D60** (1999) 091502 [[hep-ph/9903355](#)].
- [115] A.V. Smirnov, V.A. Smirnov and M. Steinhauser, *Three-loop static potential*, *Phys.Rev.Lett.* **104** (2010) 112002 [[0911.4742](#)].
- [116] C. Anzai, Y. Kiyo and Y. Sumino, *Static QCD potential at three-loop order*, *Phys.Rev.Lett.* **104** (2010) 112003 [[0911.4335](#)].
- [117] N. Brambilla, A. Vairo, X. Garcia i Tormo and J. Soto, *The QCD static energy at NNNLL*, *Phys.Rev.* **D80** (2009) 034016 [[0906.1390](#)].
- [118] S. Necco and R. Sommer, *Testing perturbation theory on the $N_f = 0$ static quark potential*, *Phys.Lett.* **B523** (2001) 135 [[hep-ph/0109093](#)].
- [119] H. Takaura, T. Kaneko, Y. Kiyo and Y. Sumino, *Determination of α_s from static QCD potential with renormalon subtraction*, *Phys. Lett.* **B789** (2019) 598 [[1808.01632](#)].
- [120] H. Takaura, T. Kaneko, Y. Kiyo and Y. Sumino, *Determination of α_s from static QCD potential: OPE with renormalon subtraction and Lattice QCD*, *JHEP* **04** (2019) 155 [[1808.01643](#)].
- [121] A. Bazavov, N. Brambilla, X. Garcia i Tormo, P. Petreczky, S. J. and A. Vairo, *Determination of α_s from the QCD static energy: An update*, *Phys.Rev.* **D90** (2014) 074038 [[1407.8437](#)].
- [122] A. Bazavov, N. Brambilla, X. Garcia i Tormo, P. Petreczky, J. Soto et al., *Determination of α_s from the QCD static energy*, *Phys.Rev.* **D86** (2012) 114031 [[1205.6155](#)].

- [123] F. Karbstein, M. Wagner and M. Weber, *Determination of $\Lambda_{\overline{MS}}^{(n_f=2)}$ and analytic parametrization of the static quark-antiquark potential*, *Phys. Rev.* **D98** (2018) 114506 [[1804.10909](#)].
- [124] F. Karbstein, A. Peters and M. Wagner, *$\Lambda_{\overline{MS}}^{(n_f=2)}$ from a momentum space analysis of the quark-antiquark static potential*, *JHEP* **1409** (2014) 114 [[1407.7503](#)].
- [125] [ETM 11C] K. Jansen, F. Karbstein, A. Nagy and M. Wagner, *$\Lambda_{\overline{MS}}$ from the static potential for QCD with $N_f = 2$ dynamical quark flavors*, *JHEP* **1201** (2012) 025 [[1110.6859](#)].
- [126] N. Husung, M. Koren, P. Krah and R. Sommer, *$SU(3)$ Yang Mills theory at small distances and fine lattices*, *EPJ Web Conf.* **175** (2018) 14024 [[1711.01860](#)].
- [127] N. Brambilla, X. Garcia i Tormo, J. Soto and A. Vairo, *Precision determination of $r_0 \Lambda_{\overline{MS}}$ from the QCD static energy*, *Phys.Rev.Lett.* **105** (2010) 212001 [[1006.2066](#)].
- [128] G. S. Bali and K. Schilling, *Running coupling and the Λ -parameter from $SU(3)$ lattice simulations*, *Phys.Rev.* **D47** (1993) 661 [[hep-lat/9208028](#)].
- [129] N. Husung, P. Marquard and R. Sommer, *Asymptotic behavior of cutoff effects in Yang–Mills theory and in Wilson’s lattice QCD*, *Eur. Phys. J. C* **80** (2020) 200 [[1912.08498](#)].
- [130] A. Bazavov, P. Petreczky and J. Weber, *Equation of State in 2+1 Flavor QCD at High Temperatures*, *Phys. Rev. D* **97** (2018) 014510 [[1710.05024](#)].
- [131] J.H. Weber, A. Bazavov and P. Petreczky, *Equation of state in (2+1) flavor QCD at high temperatures*, *PoS Confinement2018* (2019) 166 [[1811.12902](#)].
- [132] M. Berwein, N. Brambilla, P. Petreczky and A. Vairo, *Polyakov loop correlator in perturbation theory*, *Phys. Rev. D* **96** (2017) 014025 [[1704.07266](#)], [Addendum: *Phys.Rev.D* 101, 099903 (2020)].
- [133] K.G. Chetyrkin, A.L. Kataev and F.V. Tkachov, *Higher Order Corrections to Sigma-t ($e^+ e^- \rightarrow \text{Hadrons}$) in Quantum Chromodynamics*, *Phys. Lett.* **85B** (1979) 277.
- [134] L.R. Surguladze and M.A. Samuel, *Total hadronic cross-section in $e^+ e^-$ annihilation at the four loop level of perturbative QCD*, *Phys. Rev. Lett.* **66** (1991) 560 [Erratum: *Phys. Rev. Lett.* 66,2416(1991)].
- [135] S.G. Gorishnii, A.L. Kataev and S.A. Larin, *The $O(\alpha_s^3)$ corrections to $\sigma_{tot}(e^+e^- \rightarrow \text{hadrons})$ and $\Gamma(\tau^- \rightarrow \nu_\tau + \text{hadrons})$ in QCD*, *Phys. Lett.* **B259** (1991) 144.
- [136] P.A. Baikov, K.G. Chetyrkin and J.H. Kuhn, *Order α_s^4 QCD Corrections to Z and tau Decays*, *Phys. Rev. Lett.* **101** (2008) 012002 [[0801.1821](#)].
- [137] I. Balitsky, M. Beneke and V.M. Braun, *Instanton contributions to the τ decay widths*, *Phys.Lett.* **B318** (1993) 371 [[hep-ph/9309217](#)].

- [138] K. Chetyrkin and A. Maier, *Massless correlators of vector, scalar and tensor currents in position space at orders α_s^3 and α_s^4 : Explicit analytical results*, *Nucl. Phys. B* **844** (2011) 266 [[1010.1145](#)].
- [139] [JLQCD/TWQCD 08C] E. Shintani et al., *Lattice study of the vacuum polarization function and determination of the strong coupling constant*, *Phys.Rev.* **D79** (2009) 074510 [[0807.0556](#)].
- [140] [JLQCD 10] E. Shintani, S. Aoki, H. Fukaya, S. Hashimoto, T. Kaneko et al., *Strong coupling constant from vacuum polarization functions in three-flavor lattice QCD with dynamical overlap fermions*, *Phys.Rev.* **D82** (2010) 074505, Erratum [[1002.0371](#)].
- [141] R.J. Hudspith, R. Lewis, K. Maltman and E. Shintani, *α_s from the Lattice Hadronic Vacuum Polarisation*, [1804.10286](#).
- [142] R.J. Hudspith, R. Lewis, K. Maltman and E. Shintani, *Determining the QCD coupling from lattice vacuum polarization*, in *Proceedings, 33rd International Symposium on Lattice Field Theory (Lattice 2015)*, vol. LATTICE2015, p. 268, 2016, <http://inspirehep.net/record/1398355/files/arXiv:1510.04890.pdf> [[1510.04890](#)].
- [143] [RBC/UKQCD 14B] T. Blum et al., *Domain wall QCD with physical quark masses*, *Phys. Rev.* **D93** (2016) 074505 [[1411.7017](#)].
- [144] R. Hudspith, R. Lewis, K. Maltman and E. Shintani, *α_s from the Hadronic Vacuum Polarisation*, *EPJ Web Conf.* **175** (2018) 10006.
- [145] [HPQCD 05A] Q. Mason et al., *Accurate determinations of α_s from realistic lattice QCD*, *Phys. Rev. Lett.* **95** (2005) 052002 [[hep-lat/0503005](#)].
- [146] [HPQCD 08A] C. T. H. Davies et al., *Update: accurate determinations of α_s from realistic lattice QCD*, *Phys. Rev.* **D78** (2008) 114507 [[0807.1687](#)].
- [147] G.P. Lepage and P.B. Mackenzie, *On the viability of lattice perturbation theory*, *Phys.Rev.* **D48** (1993) 2250 [[hep-lat/9209022](#)].
- [148] K. Hornbostel, G. Lepage and C. Morningstar, *Scale setting for α_s beyond leading order*, *Phys.Rev.* **D67** (2003) 034023 [[hep-ph/0208224](#)].
- [149] [HPQCD 10] C. McNeile, C. T. H. Davies, E. Follana, K. Hornbostel and G. P. Lepage, *High-precision c and b masses and QCD coupling from current-current correlators in lattice and continuum QCD*, *Phys. Rev.* **D82** (2010) 034512 [[1004.4285](#)].
- [150] K. Maltman, D. Leinweber, P. Moran and A. Sternbeck, *The realistic lattice determination of $\alpha_s(M_Z)$ revisited*, *Phys. Rev.* **D78** (2008) 114504 [[0807.2020](#)].
- [151] [QCDSF/UKQCD 05] M. Göckeler, R. Horsley, A. Irving, D. Pleiter, P. Rakow, G. Schierholz et al., *A determination of the Lambda parameter from full lattice QCD*, *Phys.Rev.* **D73** (2006) 014513 [[hep-ph/0502212](#)].
- [152] [SESAM 99] A. Spitz et al., *α_s from upsilon spectroscopy with dynamical Wilson fermions*, *Phys.Rev.* **D60** (1999) 074502 [[hep-lat/9906009](#)].

- [153] M. Wingate, T.A. DeGrand, S. Collins and U.M. Heller, *From spectroscopy to the strong coupling constant with heavy Wilson quarks*, *Phys.Rev.* **D52** (1995) 307 [[hep-lat/9501034](#)].
- [154] C. T. H. Davies, K. Hornbostel, G. Lepage, A. Lidsey, J. Shigemitsu et al., *A precise determination of α_s from lattice QCD*, *Phys.Lett.* **B345** (1995) 42 [[hep-ph/9408328](#)].
- [155] S. Aoki, M. Fukugita, S. Hashimoto, N. Ishizuka, H. Mino et al., *Manifestation of sea quark effects in the strong coupling constant in lattice QCD*, *Phys.Rev.Lett.* **74** (1995) 22 [[hep-lat/9407015](#)].
- [156] M. Kitazawa, T. Iritani, M. Asakawa, T. Hatsuda and H. Suzuki, *Equation of State for $SU(3)$ Gauge Theory via the Energy-Momentum Tensor under Gradient Flow*, *Phys. Rev.* **D94** (2016) 114512 [[1610.07810](#)].
- [157] [FlowQCD 15] M. Asakawa, T. Iritani, M. Kitazawa and H. Suzuki, *Determination of Reference Scales for Wilson Gauge Action from Yang–Mills Gradient Flow*, [1503.06516](#).
- [158] A. X. El-Khadra, G. Hockney, A.S. Kronfeld and P.B. Mackenzie, *A determination of the strong coupling constant from the charmonium spectrum*, *Phys.Rev.Lett.* **69** (1992) 729.
- [159] [QCDSF/UKQCD 04A] M. Göckeler, R. Horsley, A. Irving, D. Pleiter, P. Rakow, G. Schierholz et al., *Determination of Λ in quenched and full QCD: an update*, *Nucl.Phys.Proc.Suppl.* **140** (2005) 228 [[hep-lat/0409166](#)].
- [160] S. Booth, M. Göckeler, R. Horsley, A. Irving, B. Joo, S. Pickles et al., *The strong coupling constant from lattice QCD with $N_f = 2$ dynamical quarks*, *Nucl.Phys.Proc.Suppl.* **106** (2002) 308 [[hep-lat/0111006](#)].
- [161] [QCDSF/UKQCD 01] S. Booth, M. Göckeler, R. Horsley, A. Irving, B. Joo, S. Pickles et al., *Determination of $\Lambda_{\overline{MS}}$ from quenched and $N_f = 2$ dynamical QCD*, *Phys.Lett.* **B519** (2001) 229 [[hep-lat/0103023](#)].
- [162] [HPQCD 03A] C. T. H. Davies et al., *High-precision lattice QCD confronts experiment*, *Phys. Rev. Lett.* **92** (2004) 022001 [[hep-lat/0304004](#)].
- [163] Q.J. Mason, *High-precision lattice QCD: Perturbations in a non-perturbative world*, Ph.D. thesis, Cornell U., LNS, 2004.
- [164] K. Maltman, *Two recent high-precision determinations of $\alpha(s)$* , *AIP Conf. Proc.* **1261** (2010) 159.
- [165] [HPQCD 08B] I. Allison et al., *High-precision charm-quark mass from current-current correlators in lattice and continuum QCD*, *Phys. Rev.* **D78** (2008) 054513 [[0805.2999](#)].
- [166] A. Bochkarev and P. de Forcrand, *Determination of the renormalized heavy quark mass in lattice QCD*, *Nucl.Phys.* **B477** (1996) 489 [[hep-lat/9505025](#)].
- [167] [HPQCD 14A] B. Chakraborty, C.T.H. Davies, G.C. Donald, R.J. Dowdall, B. Galloway, P. Knecht et al., *High-precision quark masses and QCD coupling from $n_f = 4$ lattice QCD*, *Phys.Rev.* **D91** (2015) 054508 [[1408.4169](#)].

- [168] [JLQCD 16] K. Nakayama, B. Fahy and S. Hashimoto, *Short-distance charmonium correlator on the lattice with Möbius domain-wall fermion and a determination of charm quark mass*, *Phys. Rev.* **D94** (2016) 054507 [[1606.01002](#)].
- [169] B. Dehnadi, A.H. Hoang and V. Mateu, *Bottom and Charm Mass Determinations with a Convergence Test*, *JHEP* **08** (2015) 155 [[1504.07638](#)].
- [170] K. Chetyrkin, J.H. Kuhn and C. Sturm, *Four-loop moments of the heavy quark vacuum polarization function in perturbative QCD*, *Eur.Phys.J.* **C48** (2006) 107 [[hep-ph/0604234](#)].
- [171] R. Boughezal, M. Czakon and T. Schutzmeier, *Charm and bottom quark masses from perturbative QCD*, *Phys.Rev.* **D74** (2006) 074006 [[hep-ph/0605023](#)].
- [172] A. Maier, P. Maierhofer and P. Marquard, *The second physical moment of the heavy quark vector correlator at $O(\alpha_s^3)$* , *Phys.Lett.* **B669** (2008) 88 [[0806.3405](#)].
- [173] A. Maier, P. Maierhofer, P. Marquard and A. Smirnov, *Low energy moments of heavy quark current correlators at four loops*, *Nucl.Phys.* **B824** (2010) 1 [[0907.2117](#)].
- [174] Y. Kiyo, A. Maier, P. Maierhofer and P. Marquard, *Reconstruction of heavy quark current correlators at $O(\alpha_s^3)$* , *Nucl.Phys.* **B823** (2009) 269 [[0907.2120](#)].
- [175] Y. Maezawa and P. Petreczky, *Quark masses and strong coupling constant in 2+1 flavor QCD*, *Phys. Rev.* **D94** (2016) 034507 [[1606.08798](#)].
- [176] J.H. Kühn, M. Steinhauser and C. Sturm, *Heavy quark masses from sum rules in four-loop approximation*, *Nucl. Phys.* **B778** (2007) 192 [[hep-ph/0702103](#)].
- [177] K. Chetyrkin, J. Kuhn, A. Maier, P. Maierhofer, P. Marquard et al., *Charm and Bottom Quark Masses: An Update*, *Phys.Rev.* **D80** (2009) 074010 [[0907.2110](#)].
- [178] [HPQCD 13A] R. Dowdall, C. Davies, G. Lepage and C. McNeile, *V_{us} from π and K decay constants in full lattice QCD with physical u , d , s and c quarks*, *Phys.Rev.* **D88** (2013) 074504 [[1303.1670](#)].
- [179] A. Cucchieri, *Gribov copies in the minimal Landau gauge: The Influence on gluon and ghost propagators*, *Nucl.Phys.* **B508** (1997) 353 [[hep-lat/9705005](#)].
- [180] L. Giusti, M. Paciello, C. Parrinello, S. Petrarca and B. Taglienti, *Problems on lattice gauge fixing*, *Int.J.Mod.Phys.* **A16** (2001) 3487 [[hep-lat/0104012](#)].
- [181] A. Maas, J.M. Pawłowski, D. Spielmann, A. Sternbeck and L. von Smekal, *Strong-coupling study of the Gribov ambiguity in lattice Landau gauge*, *Eur.Phys.J.* **C68** (2010) 183 [[0912.4203](#)].
- [182] B. Alles, D. Henty, H. Panagopoulos, C. Parrinello, C. Pittori et al., *α_s from the nonperturbatively renormalised lattice three gluon vertex*, *Nucl.Phys.* **B502** (1997) 325 [[hep-lat/9605033](#)].
- [183] P. Boucaud, J. Leroy, H. Moutarde, J. Micheli, O. Pene et al., *Preliminary calculation of α_s from Green functions with dynamical quarks*, *JHEP* **0201** (2002) 046 [[hep-ph/0107278](#)].

- [184] P. Boucaud, J. Leroy, A. Le Yaouanc, A. Lokhov, J. Micheli et al., *Asymptotic behavior of the ghost propagator in SU(3) lattice gauge theory*, *Phys.Rev.* **D72** (2005) 114503 [[hep-lat/0506031](#)].
- [185] P. Boucaud, J. Leroy, A. Le Yaouanc, A. Lokhov, J. Micheli et al., *Non-perturbative power corrections to ghost and gluon propagators*, *JHEP* **0601** (2006) 037 [[hep-lat/0507005](#)].
- [186] A. Sternbeck, K. Maltman, L. von Smekal, A. Williams, E. Ilgenfritz et al., *Running α_s from Landau-gauge gluon and ghost correlations*, *PoS LAT2007* (2007) 256 [[0710.2965](#)].
- [187] Ph. Boucaud, F. De Soto, J. Leroy, A. Le Yaouanc, J. Micheli et al., *Ghost-gluon running coupling, power corrections and the determination of $\Lambda_{\overline{\text{MS}}}$* , *Phys.Rev.* **D79** (2009) 014508 [[0811.2059](#)].
- [188] [ETM 13D] B. Blossier et al., *High statistics determination of the strong coupling constant in Taylor scheme and its OPE Wilson coefficient from lattice QCD with a dynamical charm*, *Phys.Rev.* **D89** (2014) 014507 [[1310.3763](#)].
- [189] [ETM 12C] B. Blossier, P. Boucaud, M. Brinet, F. De Soto, X. Du et al., *The strong running coupling at τ and Z_0 mass scales from lattice QCD*, *Phys.Rev.Lett.* **108** (2012) 262002 [[1201.5770](#)].
- [190] [ETM 11D] B. Blossier, P. Boucaud, M. Brinet, F. De Soto, X. Du et al., *Ghost-gluon coupling, power corrections and $\Lambda_{\overline{\text{MS}}}$ from lattice QCD with a dynamical charm*, *Phys.Rev.* **D85** (2012) 034503 [[1110.5829](#)].
- [191] A. Sternbeck, K. Maltman, M. Müller-Preussker and L. von Smekal, *Determination of $\Lambda_{\overline{\text{MS}}}$ from the gluon and ghost propagators in Landau gauge*, *PoS LAT2012* (2012) 243 [[1212.2039](#)].
- [192] A. Sternbeck, E.-M. Ilgenfritz, K. Maltman, M. Müller-Preussker, L. von Smekal et al., *QCD Lambda parameter from Landau-gauge gluon and ghost correlations*, *PoS LAT2009* (2009) 210 [[1003.1585](#)].
- [193] [ETM 10F] B. Blossier et al., *Ghost-gluon coupling, power corrections and $\Lambda_{\overline{\text{MS}}}$ from twisted-mass lattice QCD at $N_f = 2$* , *Phys.Rev.* **D82** (2010) 034510 [[1005.5290](#)].
- [194] E.-M. Ilgenfritz, C. Menz, M. Müller-Preussker, A. Schiller and A. Sternbeck, *SU(3) Landau gauge gluon and ghost propagators using the logarithmic lattice gluon field definition*, *Phys.Rev.* **D83** (2011) 054506 [[1010.5120](#)].
- [195] F. De Soto and J. Rodriguez-Quintero, *Notes on the determination of the Landau gauge OPE for the asymmetric three gluon vertex*, *Phys.Rev.* **D64** (2001) 114003 [[hep-ph/0105063](#)].
- [196] P. Boucaud, A. Le Yaouanc, J. Leroy, J. Micheli, O. Pene et al., *Testing Landau gauge OPE on the lattice with a $\langle A^2 \rangle$ condensate*, *Phys.Rev.* **D63** (2001) 114003 [[hep-ph/0101302](#)].

- [197] P. Boucaud, A. Le Yaouanc, J. Leroy, J. Micheli, O. Pene et al., *Consistent OPE description of gluon two point and three point Green function?*, *Phys.Lett.* **B493** (2000) 315 [[hep-ph/0008043](#)].
- [198] P. Boucaud, G. Burgio, F. Di Renzo, J. Leroy, J. Micheli et al., *Lattice calculation of $1/p^2$ corrections to α_s and of Λ_{QCD} in the MOM scheme*, *JHEP* **0004** (2000) 006 [[hep-ph/0003020](#)].
- [199] D. Bećirević, P. Boucaud, J. Leroy, J. Micheli, O. Pene et al., *Asymptotic scaling of the gluon propagator on the lattice*, *Phys.Rev.* **D61** (2000) 114508 [[hep-ph/9910204](#)].
- [200] D. Bećirević, P. Boucaud, J. Leroy, J. Micheli, O. Pene et al., *Asymptotic behavior of the gluon propagator from lattice QCD*, *Phys.Rev.* **D60** (1999) 094509 [[hep-ph/9903364](#)].
- [201] P. Boucaud, J. Leroy, J. Micheli, O. Pene and C. Roiesnel, *Three loop beta function and nonperturbative α_s in asymmetric momentum scheme*, *JHEP* **9812** (1998) 004 [[hep-ph/9810437](#)].
- [202] P. Boucaud, J. Leroy, J. Micheli, O. Pene and C. Roiesnel, *Lattice calculation of α_s in momentum scheme*, *JHEP* **9810** (1998) 017 [[hep-ph/9810322](#)].
- [203] [ETM 13] K. Cichy, E. Garcia-Ramos and K. Jansen, *Chiral condensate from the twisted mass Dirac operator spectrum*, *JHEP* **1310** (2013) 175 [[1303.1954](#)].
- [204] P. Boucaud, F. De Soto, K. Raya, J. Rodríguez-Quintero and S. Zafeiropoulos, *Discretization effects on renormalized gauge-field Green's functions, scale setting, and the gluon mass*, *Phys. Rev. D* **98** (2018) 114515 [[1809.05776](#)].
- [205] K.G. Chetyrkin and J.H. Kuhn, *Quartic mass corrections to $R(\text{had})$* , *Nucl. Phys.* **B432** (1994) 337 [[hep-ph/9406299](#)].
- [206] J.-L. Kneur and A. Neveu, *Chiral condensate from renormalization group optimized perturbation*, *Phys. Rev.* **D92** (2015) 074027 [[1506.07506](#)].
- [207] K. Nakayama, H. Fukaya and S. Hashimoto, *Lattice computation of the Dirac eigenvalue density in the perturbative regime of QCD*, *Phys. Rev.* **D98** (2018) 014501 [[1804.06695](#)].
- [208] [CERN 08] L. Giusti and M. Lüscher, *Chiral symmetry breaking and the Banks–Casher relation in lattice QCD with Wilson quarks*, *JHEP* **03** (2009) 013 [[0812.3638](#)].
- [209] [JLQCD 16B] G. Cossu, H. Fukaya, S. Hashimoto, T. Kaneko and J.-I. Noaki, *Stochastic calculation of the Dirac spectrum on the lattice and a determination of chiral condensate in 2+1-flavor QCD*, *PTEP* **2016** (2016) 093B06 [[1607.01099](#)].
- [210] PARTICLE DATA GROUP collaboration, *Review of Particle Physics*, *Chin. Phys.* **C40** (2016) 100001.
- [211] PARTICLE DATA GROUP collaboration, *Review of Particle Physics*, *Chin. Phys.* **C38** (2014) 090001 and 2015 update.
- [212] PARTICLE DATA GROUP collaboration, *Review of Particle Physics*, *Phys.Rev.* **D86** (2012) 010001 and 2013 partial update for the 2014 edition.

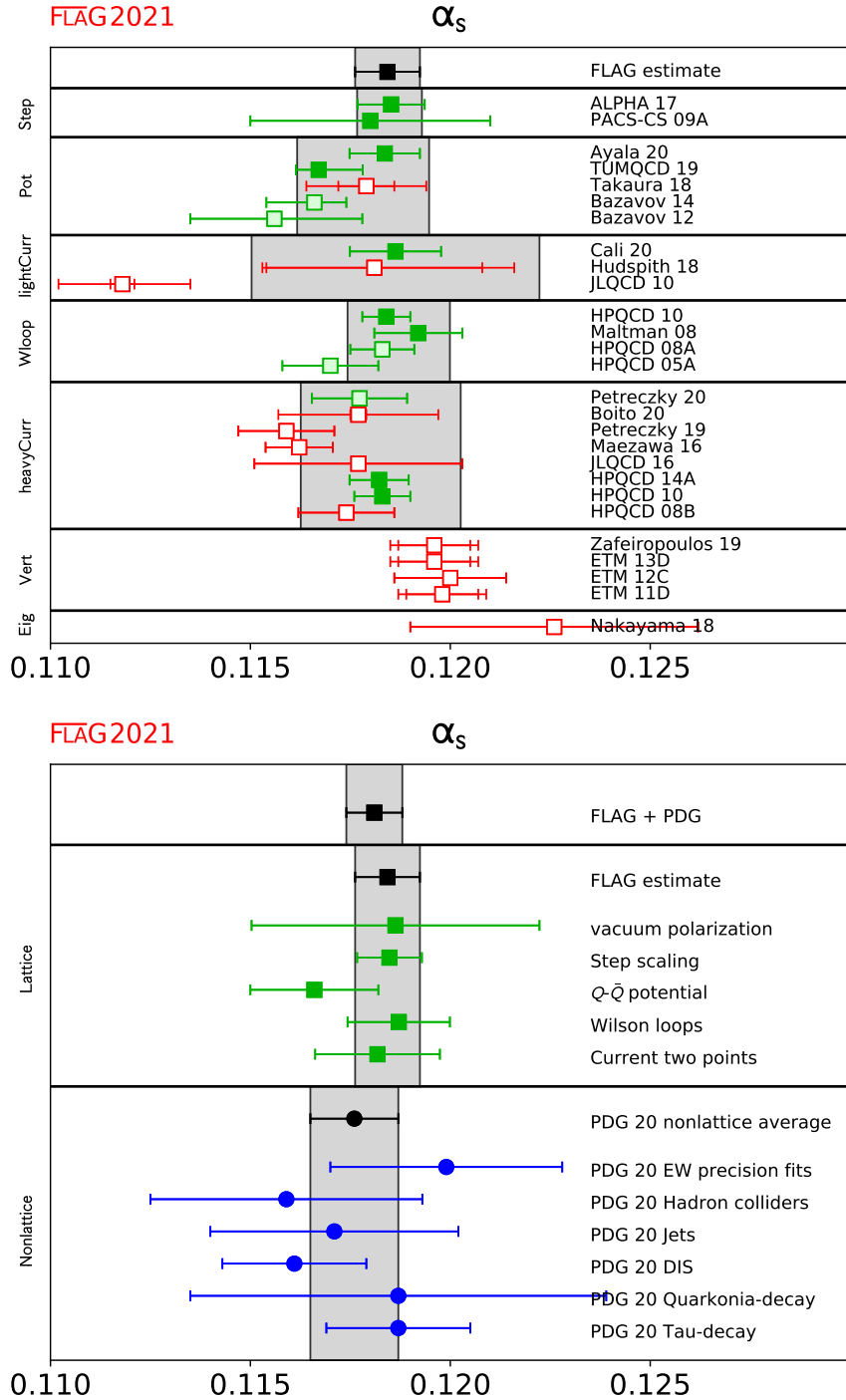


Figure 41: $\alpha_{\overline{\text{MS}}}^{(5)}(M_Z)$, the coupling constant in the $\overline{\text{MS}}$ scheme at the Z mass. Top: lattice results, pre-ranges from different calculation methods, and final average. Bottom: Comparison of the lattice pre-ranges and average with the nonlattice ranges and average. The first PDG 20 entry gives the outcome of their analysis excluding lattice results (see Sec. 9.11.4).